



1997

Amyloid- $\text{A}\beta$ Deposition in Rat Brain: Histopathological and Functional Sequelae

Einar M. Sigurdsson
Loyola University Chicago

Follow this and additional works at: https://ecommons.luc.edu/luc_diss

 Part of the [Pharmacology Commons](#)

Recommended Citation

Sigurdsson, Einar M., "Amyloid- $\text{A}\beta$ Deposition in Rat Brain: Histopathological and Functional Sequelae" (1997). *Dissertations*. 3416.
https://ecommons.luc.edu/luc_diss/3416

This Dissertation is brought to you for free and open access by the Theses and Dissertations at Loyola eCommons. It has been accepted for inclusion in Dissertations by an authorized administrator of Loyola eCommons. For more information, please contact ecommons@luc.edu.



This work is licensed under a [Creative Commons Attribution-Noncommercial-No Derivative Works 3.0 License](#).
Copyright © 1997 Einar M. Sigurdsson

LIBRARY-LOYOLA UNIVERSITY
MEDICAL CENTER,

LOYOLA UNIVERSITY CHICAGO

AMYLOID- β DEPOSITION IN RAT BRAIN:
HISTOPATHOLOGICAL AND FUNCTIONAL SEQUELAE

A DISSERTATION SUBMITTED TO
THE FACULTY OF THE GRADUATE SCHOOL
IN CANDIDACY FOR THE DEGREE OF
DOCTOR OF PHILOSOPHY

DEPARTMENT OF PHARMACOLOGY AND EXPERIMENTAL THERAPEUTICS

BY

EINAR M. SIGURDSSON

CHICAGO, ILLINOIS

MAY, 1997

Copyright by Einar M. Sigurdsson, 1997

All rights reserved.

ACKNOWLEDGEMENTS

I sincerely thank my advisor, Dr. Stanley A. Lorens, and Dr. John M. Lee for their guidance and support during my research endeavors in their laboratories. I thank the other members of my dissertation committee, Drs. Thackery Gray, Nancy Muma, and T. Celeste Napier, for their guidance and review of this work. I am indebted to Matthew J. Hejna, Debra Magnuson and Xin-Wen Dong for their technical support. My gratitude goes to Connie Polchan for secretarial assistance, and to Therman Banks for excellent animal care. I also wish to thank all the staff, students and faculty of the Department of Pharmacology and Experimental Therapeutics.

TABLE OF CONTENTS

ACKNOWLEDGEMENTS	iii
LIST OF FIGURES	vi
LIST OF TABLES	viii
LIST OF ABBREVIATIONS	ix
ABSTRACT	xi
Chapter	
I. INTRODUCTION	1
REVIEW OF THE RELEVANT LITERATURE	3
Amyloid- β Precursor Protein	3
A β Peptide	6
Effects of A β Peptide on Behavior	10
Tau protein	14
Apolipoprotein E	15
Presenilins	16
Glial cells in Alzheimer's Disease	17
Macrogliia: Astrocytes	17
Microglia	18
Distribution of Alzheimer's Disease Histopathology	20
Laterality in Alzheimer's Disease	22
Animal Models for Alzheimer's Disease	23
II. AIMS OF THE PRESENT STUDY	30
III. LOCAL AND DISTANT HISTOPATHOLOGICAL EFFECTS OF UNILATERAL INJECTIONS OF AMYLOID- β 25-35 INTO THE AMYGDALA OF YOUNG MALE FISCHER RATS	38
Abstract	
Introduction	
Materials and Methods	
Results	
Discussion	

IV. LATERALITY IN THE HISTOLOGICAL	
EFFECTS OF INJECTIONS OF AMYLOID- β 25-35	
INTO THE AMYGDALA OF YOUNG MALE FISCHER RATS67
Abstract	
Introduction	
Materials and Methods	
Results	
Discussion	
V. TIME COURSE OF THE HISTOPATHOLOGICAL	
EFFECTS OF INJECTIONS OF AMYLOID- β 25-35	
INTO THE AMYGDALA OF YOUNG MALE FISCHER RATS 90
Abstract	
Introduction	
Materials and Methods	
Results	
Discussion	
VI. GENERAL DISCUSSION 133
Appendix	
REFERENCES 144
VITA 173

LIST OF FIGURES

Figure	Page
1. APP processing enzymes	4
2. Amino acid sequence of A β 1-42 and A β 25-35 (underlined)	6
3. Cresyl violet staining at 8 days postinjection	49
4. Tau-2 IR at 8 days postinjection	51
5. Tau-2 IR at 8 days postinjection	52
6. Quantitation of tau-2 IR cells at 8 days and 32 days postinjection	55
7. Alz-50 IR at 32 days postinjection	56
8. GFAP IR 32 days postinjection	58
9. Schematic diagram of the right hemisphere of a coronal section through the A β 25-35 injection site	61
10. Neuronal shrinkage within the right amygdala	76
11. Congo red positive A β deposit	77
12. Laterality in tau-2 IR	79
13. Laterality in GFAP staining	81
14. A β deposits, neuronal shrinkage, tau-2 and GFAP staining	82
15. Tau-2 IR within the right amygdala following injection of A β 25-35 into the left amygdala	84
16. Congo red positive A β deposits at 32 and 128 days postoperatively	106
17. Size of the A β deposits within the left and right amygdala at 8, 32, 64, 96, and 128 days postoperatively	107
18. Tau-2 IR at 32 days postinjection	110
19. Time course of neuronal tau-2 IR within the left and right amygdala or hippocampus	111

20. Neuronal tau-2 IR within the left and right amygdala (A) and hippocampus (B) at 32 and 128 days postinjection	112
21. GFAP IR at 32 and 128 days postinjection	114
22. Time course of reactive astrogliosis within the left and right hippocampus	115
23. Cresyl violet staining at 32 days postinjection	117
24. Neuronal shrinkage in cresyl violet stained sections within the right amygdala vs. the left amygdala at 32 and 128 days postoperatively	118
25. Amygdaloid IL-1 β IR at 32 days postinjection	120
26. Hippocampal IL-1 β IR at 32 days postinjection	121
27. Behavior in the open field (12 min)	123
28. Behavior in the Morris water maze	125
29. Pathological effects of A β	141

LIST OF TABLES

Table	Page
1. One-way CAR acquisition and retention	124
2. Amygdaloid ChAT activity	126

LIST OF ABBREVIATIONS

A β	amyloid- β
ACh	acetylcholine
AChE	acetylcholinesterase
AD	Alzheimer's disease
ANOVA	analysis of variance
ApoE	apolipoprotein E
AP	anteroposterior
APP	amyloid- β precursor protein
APPs	APP secreted form
C	complement factor
CAR	one-way conditioned avoidance response
ChAT	choline acetyltransferase
CNS	central nervous system
DAB	3, 3' diaminobenzidine tetrahydrochloride
DV	dorsoventral
GFAP	glial fibrillary acidic protein
GS	glutamine synthetase
i.c.v.	intracerebroventricular
Ig	immunoglobulin
i.p.	intraperitoneally
IL	interleukin
IR	immunoreactivity, immunoreactive

ML	mediolateral
PB	sodium/potassium phosphate buffer
PBS	phosphate buffered saline
SEC	serpin-enzyme complex
TBS	tris buffered saline
TFA	trifluoroacetic acid
TPK I	tau protein kinase I
VEH	vehicle
VP/SI	ventral pallidum/substantia innominata

ABSTRACT

Alzheimer's disease (AD) is characterized histopathologically by neurofibrillary tangles, senile plaques, reactive astrocytes and microglia, neuronal shrinkage, and cell loss in various brain regions. These pathological changes are associated with neurochemical deficits and cognitive impairments. Senile plaques consist predominantly of amyloid- β ($A\beta$) peptide, that has been proposed to have a prominent role in the pathogenesis of AD. The main component of the tangles is paired helical filaments, which consist largely of the protein tau in an abnormal state of phosphorylation. There is currently no treatment available that effectively slows or halts the progression of AD. The main reason for this is the relative lack of an animal model that has the features of the disease, in which potential therapeutic drugs could be screened. The main objective of this dissertation work was to develop a rat model of the histopathological hallmarks of AD.

Because the early and primary histopathological changes in AD are predominantly found in temporal lobe structures, it was determined if intra-amygdaloid injections of $A\beta$ 25-35 in the rat induced the appearance of abnormal tau proteins and reactive astrocytes as seen in AD. It was also examined if the effects of $A\beta$ were time dependent, included neuronal shrinkage and microglial activation, and if these changes were associated with neurochemical and behavioral alterations.

$A\beta$ induced abnormal neuronal tau staining in the right amygdala and hippocampus. $A\beta$ also induced reactive astrocytosis and neuronal shrinkage within the right hippocampus and amygdala, respectively. The same brain regions within the left hemisphere were significantly less affected. In addition, $A\beta$ appeared to induce microglial proliferation and

neuronal interleukin-1 β staining. The histopathological effects of A β peaked at 32 days postoperatively and were associated with minimal behavioral impairments. These effects were not associated with a reduction in amygdaloid choline acetyltransferase activity at 32 days postinjection.

These data demonstrate that intra-amygdaloid injections of A β induce transsynaptic cytoskeletal and astroglial reactions. These findings also suggest a laterality in the histopathological effects of A β and that the effects of single injections are in part transient. Identification of the cause for the lateralized effect of A β may prove valuable for understanding the etiology of AD and provide possible therapeutic strategies designed to slow the progression of the disease. In addition, these results suggest a direct association between plaque and tangle formation in AD, and support the use of this rat model to screen drugs that may alter the initial pathological events associated with AD.

CHAPTER I

INTRODUCTION

Alzheimer's disease (AD) was originally characterized by Alois Alzheimer in 1907. The histopathological characteristics of AD include neurofibrillary tangles, senile plaques, reactive astrocytes and microglia, neuronal shrinkage, and cell loss in several brain regions. These pathological changes are associated with neurochemical deficits and cognitive impairments. The main component of the neurofibrillary tangles is paired helical filaments (168,335), that consist largely of the microtubule associated protein tau in an abnormal state of phosphorylation (171,183,355,356). Reactive astrocytes and microglia have larger cytoplasm and thicker and more branched processes than they do when in their resting states. Senile plaques in the AD brain are associated with reactive astrocytes (70,126,128,250) and microglia (122,155,228). Senile plaques consist predominantly of amyloid- β (A β) 1-42 peptide (103,214,233,285), which is derived from a large membrane spanning protein, the amyloid- β precursor protein (APP) (166). Mutations in APP in some forms of familial AD are associated with an elevated production of A β (33,39,331). APP is overexpressed in Down's syndrome (248,291), and individuals with this disease invariably develop the neuropathological hallmarks of AD (23,187). The proposed role for A β in the pathogenesis of AD is further supported by the neurotoxicity of A β (369,370), which includes amino acids 25-35 of the peptide (370). Currently, AD is the fourth leading cause of death in the developed world. Advanced age is the major risk factor for AD, and the prevalence of AD is expected to rise substantially in the near future because of the aging population. Numerous advances have been made in recent years in elucidating the

mechanism of neuronal degeneration in AD. Several risk factors for AD are now known but the sequence of pathogenic events that eventually lead to dementia remains a mystery.

There is currently no treatment available that effectively slows or halts the progression of the disease. The main reason for this is a lack of an adequate animal model that has all the features of the disease, in which potential therapeutic drugs could be screened. The main objective of this dissertation work was to develop a rat model of the histopathological hallmarks of AD.

Because the early and primary histopathological changes in AD are predominantly found in temporal lobe structures, we assessed the hypotheses that A β 25-35 injections into the amygdala of the rat would induce the appearance of abnormal microtubule associated protein tau and reactive astrocytes as seen in AD. We also tested the hypotheses that the effects of A β 25-35 would be time dependent and include neuronal shrinkage and microglial activation. Furthermore, we examined the hypotheses that these histological changes would be associated with neurochemical and behavioral alterations.

REVIEW OF THE RELEVANT LITERATURE

Amyloid- β Precursor Protein

Three major isoforms of APP are produced by alternative splicing. Isoforms of 751 and 770 amino acids are expressed in both neural and non-neural tissue (169,275,333), whereas a 695 amino acid isoform is mostly expressed in neurons (172,365). APP is processed through at least two proteolytic pathways. The major pathway is a secretory pathway which leads to cleavage of APP within the extracellular portion of the A β peptide (between residues 16 and 17) (78), that generates a 90-100 kDa secreted form (APPs) (78,318,349). This cleavage is performed by an unknown enzyme named α -secretase. This pathway is considered non-amyloidogenic because intact A β is not formed. APP also is processed through an amyloidogenic endosomal/lysosomal pathway (44,80,107,119). This alternative pathway generates intact A β that is processed from APP by unknown enzymes termed β - and γ -secretase. It was believed that intact A β was not generated during normal APP processing (318), but it has recently been demonstrated that A β is produced and secreted during normal metabolism (24,120,307,313). Analysis of APP metabolism in primary cell cultures of neurons, astrocytes and microglia indicates that neurons generate more A β than astrocytes or microglia (190).

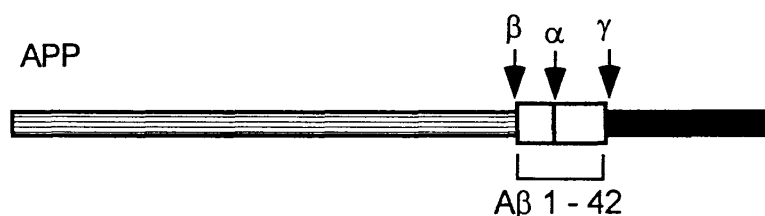


Figure 1. APP processing enzymes. Schematic presentation of the enzymatic cleavage of APP. A cleavage of APP by β - and γ -secretases is considered amyloidogenic because it leads to the production of $A\beta$ 1-42, the most prominent form of $A\beta$ in senile plaques. Alternatively, a cleavage by α -secretase is considered non-amyloidogenic because intact $A\beta$ is not formed. The arrows labeled α , β , and γ represent the respective secretases.

The role of APP, APPs and A β in the brain is not well understood. APP associates with G proteins (251), suggesting that it may serve as a receptor. Overexpression of APP has synaptotrophic effects in the cortex of transgenic mice and protects against the neurotoxicity of the gp 120 protein found in the human immunodeficiency virus (240,241). APP is not essential during development because homozygous APP-knockout mice proceed through gestation normally (371). As adults, they are fertile but exhibit a 15-20% decrease in body weight, decreased locomotor activity, and a loss of forelimb grip strength. Diffuse reactive gliosis is observed in the brains of these animals without clear neuronal degeneration.

Cerebrospinal fluid levels of APPs are decreased in AD (339). APPs stimulates cell growth (295), promotes cell adhesion (20,38,167,234,303), and mediates the effects of nerve growth factor on neurite outgrowth (234). At the molecular level, APPs activates potassium channels (96) and increases the activity of microtubule associated protein kinase (116). APPs protects cultured neurons from the damaging effects of glucose deprivation, excitatory amino acids, and oxidation, possibly through stabilization of intracellular calcium (217,302). It is possible that a reduction in the production of APPs is associated with an increase in A β production, both of which would result in increased neuronal vulnerability to toxic insults.

A β Peptide

The proposed direct role for A β in the pathogenesis of AD is supported by the association of AD with inherited APP mutations; APP overexpression in Down's syndrome; and, the neurotoxicity of A β fibrils.

H₂N-Asp-Ala-Glu-Phe-Arg-His-Asp-Ser-Gly-Tyr-Glu-Val-His-His-Gln-Lys-Leu-Val-Phe-Phe-Ala-Glu-Asp-Val-Gly-Ser-Asn-Lys-Gly-Ala-Ile-Ile-Gly-Leu-Met-Val-Gly-Gly-Val-Val-Ile-Ala-OH

Figure 2. Amino acid sequence of A β 1-42 and A β 25-35 (underlined).

Normal processing of APP results in more production of A β 1-40 than A β 1-42 (331,336). The preferential deposition of A β 1-42 in senile plaques (285) is likely due to its lesser solubility than A β 1-40, and that it is more prone to aggregate and form β -pleated sheets (11,22,81,124,161,162). The first APP mutation found in AD kindreds was identified at codon 717 (104). Expression of this mutant APP in cultured cells results in increased production of A β 1-42 (331). Another inherited double APP mutation at codons 670 and 671 (242) results in an increase in A β production in transfected cells (33,39). APP is overexpressed in Down's syndrome (248,291) and individuals with this disease invariably develop the neuropathological hallmarks of AD (23,187).

In vitro studies indicate that A β 1-28 has a neurotrophic effect on cultured hippocampal neurons (353), and that A β 25-35 is a neurotrophic factor at low concentrations (nM) in differentiating neurons but is neurotoxic at high concentrations (μ M) in mature neurons (370). A β toxicity in cell culture (273,284,368-370) depends on its aggregation state (25,220,269,273), and requires the assembly of A β into amyloid fibrils composed of a β -pleated sheet structure (26,144,203). These *in vitro* findings correlate

well with the observation that histopathological changes in AD are associated with senile plaques that are composed of A β fibrils, but not with diffuse plaques composed of amorphous A β aggregates (210,366). Various compounds bind to A β and enhance its fibrillation *in vitro*, including apolipoprotein E (ApoE) (205,296,326,359), heparan sulfate proteoglycan (90), and aluminum, iron and zinc ions (29,83,213). In addition, metal-catalyzed oxidation of A β results in the formation of highly insoluble aggregates (71). A β *in vitro* develops resistance to protease degradation when polymerized into fibrils (252). Other amyloidogenic peptides also are toxic to neurons *in vitro*, including amylin, serum amyloid P component, and a peptide derived from the prion protein (87,202,222,338). These findings suggest that the tertiary structure of the fibril, rather than its amino acid sequence, is responsible for its toxicity.

A β 1-42 has been shown to bind to the serpin-enzyme complex (SEC) receptor on cultured hepatoma cells (165). A β 25-35, 31-35, 1-39, and A β 1-40 have similar affinity as A β 1-42 for the receptor (19). The SEC receptor is present on PC12 cells as well as in primary culture of murine cortical neurons, and the selectivity of neuronal SEC receptor for A β is identical to that of hepatoma cells (19). The SEC receptor has been demonstrated to mediate internalization and degradation of A β in PC12 cells (19). In addition, this receptor recognizes the soluble non-toxic A β but not the aggregated cytotoxic A β , suggesting that the receptor may have a protective role by mediating clearance and metabolism of soluble A β (18). Furthermore, A β binds to the receptor for advanced glycation end products (RAGE) in neurons, microglia and vascular endothelial cells (367). This interaction mediates cell adhesion to A β and induces production of reactive oxygen species in microglia. The class A scavenger receptor has also been demonstrated to mediate adhesion of microglia to A β that causes secretion of reactive oxygen species and cell immobilization (76). In addition, A β has been observed to form an ion channel in artificial lipid membranes (6).

A β *in vitro* has been observed to potentiate the neurotoxicity of excitatory amino acids (170,218), glucose deprivation (48), and oxidative stress (196). Conversely, other studies have reported that glutamate antagonists do not prevent A β toxicity (28,269). A β also impairs mitochondrial redox activity and increases the generation of free radicals (14,308). Some reports have suggested that antioxidants inhibit the toxicity of A β and other amyloidogenic peptides (14), whereas other studies find no protective effect of the same antioxidants (196,202). The neurotoxicity of A β and other amyloidogenic peptides has been shown to be mediated by an increase in intracellular calcium (218,219), but calcium channel blockers and calcium chelating agents do not inhibit A β neurotoxicity (202,352). These discrepancies, which may be due to differences in culture conditions, clearly demonstrate the limitations of *in vitro* culture systems and show that caution must be taken in extrapolating *in vitro* findings to *in vivo* situations.

The two basic pathways or mechanisms of cell death are necrosis and apoptosis. *In vitro* studies have observed that A β induces both apoptosis (88,200,347) and necrosis (13). Another amyloidogenic peptide, amylin, has been shown to induce apoptosis in pancreatic islet cells (202). Some neurons in AD brain appear to undergo apoptosis (2,189,328), and cortical neurons from Down's syndrome brains generate increased levels of reactive oxygen species that leads to apoptotic cell death in culture (27).

The reproducibility of A β toxicity *in vivo* has been inconsistent (42,91,99,101,102,178,180,314,320,354). This may be due to variations in: 1) the conformational state (25,269,273), dose, and sequence of A β ; 2) method of administration; 3) pathological endpoints measured; 4) what brain region and/or hemisphere is injected; 5) postoperative interval; and, 6) species and/or strain used. The consistency and persistence of A β deposits within the brain may also depend on similar factors. A β *in vitro* develops protease resistance to degradation when polymerized into fibrils (252). The presence of heparan sulfate proteoglycans has been shown to be important for consistent *in vivo*

deposition of A β 1-40 and persistence of fibrillar A β in the rat hippocampus (321). Also, A β 25-35 deposits within the rat nucleus basalis are degraded more rapidly than A β 1-40 deposits (102). Furthermore, acetylcholinesterase (AChE) has been shown to promote the formation of and/or stabilization of A β fibrils (150).

It can be argued that because A β 1-42 is the most prevalent form of A β in senile plaques, it is appropriate to use that peptide for injections into brain instead of A β 25-35. However, the main problem with using A β 1-42 is its insolubility in physiological solvents. Therefore, there is a risk of potentially toxic solvents interfering with the properties and effects of A β 1-42. On the other hand, A β 25-35 is readily soluble in H₂O and acquires the same β -pleated sheet conformation as A β 1-42, which is the toxic conformation of A β .

Only recently have a few studies demonstrated a direct association between plaque and tangle formation in AD. *In vitro* studies have demonstrated that A β increases tau protein kinase I (TPK I) activity (332), induces abnormal tau immunoreactivity (IR) (26,207), and that the neuronal death caused by A β can be prevented with TPK I antisense oligonucleotides (332). These findings suggest an association between plaque and tangle formation in AD. A few *in vivo* studies have investigated the effects of A β injected into the central nervous system (CNS) on tau IR (42,91,99,178,180,274). Some of these studies indicate that A β can induce the appearance of abnormal tau proteins in the vicinity of the injection site (rat cerebral cortex and hippocampus) (91,178,180). Other studies have failed to show any effect (42,99,274). For the most part, these *in vivo* studies have only been qualitative or descriptive in nature. No attempts have been made to quantify A β induced effects by counting neuronal tau IR cells.

The effects of A β on tau IR may be mediated through an increase in intracellular calcium. A β has been shown to increase intracellular calcium (7,218), and calcium influx in cultured rat hippocampal neurons caused by glutamate induces tau IR as recognized by the antibodies Alz-50 and 5E2 (216). Protein kinases are generally activated by increases in

intracellular calcium and several of those have been shown to phosphorylate different sites on tau proteins (238). Therefore, A β may increase the phosphorylation of tau proteins through an activation of kinases mediated by an increase in intracellular calcium. The activities of some phosphatases that may dephosphorylate tau proteins have been shown to be decreased in AD (111,311). Therefore, A β 25-35 may also be decreasing the dephosphorylation of tau proteins through an inhibition of phosphatases.

Effects of A β Peptide on Behavior

Only a few studies have investigated the effects of A β injections on behavior and the experimental procedures vary substantially. It is, therefore, appropriate to give a somewhat detailed description of these findings. Because of the nature of behavioral experiments, it is necessary to support alterations in behavior with neurochemical and/or histological findings.

Flood et al. (85) observed that intracerebroventricular (i.c.v.) administration in mice of [Gln11]A β 1-28, A β 12-28, A β 18-28 and A β 12-20 immediately after training in a footshock active avoidance test caused dose dependent retention deficits in the same test one week later. This effect may be specific to memory processing because the peptides did not cause amnesia when injected 24 h after training nor did they disturb storage or retrieval of older memories. Intrahippocampal injection of [Gln11]A β 1-28 produced amnesia at much lower doses (<1 nmol) than an i.c.v. injection (approximately 1.5 - 6 nmol).

Maurice et al. (221) showed that A β 25-35 injected i.c.v. in mice induced dose dependent decreases in both alternation behavior in the Y-maze 6 days postinjection and passive avoidance test 7-8 days postoperatively, at doses of 3 and 9 nmol/mouse. Both the cholinesterase inhibitor tacrine and the nicotinic receptor agonist (-)-nicotine induced a dose

dependent abrogation of the A β 25-35 induced behavioral impairments. Furthermore, tacrine also reversed A β 25-35 induced impairment of place learning and retention in a water maze. A moderate bilateral cell loss and Congo red positive amyloid deposits were observed at 21 days postoperatively within the frontoparietal cortex and in the CA3 region of the hippocampal formation in animals that received 9 nmol A β 25-35. These results indicate that the deposition of A β in the brain is in some way related to impairment of learning and cholinergic degeneration, and furthermore suggest that the 25-35 fragment of A β that is sufficient to induce neuronal death in cultures also induces an AD type amnesia in mice.

One of the first studies to demonstrate a behavioral effect of A β in rats was performed by Tate et al. (334), and did not use injections of A β but rather a grafting of transfected cells that overexpress A β . These cells were grafted into the suprachiasmatic nuclei of adult rats and led to disruption of circadian activity. AD patients exhibit irregularities in the patterns of circadian rhythms and this finding suggests that A β may have a role in these changes. However, it should be noted that the control groups did not include animals grafted with non-transfected cells.

Nabeshima et al. (244) demonstrated that continuous infusions of A β 1-40 (3, 30 and 300 pmol/day) for two weeks into the cerebral ventricles in adult rats led to impaired performance in water maze (9-13 days postinfusion) and passive avoidance tasks (14-15 days postinfusion). These behavioral impairments were associated with a moderate reduction in choline acetyltransferase (ChAT) activity in the frontal cortex (3 and 30 pmol/day) and hippocampus (300 pmol/day). No differences were observed in AChE activity between treatment groups. Also, Itoh et al. (156) demonstrated in this model that A β infusions (300 pmol/day) reduced nicotine stimulated release of acetylcholine and dopamine determined 11-13 days postoperatively by an *in vivo* brain microdialysis method. Furthermore, dopamine release induced by high potassium stimulation was also decreased in

these rats. These results suggest that learning deficits in these animals are partly due to the impairment of neurotransmitter release.

McDonald et al. (223) observed that single bilateral hippocampal injections of A β 1-40 (2 nmol) impaired learning of a signaled footshock avoidance and a food reinforcing task in a Y-maze, suggesting a detrimental effect of A β on memory consolidation. Chronic daily A β 1-40 injections (0.5 nmol/day) for 26 days had no effects on an eight-arm radial maze performance, and no aggregation of A β or significant necrosis was observed upon postmortem histological analysis. These experiments suggest that single injections of A β impair memory consolidation but repeated injections do not affect well-learned behavior. In a follow-up study (224), these authors sought to determine if the amnesia was specific to the A β 1-40 sequence, and if the amnesia could be attributed to a consolidation process. The results indicate that the reverse peptide A β 40-1 has no behavioral effect, and that A β 1-40 injected after partial training does not interfere with a consolidation process.

Cleary et al. (41) showed that acute bilateral hippocampal A β 1-40 (1-3 nmol) administrations 20 min before testing did not alter the behavior of rats performing under stable food-maintained schedules of reinforcement or under a delayed conditional discrimination procedure. Also, no behavioral changes were observed during chronic 15 days A β 1-40 (1 nmol/day) injections but lever-pressing performance declined significantly 30 days after termination of the chronic daily regimen. Thioflavin S positive staining, indicating the presence of A β deposits, was observed in 3 of 6 rats in and around the area of cannula termination approximately 60 days after the last A β 1-40 injection.

Giovannelli et al. (102) demonstrated that unilateral injections of A β 1-40 (2.3 nmol) and A β 25-35 (9.4 nmol) into the right nucleus basalis of rats resulted in Congo red positive A β deposits at the injection site. These deposits were visible for about 21 days in the A β 25-35 treated rats and for at least two months in the A β 1-40 injected rats. The presence of these deposits was associated with a reduction in the number of ChAT immunopositive

neurons in the A β 25-35 rats at 7 and 14 days postoperatively, and in the A β 1-40 rats at 7, 14, 21, 30 and 60 days postinjection. This reduction in ChAT IR was paralleled by a decrease in basal acetylcholine release from the parietal cortex ipsilateral to the lesion. Disruption of object recognition was observed at 7 and 14 days after A β 25-35 injection, whereas A β 1-40 caused a slight impairment only two months after lesion.

In addition to injections of A β alone, a report by Dornan et al. (65) indicated that bilateral injections of 4 nmol of A β 25-35 and 6 nmol of ibotenic acid into the rat hippocampus disrupted acquisition of spatial learning in the radial arm maze 8-32 days postinjection, whereas A β 25-35 alone had no effect. Histological examination revealed that only the combination of A β 25-35 with ibotenic acid produced a lesion along with focal deposits in the hippocampus.

We observed that A β 25-35 (1 or 8 nmol) injected bilaterally into the ventral pallidum/substantia innominata (VP/SI) of rats failed to produce behavioral, histological or neurochemical signs of toxicity (314). Also, neither dose of A β 25-35 potentiated the effects of quinolinic acid (37.5 nmol) on behavior or amygdaloid ChAT activity, and did not appear to increase the histological damage caused by quinolinic acid. These results suggest that A β 25-35 is not neurotoxic within the VP/SI and that it does not potentiate the neurotoxicity of quinolinic acid in the VP/SI.

All the above studies analyzed young animals and injected peptide sequences that correlate with the human A β . In one study by Winkler et al. (354), a rat A β 1-42 was injected bilaterally into the hippocampus or the lateral ventricle of 3 month old rats. Fifteen months later, these rats did not differ from vehicle treated rats in their ability to learn a spatial memory task in the Morris water maze. A β IR was detected at the injection site at 16 months following injection but no qualitative neuronal loss was observed.

In addition to these findings, behavioral effects have also been demonstrated for amylin, which is a 37 amino acid amyloidogenic peptide of a different sequence than A β .

Kovacs et al. (175) observed that a unilateral administration of amylin (64-255 pmol) into the lateral brain ventricle of rats led to an increase in the latency of passive avoidance behavior, and caused facilitation of the extinction of active avoidance behavior 24 h postinjection. Amylin also inhibited locomotion in an open field, and increased rearing and grooming activity during the first 24 h postinjection. According to the authors, these findings suggest that amylin influences the behavioral reaction in these paradigms mainly by acting on locomotion, and not by modifying learning and memory processes.

Tau Protein

The main component of neurofibrillary tangles is paired helical filaments (168,335), which consist largely of the protein tau in an abnormal state of phosphorylation (171,183,355,356). Tau consists of six isoforms of a molecular weight of 55 to 62kD that are generated by alternative splicing of a single gene (106,140). Tau is a potent promoter of tubulin assembly *in vitro* (43), and is often associated with microtubules in neuronal axons. However, it is also found normally in the somatodendritic compartments and in glia (201,232,259). In AD, neurofibrillary tangles are found predominantly in the perinuclear region encircling the nucleus (231), but prominent tau IR fibers without classical tangle formation are also found in cell bodies of affected neurons (259). There is a correlation between the number of cortical tangles and the degree of cognitive impairment (17,289), and it has been reported that tangles, but not senile plaques, parallel duration and severity of AD (8). Tau isolated from paired helical filaments is extensively phosphorylated compared to normal tau but there has also been isolated from AD brain abnormally phosphorylated non-paired helical filament tau (173). Presently, the kinases that mediate tau phosphorylation have not been conclusively identified but various kinases have been

implicated (67,151,152,194,260,341,345). There may also be alterations in the activities of certain protein phosphatases in AD (111,185,215,266), that have been shown to dephosphorylate tau *in vitro* (66,109,110,112,294,343). It should be noted, however, that the significance of the hyperphosphorylated state of tau to the etiology and progression of AD remains to be determined. Interestingly, intracerebral injection of abnormally phosphorylated tau proteins purified from AD brains has been shown to enhance A β IR in rat brain (312), suggesting an association between plaque and tangle formation in AD.

Various antibodies recognize tau proteins, such as tau-2 and Alz-50. The tau-2 antibody recognizes tau proteins in both the phosphorylated and non-phosphorylated form. This antibody does not discriminate between normal tau and hyperphosphorylated Alzheimer's tau in unfixed tissue, but recognizes only the Alzheimer's tau in fixed tissue (259). The Alz-50 antibody in immunocytochemical studies stains AD brain tissue (55), but its IR in normal brain tissue appears to depend on the method used (293). It demonstrates early changes in AD by recognizing abnormally phosphorylated tau protein (337).

Apolipoprotein E

The gene for ApoE is located on chromosome 19 and is the first known gene that confers susceptibility for the sporadic late-onset form of AD. The three major alleles of ApoE are E2, E3, and E4. An increased frequency of the ApoE4 allele is associated with late-onset AD (325), and leads to an increased number of amyloid plaques compared to AD cases that do not have this risk factor (280,299). Conversely, the ApoE2 allele decreases the risk of AD and delays disease onset (49,290). ApoE binds to soluble A β *in vitro* (326) and enhances fibrillogenesis in an isoform specific manner, with ApoE4 being more active than ApoE3 (205,296,359). These *in vitro* studies correlate with findings that ApoE is

associated with amyloid plaques (245,246,280,360). ApoE is found in the neuronal cytoplasm (125) and is also associated with neurofibrillary tangles in AD (245,280). It binds to nonphosphorylated tau *in vitro*, and ApoE3 binds with higher affinity than ApoE4 (324).

Presenilins

Mutations in three genes account for a portion of cases of the early-onset familial form of AD. The first of these genes to be associated with AD was the gene for APP on chromosome 21. However, mutations in this gene account only for a small fraction of the early-onset AD cases. The most common mutations are found on chromosome 14 (297,322), in a gene that encodes the protein presenilin 1 (310). This protein appears to be an integral membrane protein containing seven to nine transmembrane domains. A second transmembrane protein, presenilin 2, is 67% homologous in amino acid sequence to presenilin 1. The gene coding for presenilin 2 is found on chromosome 1 and is the likely genetic locus of familial AD in Volga German families (192,193). More than 25 different inherited mutations have been identified in these two presenilin genes (344). The functions of the proteins encoded by the presenilins are unknown but they may be localized to the endoplasmic reticulum and Golgi complex in transfected cells (176). This finding suggests that the presenilins may affect protein transport and/or processing, possibly modulating the processing of APP and production of A β . In support of this scenario, a recent report indicates that levels of A β 1-42 and/or A β 1-43 are increased in fibroblast media and plasma from carriers of mutations in these genes (298). In addition, increased A β 1-42 and/or A β 1-43 levels are found in brains of mice that express mutant presenilin 1 (69). Overexpression of presenilin 2 in PC12 cells has been demonstrated to increase apoptosis

induced by trophic factor withdrawal or $A\beta$, and a presenilin 2 mutation associated with familial AD enhances basal apoptotic activity (362).

Glia in Alzheimer's Disease

More than half of the volume of the brain consists of non-neuronal cells (93). The largest class of these cells are comprised of neuroglia, and there are up to 10 times as many neuroglial cells in the brain as there are neurons. The neuroglia are further categorized as microglia or macroglia.

Macroglia: Astrocytes

The majority of the neuroglia are macroglia which are further subdivided into oligodendrocytes and astrocytes. Astrocytes modulate inflammatory and immune responses in the CNS, induce and help maintain the blood-brain-barrier, regulate the neuronal environment, and facilitate neuronal growth, repair and regeneration. The transformation of resting astrocytes to reactive astrocytes is one of the earliest and most dominant responses of the CNS to tissue injury. The reactive state is characterized by nuclear changes and a cytoplasmic enlargement that is associated with the generation of thicker, longer and more complex processes. In the AD brain, reactive astrocytes are found in high abundance surrounding senile plaques (70,126,128,250). They colocalize with plaques at a relatively early stage in AD and apparently prior to the appearance of plaque associated dystrophic neurites (270). Glial fibrillary acidic protein (GFAP) (77) is a component of the glial intermediate filaments that form part of the cytoskeleton, and is found predominantly in astrocytes. GFAP levels in AD brains are increased 8 to 16 fold compared to control brains (21,60).

There are several possible roles for astrocytes in AD. Reactive astrocytosis may occur merely as a response to an underlying pathology. Astrocytes may be recruited in an attempt to attenuate the progression of the disease and/or to enclose degenerating areas with astrogliotic scar. Astrocytes may also have a causal or contributory role in the pathology. In this scenario, the primary pathology may be astrocytic and lead to A β production and/or subsequent events that lead to neuritic damage and tangle formation. Also, A β may be toxic to astrocytes and that may indirectly lead to neuronal damage. Recent reports suggest that A β induces reactive astrocytosis *in vitro* (34,141,271), but does not decrease astrocyte viability (271).

Excitotoxicity has been hypothesized to have a role in the pathology of AD (114). Glutamate is the major excitatory neurotransmitter in the brain, and the distribution of plaques in AD correlates well with the termination of glutamatergic fibers (79,264,283). Both astrocytes and neurons are involved in glutamate transport and metabolism. Glutamate uptake is primarily performed by astrocytes, both in culture and *in vivo* (135,136,142,229). A β in some culture systems has been observed to potentiate neuronal excitotoxicity (170,218). This suggests that the glutamate transporting activity of astrocytes may be impaired by A β but no reports have investigated this phenomenon. However, A β has been shown to increase expression of glutamine synthetase (GS) in cultured astrocytes, suggesting that A β -related reactive astrocytosis in AD may benefit local neurons by enhancing glial capacity to regulate levels of glutamate (272). Conversely, A β has been reported to produce a mild but significant impairment in GS activity in mixed cultures (127). Whether GS levels and activity are affected in AD is unclear (164,319).

Microglia

Over the last decade several investigators have noted that the AD brain exhibits many classical markers of immune-mediated damage. Microglia are the brain's

representatives of the immune system and express many leukocyte surface antigens which are upregulated in AD (227). In AD, there is a vigorous activation of the classical, but not the alternative complement pathway (74,75,153,154,225,226). AD lesions are easily revealed by antibodies to complement factor (C) 1q, C3d, and C4d (225,226). All these antibodies recognize extracellular amyloid deposits, dystrophic neurites, neurophil threads, extracellular neurofibrillary tangles, and even some intraneuronal tangles. The components of the complement pathway may be partly derived from reactive microglia (123). It is not known what causes activation of the classical complement pathway in AD, but it is of interest that A β can bind C1q (304). This interaction activates the classical cascade *in vitro* (282), and enhances the cytotoxicity of A β (304), likely by increasing A β aggregation into a β -pleated sheet structure and by stabilizing preformed aggregates (348). In the AD brain, microglia are known to associate with plaques (122,155,228). Microglia in culture scavenge A β (5) and microglia-like phagocytes have a role in A β clearance following intraventricular infusions of A β (92). However, A β can induce degeneration of cultured microglia (174).

Cytokines are polypeptides with diverse actions on many cell types, and are particularly important as mediators of inflammation and regulation of cell growth and differentiation. The cytokines are generally classified into four groups; the interleukins, tumor necrosis factors, interferons, and growth factors. Inflammatory cytokines found in senile plaque regions include interleukin (IL) 1, IL-6, and tumor necrosis factor (62,117,309). Microglia seems to be the major source of IL-1 within the CNS, but this cytokine is also found in astrocytes and neurons (300). In rat, mouse, human and other species, IL-1 exists in two forms, IL-1 α (199) and IL-1 β (9), that are the products of two separate genes (40,97). Human IL-1 α and IL-1 β have 25% homology and appear to have a similar biological activity (63). IL-1 β *in vitro* stimulates the APP promoter (64), induces APP mRNA (59,89,108), stimulates APPs secretion (31), and enhances A β cytotoxicity in PC12

cells (82). $A\beta$ *in vitro* induces IL-1 β mRNA in astroglial cells (59), enhances astro- and microglial secretion of IL-1 (4), and stimulates the proliferation and morphological transformation of microglia (4). $A\beta$ also increases nitric oxide production from microglial cells in culture but not from astrocytes or cortical neurons. This production is potentiated by the cytokine interferon- γ and leads to an injury of cortical neurons (149). Furthermore, the synergistic activation of cultured microglia by $A\beta$ and interferon- γ causes the production of neurotoxic free radicals (230).

Distribution of Alzheimer's Disease Pathology

Individuals with Down's syndrome (trisomy 21) invariably develop the neuropathological hallmarks of AD (23,187). Therefore, it is likely that the sequence of pathogenic alterations in Down's syndrome resembles that of AD. Overexpression of APP mRNA has been observed in Down's syndrome brains (248,291), and senile plaques appear at a younger age than do neurofibrillary tangles in Down's syndrome (100,212,291,358), suggesting that $A\beta$ may have a role in tangle formation. In AD, the distribution of plaques and tangles suggests that neurons that have efferent projections to areas that contain amyloid deposits often contain tangles (265). For example, senile plaques accumulate within the amygdala in the terminal zone of tangle bearing hippocampal neurons (181). This suggests that $A\beta$ may act on nerve terminals to cause cytoskeletal alterations in axons that ultimately lead to tangle formation within the perikarya (265). This notion is supported by the observation that the APP is predominantly located in the synaptic zone of neurons (301). Therefore, deposition of $A\beta$ fibrils and their initial toxic effects would primarily occur near their site of generation, namely at the nerve terminals. These effects then would gradually spread to distal brain regions that send axons to the area of initial deposition.

However, there are areas severely affected by neurofibrillary tangles whose projection zone is not frequently affected by senile plaques (279). For example, subicular/CA1 hippocampal neurons develop tangles and project strongly to layer IV of the entorhinal cortex, which contains tangles but few senile plaques (147). The pathological process in AD occurs over decades. It is possible that different regions and/or cell types of the brain have different kinetics for the development and/or degradation of neurofibrillary tangles and senile plaques.

The major pathological changes in AD are in regions of the medial temporal lobe, including the hippocampus, amygdala, entorhinal cortex and parahippocampal gyrus (265). Within these brain regions, the number of senile plaques has been reported to be highest in the amygdala (8). Some reports indicate that the amygdala is affected earlier in the disease than the hippocampal or cortical areas (158,258). Severe ChAT deficits have been reported in the amygdala in cases of histopathologically confirmed AD with no significant deficits in the neocortex or hippocampus (258). Also, in at least one AD case report, senile plaques and neurofibrillary tangles were almost exclusively restricted to the amygdala (158). The presence of numerous senile plaques without neurofibrillary tangles in the amygdala of a 19 year old patient with Down's syndrome suggests that the amygdala is a focus of early pathological changes in Down's syndrome and possibly AD (243). In patients with Down's syndrome between the ages of 35-45, many classic senile plaques are found in the amygdala but neocortical senile plaques are sparse and usually primitive, and neurofibrillary tangles are rare (208-210). A study (211) of non-demented patients of all ages showed the greatest severity of senile plaques primarily within the amygdala, whereas neurofibrillary tangles were found predominantly within the hippocampus.

Laterality in Alzheimer's Disease

The human brain is asymmetric, as are the brains of other animals. Although the left hemisphere is significantly different in function from the right, there appears to be no structure or chemical constituent that is present in one hemisphere but not in the other. However, there are quantitative differences between the hemispheres that may lead to qualitative differences. Asymmetry has been observed in neurotransmitter, neuroendocrine, and neuroimmunologic activity (361).

Some investigators have demonstrated lateralization in the involvement of the rat amygdala in learning and memory (15,45-47), and lesions of various brain regions in rats (36,61,121,184,262,281,329,342) and mice (10) have asymmetrical effects. Ligation of the right middle cerebral artery has been shown to lead to hyperactivity and reductions in norepinephrine and dopamine, whereas ligation of the left middle cerebral artery has no behavioral or neurochemical effects (281). Also, occlusion of the left or right middle cerebral artery has different effects on mean arterial pressure, renal sympathetic nerve discharge, and plasma norepinephrine levels (121). Suction lesions of the right frontal cerebral cortex induce hyperactivity (61,262), that is accompanied by a bilateral decrease in norepinephrine concentrations (262). However, identical lesions of the left cortex do not produce hyperactivity (61,262) or a decrease in norepinephrine concentrations (262). Left cortical ablations affect mainly the activity of serotonergic inputs to the right neocortex, whereas ablations of the right cortex influence the activity of the catecholaminergic inputs to the left cortex (10). Ablations of the prefrontal or parietal cortices lead to lateralized brain immunomodulation (342). Kainic acid injections into the right frontal cortex produce a significantly greater hyperactivity than identical injections into the left hemisphere (184). Striatal lesions with 6-hydroxydopamine lead to greater dopamine depletion in right-lesioned rats than in left-lesioned rats (329). Also, left and right 6-hydroxydopamine lesions of the

medial prefrontal cortex differentially alter subcortical dopamine utilization and the behavioral response to stress (36).

Asymmetries have been observed in the histopathological hallmarks (52,235), and in the reductions in ChAT activity (235,287) in individual cases of AD, but preferential involvement of either hemisphere has not been demonstrated in groups of AD patients. Interestingly, asymmetry in the density of senile plaques diminishes with increasing neuropathological severity (235), suggesting that laterality may be more prominent in the initial stages of the disease. In AD, there is an extensive neuronal loss and shrinkage in all subdivisions of the amygdala (340), but no left-right hemispheric differences were detected in total neuron numbers in a study of 9 AD cases (340). However, hemispheric laterality in cerebral metabolism and perfusion in AD has been demonstrated in several studies. In most of these reports, there is no directional preference in asymmetry (37,68,95,113,129-132,254), whereas some findings indicate preferential involvement of the left (197,306) or the right hemisphere (239). Early onset cases of AD have been associated with a greater prevalence of left (247,306) or right (148) hemispheric dysfunction compared to late onset AD cases. Other studies have found no correlation between asymmetry in hemispheric dysfunction and the duration or severity of the illness (197,239), suggesting that laterality in AD reflects subtypes more than the evolution of the disease.

Animal Models for Alzheimer's Disease

There is a loss of cholinergic neurons in the basal forebrain in AD, that contributes to the amnesic deficits observed in the disease (12,57,351). The early animal models of AD attempted to mimic the degeneration of the basal forebrain cholinergic neurons by lesioning the nucleus basalis magnocellularis (84,134,195) and/or the medial septal area

(134). This approach was limited as a model of AD because it lacked the broad spectrum of pathological features of the disease. Neurons producing norepinephrine, serotonin, dopamine, glutamate, γ -aminobutyric acid, somatostatin, neuropeptide Y, corticotrophin releasing factor, substance P, and other neuromodulators are also affected in AD (54,56,157,177,288,327). Because of these broad deficits in neurotransmitter systems, it is unlikely that AD can be treated by transmitter replacement therapy alone. A more feasible approach is to develop compounds that interfere with neuritic plaque and tangle formation, the major histopathological hallmarks of the disease.

The discovery of $A\beta$ as a major component of senile plaques and subsequent findings of its *in vitro* neurotoxicity led to model approaches examining the direct effects of $A\beta$ *in vivo* by microinjection of $A\beta$ into the brains of rats and monkeys (see $A\beta$ Peptides and Effects of $A\beta$ Peptides on Behavior). The reproducibility of $A\beta$ toxicity *in vivo* has been inconsistent (42,91,99,101,102,178,180,314,320,354). This may be due to variations in: 1) the conformational state (25,269,273), dose, and sequence of $A\beta$; 2) method of administration; 3) pathological endpoints measured; 4) what brain region and/or hemisphere is injected; 5) postoperative interval; and, 6) species and/or strain used. Therefore, further studies on the *in vivo* effects of $A\beta$ are warranted.

Various transgenic approaches toward an animal model for AD have recently been described. The approaches differ in several aspects such as: 1) in the selection of a promoter to drive APP expression; 2) in the isoform or segment of APP expressed; 3) in the strain of mouse used; and, 4) in the age of the animals at the time of behavioral testing and/or histological analysis.

$A\beta$ Transgene: Overexpression of mouse $A\beta$ in mice by LaFerla et al. (186) resulted in extensive neuronal apoptotic degeneration and reactive astrogliosis without any evidence of amyloid deposition or neurofibrillary pathology. The mouse $A\beta$ was selected in case an

interaction with species specific factors was required for its toxicity. These animals had approximately half the lifespan of normal mice and some of them developed seizures.

APP Transgenes: Approaches using full length mouse or human APP can be divided into three groups: 1) expression of normal individual APP isoforms; 2) expression of individual or several APP isoforms that carry mutations that have been associated with AD; and, 3) generation of mice transgenic for the intact APP gene.

The initial report on behavioral impairments in transgenic APP mice by Yamaguchi et al. (364) demonstrated that mice expressing the normal human APP695 isoform had impaired spatial memory in the Morris water maze. Training commenced when the mice were 8 weeks old and behavioral testing continued until the animals were 20 weeks old at which time they were sacrificed for histological analysis. These animals were significantly retarded in initial learning and in learning a new escape location, but they eventually reached control levels. However, these mice also had slower swimming speed and reduced nocturnal activity, that may have contributed to their deficit in spatial learning. No A β deposits were observed in these mice, and no neuropathological hallmarks of AD have been detected in this same transgenic line at 1-3 years of age. The authors suggest that gene dosage effect of APP695 may account for the memory impairment. The authors also raise the question of whether insertion of multiple copies of any gene construct may impair cognitive function, because inheritance of relatively small amounts of extra genomic DNA in human imbalanced translocation karyotypes results in mental retardation.

Czech et al. (53) showed that transgenic mice containing the three major neuronal isoforms for the normal human APP, that is APP695, APP751, and APP770, expressed the transgenic APP in several tissues including brain but expression levels never exceeded those of the endogenous mouse APP (53). No pathological changes resembling those of AD and Down's syndrome were observed in these animals. However, the mice transgenic for APP695 showed an impairment in a spatial navigation task, and the mice transgenic for

APP751 showed deficits in motor performance. The authors of this study stress that it is not clear whether these behavioral effects are due to the expression of the transgene or to position effect of transgene integration.

Hsiao et al. (146) demonstrated that transgenic mice overexpressing normal human or mouse APP695 died usually within a year and developed a CNS disorder that included neophobia and impaired spatial alternation, with diminished glucose utilization and astrogliosis mainly in the cerebrum. Human APP transgenes induced death much earlier than mouse APP transgenes expressed at similar levels. No extracellular amyloid was detected, indicating that some deleterious processes related to APP overexpression are dissociated from formation of amyloid.

Transgenic mice expressing normal human APP751 have been shown by Higgins et al. (137,138) and Quon et al. (277) to develop diffuse A β deposits and rarely an induction in Alz-50 IR, particularly in the hippocampus, cortex, and amygdala. The A β deposits were not Congo red positive and lacked neuritic involvement. Because the deposits did not show birefringence under polarized light when stained with Congo red, they did not have the β -pleated sheet structure of A β that is found in senile plaques. These histopathological changes increased somewhat in frequency with aging (139). These mice also exhibited age dependent deficits in spatial learning in a water maze task and in working memory in spontaneous alternation in a Y maze (236). Interestingly, these transgenic mice also exhibited a greater latency in locating a visible platform in the water maze. This suggests that vision impairment may account for differences in performance. These deficits were mild or absent in 6 month old mice but were severe in 12 month old mice compared to age-matched wild-type control mice. Neither age group of the transgenic APP751 mice showed any changes in string test, rotarod, plus maze, or circadian variation in spontaneous activity. These findings show that these mice did not have any gross motor, physiological or behavioral impairments that may have confounded interpretation of the learning tasks.

These mice may model the progressive learning and memory impairment that is a cardinal feature of AD, but further tests are necessary to investigate possible vision impairments.

The discovery of the association of AD with inherited APP mutations led to the development of transgenic mouse models containing these mutations. Malherbe et al. (206) reported that transgenic mice expressing various familial AD missense mutations, that were maximally 1.3 fold of those of wild-type mouse APP, showed no AD-like pathology and had no behavioral impairments. However, recently two mouse models have been described by Games et al. (98) and Hsiao et al. (145), that contained age dependent compact congophilic A β plaques similar to those observed in AD, and in one of these models these changes were associated with behavioral impairments (145). The first of these models to be described overexpressed APP containing the APP717 mutation that is associated with familial AD (98). These mice expressed 8-10 fold the normal level of APP and had large numbers of amyloid plaques in the hippocampus, corpus callosum, and cerebral cortex that first appeared at 6-9 months of age. The majority of the plaques were associated with reactive astrocytes and dystrophic neurites. The neocortices of these mice exhibited diffuse synaptic and dendritic loss, and contained diffusely activated microglia. This histopathology was region specific and age dependent as in AD, despite expression of the APP transgene throughout the brain. These results suggest that region and/or cell type specific vulnerability of the aging brain may dictate the pattern of plaque formation. A significant limitation of this model is the lack of neurofibrillary tangles, and their absence may reflect species variations in neuronal response to injury. Also, in this model there have been no reports of behavioral impairments associated with the histopathological changes.

The other promising transgenic mouse model (145) overexpressed a mutated form of APP695, that has been found in a Swedish family with early-onset AD (242). These mice expressed this human form at 5-6 fold the levels of endogenous mouse APP, that remained unchanged between 2 and 14 months of age. These mice demonstrated normal learning

and memory in the Morris water maze and the Y maze at 3 months of age but were impaired by 9 to 10 months of age. A five fold increase in A β 1-40 and a 14 fold increase in A β 1-42 was associated with these behavioral deficits. Numerous Congo red positive A β plaques were present in mice with elevated A β levels. The distribution of the histopathological changes was reportedly similar to that observed by Games et al. (98). Although the authors indirectly control for impairments in motor performance, it is possible that the behavioral impairments may be caused by visual impairments. This possibility, overlooked by the investigators, is based on the impairment of the transgenic mice in swimming to a visible platform.

In contrast to other APP transgenic models, the expression of human APP variants in these two promising models (98,145) substantially exceeds those of the endogenous mouse APP gene. Because of the various proposed roles for APP, it is likely that 5-10 fold increase in APP has several biological effects besides causing an increase in A β production and subsequent plaque formation. It is also possible that insertion of multiple copies of any gene construct may impair cognitive function, because inheritance of relatively small amounts of extra genomic DNA in human imbalanced translocation karyotypes results in mental retardation. The behavioral effects may also be due to position effect of transgene integration that may interfere with the expression of other genes.

The complete human APP gene has also recently been introduced into mice by Lamb et al. (188) and Pearson et al. (263). Both sets of mice properly spliced human APP mRNA in their brains to generate the three major isoforms of APP, APP695, APP751, and APP770, but in hemizygotes their expression levels were below those of the endogenous mouse APP. No signs of AD-type pathology has been observed (188) or reported (263) in these mice. These mice may overexpress human APP once they have been bred to homozygosity.

Even though several *in vitro* studies have tested various hypotheses for the mechanism by which A β exerts its toxic effect, these hypotheses have not been adequately

assessed in *in vivo* situations. It is important to continue to explore the *in vivo* effects of A β by direct injections into brain. Findings from these studies may help elucidate the sequence of pathogenic events that ultimately lead to AD. They may also distinguish between the biological effects of A β and elevated levels of APP, respectively. There are several advantages associated with the injection approach. For example, it is substantially less expensive. The pathology appears to peak at an earlier timepoint than in transgenic animals, thereby reducing the time required for drug screening. Furthermore, the pathology is due to A β , but in the transgenic animals some of the pathology may be due to effects of elevated levels of APP and/or due to position effect of transgene integration. For example, the site of transgene integration is thought to be random and its location may affect the expression of other genes. Therefore, injection models may give a clearer picture than transgenic models of the role of A β in the progression of AD.

CHAPTER II

AIMS OF THE PRESENT STUDY

Purpose

Because the early and primary histopathological changes in Alzheimer's disease (AD) are predominantly found in temporal lobe structures, it was determined if injections of amyloid- β ($A\beta$) 25-35 into the amygdala of the rat can induce the appearance of abnormal conformations of tau proteins and reactive astrocytes as seen in AD. It also was examined whether the effects of $A\beta$ were time dependent and included neuronal shrinkage, cell loss and/or microglial activation. Finally, it was determined whether the histological effects of $A\beta$ were associated with alterations in choline acetyltransferase (ChAT) activity and/or behavioral changes. Thus, the overall objective of this project was to develop an animal model for AD.

Overall Hypothesis: *In vivo* injections of $A\beta$ will induce the appearance of abnormal conformations of tau proteins and reactive astrocytes as seen in AD. The effects of $A\beta$ will be time dependent and include neuronal shrinkage, neuronal loss and microglial activation. Furthermore, these histological changes will be associated with neurochemical and behavioral alterations.

Specific Aim 1: To determine the histological effects of unilateral intra-amygdaloid injections of $A\beta$ 25-35 (5.0 nmol) in young rats at 8 and 32 days postoperatively.

Hypothesis: A β will induce conformational changes in tau proteins. These changes will be associated with reactive astrocytosis, neuronal shrinkage and cell loss.

Methods: Cresyl violet, tau-2, Alz-50 and GFAP staining

Rationale:

The histopathological characteristics of AD include neurofibrillary tangles, senile plaques, reactive astrocytes, neuronal shrinkage, and cell loss in several brain regions. The main component of the neurofibrillary tangles is paired helical filaments (168,335), which consist largely of the microtubule associated protein tau in an abnormal state of phosphorylation (171,183,355,356). In the AD brain, reactive astrocytes are associated with senile plaques (70,126,128,250). Senile plaques consist predominantly of A β 1-42 peptide (103,214,233,285), which is derived from a large membrane spanning protein, the amyloid- β precursor protein (APP) (166). Mutations in APP in some forms of familial AD are associated with an elevated production of A β (33,39,331). APP is overexpressed in Down's syndrome (248,291), and individuals with this disease invariably develop the neuropathological hallmarks of AD (23,187). The proposed role for A β in the pathogenesis of AD is further supported by the neurotoxicity of A β *in vitro* (369,370), which includes amino acids 25-35 of the peptide (370).

The reproducibility of A β toxicity *in vivo* has been inconsistent (42,91,99,101,102,178,180,314,320,354). This may be due to variations in: 1) the conformational state (25,269,273), dose, and sequence of A β ; 2) method of administration; 3) pathological endpoints measured; 4) what brain region and/or hemisphere is injected; 5) postoperative interval; and, 6) species and/or strain used. Therefore, further studies on the *in vivo* effects of A β are warranted.

Recently a direct association between plaque and tangle formation in AD has been demonstrated by a few studies. *In vitro* studies have demonstrated that A β increases tau protein kinase I (TPK I) activity (332), induces abnormal tau immunoreactivity (IR) (26,207), and that the neuronal death caused by A β can be prevented with TPK I antisense oligonucleotides (332). These findings suggest an association between plaque and tangle formation in AD. A few *in vivo* studies have investigated the effects of A β injected into the central nervous system on tau IR (42,91,99,178,180,274). Some of these studies indicate that A β can induce the appearance of abnormal tau proteins in the vicinity of the injection site (rat cerebral cortex and hippocampus) (91,178,180). Other studies have failed to show any effect (42,99,274). For the most part, these *in vivo* studies have only been qualitative or descriptive in nature. No attempts have been made to quantify A β induced effects by counting neuronal tau IR cells.

A β has been shown to increase intracellular calcium (7,218). Calcium influx in cultured rat hippocampal neurons caused by glutamate or a calcium ionophore induces tau IR as recognized by the antibodies Alz-50 and 5E2 (216). Protein kinases are generally activated by increases in intracellular calcium and several of those have been shown to phosphorylate different sites on tau proteins (238). Therefore, A β may increase the phosphorylation of tau proteins through an activation of kinases mediated by an increase in intracellular calcium. The activities of some phosphatases that may dephosphorylate tau proteins have been shown to be decreased in AD (111,311). Therefore, A β 25-35 may also be decreasing the dephosphorylation of tau proteins through an inhibition of phosphatases.

Because of the proposed role for A β in the pathogenesis of AD, intracerebral injections of A β may induce the pathological changes that occur in AD. It can be argued that because A β 1-42 is the most prevalent form of A β in senile plaques, it is appropriate to use that peptide for injections into brain instead of A β 25-35. However, the main problem with using A β 1-42 is its insolubility in physiological solvents. Therefore, there is a risk of

potentially toxic solvents interfering with the properties and effects of A β 1-42. On the other hand, A β 25-35 is readily soluble in H₂O and acquires the same β -pleated sheet conformation as A β 1-42, which is the toxic conformation of A β .

The amygdala was chosen as a region for A β injections because it may be affected earlier in AD than hippocampal or cortical areas (158,258). The major pathological changes in AD are in regions of the medial temporal lobe, including the hippocampus, amygdala, entorhinal cortex and parahippocampal gyrus (265). Within these brain regions, the number of senile plaques has been reported to be highest in the amygdala (8). Individuals with Down's syndrome invariably develop the neuropathological hallmarks of AD (23,187). The presence of numerous senile plaques without neurofibrillary tangles in the amygdala of a 19 year old patient with Down's syndrome suggests that the amygdala is a focus of early pathological changes in Down's syndrome and possibly AD (243). In patients with Down's syndrome between the ages of 35-45 many classic senile plaques are found in the amygdala but neocortical senile plaques are sparse and usually primitive, and neurofibrillary tangles are rare (208-210). There have been no previous reports on *in vivo* injections of A β into the amygdala.

Unilateral injections were employed to determine if A β induces histopathological alterations both ipsi- and contralaterally. The time of sacrifice (8 and 32 days) and the dose of A β (5.0 nmol) were chosen because preliminary results in our laboratory indicated that these parameters were associated with tau IR adjacent to the injection site in the median raphe nucleus. Neuronal shrinkage and neuronal loss are one of the hallmarks of AD. Cresyl violet staining was used in the present study to observe these histological changes. The tau-2 antibody reacts exclusively with tau proteins in both the phosphorylated and non-phosphorylated form. This antibody does not discriminate between normal tau and hyperphosphorylated Alzheimer's tau in unfixed tissue, but recognizes only the Alzheimer's tau in fixed tissue (259), and was therefore used in the present experiment. The Alz-50

antibody was also used to detect AD-like tau proteins. Alz-50 stains AD brain tissue (55), but its IR in normal brain appears to depend on the method used (293). It demonstrates early changes in AD by recognizing abnormally phosphorylated tau protein (337). Although the epitope that Alz-50 recognizes may not be phosphorylated, the overall peptide conformation recognized by the antibody may be phosphorylation dependent (105,182,337).

Using one antibody that recognizes abnormal tau proteins is not sufficient to determine if A β can induce the appearance of AD-like tau proteins. The temporal sequence leading to abnormal phosphorylation and/or conformational changes in tau proteins is not known. It is possible that A β may be inducing early changes in tau proteins that are not detected by both the tau-2 and Alz-50 antibodies. These two antibodies recognize different conformation dependent epitopes on tau proteins. A β may be inducing multiple conformational changes in tau proteins, which are differently stained using these two antibodies. The nature and extent of these conformational changes may be time dependent, brain region specific, and differ within the neuronal structure.

GFAP (77) is a component of the glial intermediate filaments that form part of the cytoskeleton, and is found predominantly in astrocytes. GFAP levels in AD brain are increased 8 to 16 fold compared to control brains (21,60). Staining with an antibody against GFAP was performed to determine 1) if A β increases the appearance of reactive astrocytes, as seen surrounding senile plaques in AD, and 2) if there appears to be a correlation between the location and severity of tau-2 and GFAP IR.

Specific Aim 2: To determine the histological effects of bilateral intra-amygdaloid injections of A β at 8, 32, 64, 96 and 128 days postoperatively.

Hypotheses: 1) The histological effects of A β will increase with time; and, 2) will be potentiated by bilateral administration due to the inability of the intact side to compensate for the contralateral insult.

Methods: Cresyl violet, Congo red, tau-2, GFAP and IL-1 β staining.

Rationale:

The overall objective of this project was to develop an animal model for AD. Therefore, it was necessary to know how long the effects of A β lasted to prepare for screening of drugs that prevent, reduce or reverse the histopathological effects of A β . AD is a bilateral disorder and bilateral infusions are required to determine if the effects of A β are exponential and for behavioral analyses. To prepare for behavioral experiments, it was necessary to perform a time course study on the histological effects of A β . The detrimental effects had to last throughout the behavioral experiments, which typically are performed 4-6 weeks postoperatively. Congo red staining was performed to determine if the A β deposits within the rat amygdala were of the β -pleated sheet structure that is observed in senile plaques in AD. Microglia appear to be the major source of IL-1 within the CNS (300). In the AD brain, microglia are known to associate with plaques (122,155,228), and inflammatory cytokines found in senile plaque regions include IL-1 β (62). Thus, staining was performed on brain sections with an IL-1 β antibody to determine if the intra-amygdaloid A β deposits were associated with microglia.

Specific Aim 3: To determine if bilateral intra-amygdaloid injections of A β affect ChAT activity within the amygdala at 32 days postoperatively.

Hypothesis: A β injected into the amygdala reduces ChAT activity within the amygdala.

Methods: Measurements of ChAT activity.

Rationale:

The amygdala receives a prominent cholinergic input from the nucleus basalis (35,363), and ChAT activity has been reported to be severely reduced within the amygdala in AD patients (258,287,288). Measurements of amygdaloid ChAT activity were performed to investigate if the cytoskeletal changes and neuronal shrinkage within the amygdala were associated with a reduction in ChAT activity. The time of sacrifice was based on the results of the time course study that indicated that the histological effects of A β peak at 32 days postoperatively. Although neuronal loss may not be severe following intra-amygdaloid injections of A β , this compound may affect the metabolic integrity of cholinergic neurons projecting to the amygdala. The neurochemical changes in AD that best correlate with the severity of dementia are reductions in ChAT activity in temporal lobe structures (268). Thus, ChAT activity was measured within the amygdala.

Specific Aim 4: To determine if bilateral intra-amygdaloid injections of A β cause behavioral changes that may simulate those observed in AD.

Hypothesis: Bilateral intra-amygdaloid injections of A β will cause behavioral changes at 34-52 days postoperatively, that may simulate those observed in AD.

Methods: Open field, one-way active avoidance and Morris water maze.

Rationale:

Electrolytic lesions of the amygdaloid complex (51,73,163,305), lesions of the central nucleus (118,160,350), or of the lateral and basal nuclei of the amygdala (159) enhance exploratory behavior of rats in the open field test. Furthermore, lesions of the amygdala have been shown to be associated with behavioral impairments in active avoidance learning (30,286), but do not appear to impair spatial learning in the Morris water maze (58,330). Lesions of the hippocampus severely disrupt spatial learning (257,278), and this impairment has been shown to be potentiated by amygdaloid lesions (1,267). Therefore, because intra-amygdaloid injections of A β induced histopathological changes not only within the amygdala but also within the hippocampus, it was considered appropriate to use the water maze test. The time interval for behavioral testing (34-52 days postoperatively) was based on the severity of the histological effects observed in the time course study.

CHAPTER III

LOCAL AND DISTANT HISTOPATHOLOGICAL EFFECTS OF UNILATERAL INJECTIONS OF AMYLOID- β 25-35 INTO THE AMYGDALA OF YOUNG MALE FISCHER RATS

Abstract

To determine if amyloid- β (A β) induces tau-immunoreactivity (IR) and reactive astrocytosis *in vivo*, we injected A β 25-35 (5.0 nmol) into the right amygdala of rats. At 8 days postinjection, the peptide induced tau-2 IR in neuronal cell bodies and processes ipsilaterally in the amygdala, cingulate cortex and hippocampus. At 32 days postinjection, the intensity of tau-2 IR was greater than at 8 days in the amygdala and hippocampus, but not in the cingulate cortex. Induction of Alz-50 IR also was progressive but the morphology and distribution was different from tau-2 IR. Beaded fibers with occasional neuronal perikarya were visualized with Alz-50, and the IR was primarily observed in the ipsilateral amygdala. In addition, amygdaloid injections of A β 25-35 induced reactive astrocytosis, particularly in the ipsilateral hippocampus at 32 days postoperatively.

To our knowledge, this is the first study to show that *in vivo* injections of A β 25-35 induce progressive transsynaptic cytoskeletal and astrogliotic reactions, that gradually spread from the area of injection to brain regions that have prominent efferent connections with the injected area. These findings also suggest a direct association between plaque and tangle formation in Alzheimer's disease.

Introduction

Alzheimer's disease (AD) is characterized histopathologically by amyloid deposition (senile plaques), neurofibrillary tangles and neuronal cell loss in several, but not all cortical and subcortical regions. The main component of senile plaques is the amyloid- β ($A\beta$) peptide (103,214,233,285). It is derived from a large transmembrane protein, the amyloid- β precursor protein (APP) (166) and is thought to play an important role in the pathogenesis of AD. Mutations in the APP gene on chromosome 21 are associated with a subpopulation of familial AD patients (104). The main component of neurofibrillary tangles is paired helical filaments (168,335), which consist largely of the microtubule associated protein tau in an abnormal state of phosphorylation (171,183,355,356).

In AD, the distribution of plaques and tangles within subcortical nuclei suggests that neurons that have efferent projections to areas that contain amyloid deposits often contain tangles (265). Therefore, since diffuse $A\beta$ deposition precedes the development of neurofibrillary pathology (179), it has been hypothesized that $A\beta$ acts on nerve terminals to cause cytoskeletal alterations in axons that ultimately lead to tangle formation within the perikarya (265). Individuals with Down's syndrome (trisomy 21) invariably develop a neuropathology indistinguishable from AD (23,187). Therefore, it is likely that the sequence of pathogenic alterations in Down's syndrome resembles that of AD. Researchers have noted that senile plaques appear at a younger age than do neurofibrillary tangles in Down's syndrome (100,212,291,358), suggesting that $A\beta$ may have a role in tangle formation.

In vitro studies indicate that $A\beta$ has neurotrophic (353,370) as well as neurotoxic (369,370) properties. The *in vitro* neurotoxic activity includes amino acids 25-35 of the peptide (370). The reproducibility of $A\beta$ toxicity *in vivo* has been inconsistent (42,91,99,101,102,178,180,191,274,314,320,354). This may be due to variations in the conformational state of $A\beta$ (25,269,273), different biochemical and/or pathological

endpoints measured. *In vitro* studies have demonstrated that A β increases tau protein kinase I (TPK I) activity (332), induces abnormal tau immunoreactivity (IR) (26,207), and that the neuronal death caused by A β can be prevented with TPK I antisense oligonucleotides (332). There have been a few *in vivo* studies investigating the effects of A β injected into the central nervous system (CNS) on tau IR (42,91,99,178,180,274). Some of these studies indicate that A β can induce the appearance of abnormal tau proteins in the vicinity of the injection site (rat cerebral cortex and hippocampus) (91,178,180). Other studies have failed to show any effect (42,99,274). For the most part, these *in vivo* studies have only been qualitative or descriptive in nature regarding effects on tau IR. No attempts have been made to quantify A β induced effects by counting neuronal tau IR cells.

In the AD brain, reactive astrocytes are found in high abundance surrounding senile plaques (70,126,128,250). Glial fibrillary acidic protein (GFAP) is a component of the glial intermediate filaments that are found in the cytoplasm of astrocytes and form part of the cytoskeleton. GFAP levels in AD brains are increased 8 to 16 fold compared to control brains (21,60). A β has been shown to induce a reactive phenotype in cultured astrocytes but does not decrease astrocyte viability (271).

The major pathological changes in AD are in regions of the medial temporal lobe, including the hippocampus, amygdala, entorhinal cortex and parahippocampal gyrus (265). Some reports indicate that the amygdala is affected earlier in the disease than the hippocampal or cortical areas (158,258). Severe choline acetyltransferase (ChAT) deficits have been reported in the amygdala in cases of histopathologically confirmed AD with no significant deficits in the neocortex or hippocampus (258). Also, in at least one AD case report, senile plaques and neurofibrillary tangles were almost exclusively restricted to the amygdala (158). The presence of numerous senile plaques without neurofibrillary tangles in the amygdala of a 19 year old patient with Down's syndrome suggests that the amygdala is a focus of early pathological change in Down's syndrome and possibly AD (243). In

patients with Down's syndrome between the ages of 35-45 many classic senile plaques are found in the amygdala but neocortical senile plaques are sparse and usually primitive, and neurofibrillary tangles are rare (208-210). A study of non-demented patients of all ages showed the greatest severity of senile plaques primarily within the amygdala, whereas neurofibrillary tangles were found predominantly within the hippocampus (211).

Because the primary and early histopathological changes in AD are found primarily within temporal lobe structures, we determined if a unilateral A β 25-35 injection into the amygdala of the rat can induce the appearance of abnormal microtubule associated protein tau and reactive astrocytes as seen in AD. Secondly, we examined whether brain areas that project to and/or receive projections from the amygdala showed similar changes, and how long these effects last.

Materials and Methods

Animals

Male Fischer-344 rats were obtained from Harlan Sprague-Dawley Inc. (Indianapolis, IN). At the time of arrival, the rats weighed 250-300 g and were 3-4 months of age. The animals were housed individually, maintained on a 12 h light-dark cycle (lights on at 07:00 h) in a AAALAC approved facility, had access to food and water *ad libitum*, and were habituated to their new environment for 2-3 weeks prior to surgery.

Surgery

Surgery was performed under sodium pentobarbital (50 mg/kg, intraperitoneally (i.p.); Butler, Columbus, OH) anesthesia. Atropine sulfate (0.4 mg/kg; Sigma, St. Louis, MO) and ampicillin sodium salt (50 mg/kg; Sigma) were injected intramuscularly once the animals were anesthetized. The animals received a unilateral injection into the right amygdala. A Kopf stereotaxic instrument was used with the incisor bar set at 3.3 mm below the interaural line. Injection coordinates measured from bregma and the surface of the skull (AP - 3.0, ML - 4.6, DV - 8.8) were empirically determined based on the atlas of Paxinos and Watson (261). The anteroposterior (AP) coordinate was positioned where the amygdaloid structure is largest. The mediolateral (ML) coordinate was centered between the medial and lateral aspects of the amygdala (medial to the basolateral nucleus). The dorsoventral (DV) coordinate was centered between the dorsal and ventral aspects of the amygdala. A volume of 3.0 μ l was administered over 6 min (flow rate 0.5 μ l/min) using a CMA/100 microsyringe pump (Carnegie Medicin AD, Solna, Sweden). The cannula was left *in situ* for 2 min following injection, and then was slowly withdrawn. Following surgery the animals were placed on a heating pad until they regained their righting reflex.

Most of the previous studies which have injected A β into the brain have utilized a volume of 1.0 μ l or less. The choice of an appropriate volume must be based on the physiochemical properties of the substance, outside and within the brain. It has been reported that A β 25-35 at high concentrations (10 nmol/ μ l) forms a viscous gel (292), and may therefore adhere to the cannula resulting in an inaccurate dose delivery and spread of the peptide along the cannula track. In addition, A β 25-35 appears to aggregate at the site of injection and does not diffuse from the vicinity of the injection site. For these reasons, we deemed it appropriate to inject a larger volume (3.0 μ l).

Drugs

A β 25-35 and A β 35-25 (BACHEM, Torrance, CA) were supplied as a trifluoroacetic acid (TFA) salt with the peptide content 84.4 and 82.15 (\pm 3%), respectively. According to a representative at BACHEM there is no direct stoichiometric relationship between the content of A β 25-35 and TFA. In order to not underestimate the amount of TFA, we assumed that it was 15.6% of the weight of the salt. Therefore, there are approximately 2 nmol of TFA for each 1 nmol of A β 25-35. The peptide and its respective vehicle (VEH; TFA, sodium salt; Sigma) were dissolved in Nanopure[®] H₂O (H₂O) immediately before use and stored at 4[°]C between injections. The reverse peptide was handled in the same manner.

Animal Sacrifice and Tissue Preparation

Animals were anesthetized with sodium pentobarbital (100 mg/kg, i.p.) and perfused transaortically at 8 or 32 days postoperatively with 250 ml of 0.1 M sodium/potassium phosphate buffer (PB, pH 7.4), followed by 500 ml of 4% paraformaldehyde in PB at a rate of 500 ml/h at room temperature. Immediately after beginning the perfusion, 1.0 U/g heparin (Upjohn, Kalamazoo, MI) was administered transaortically. Following perfusion the

brain was placed in the buffered fixative with 20% sucrose for 1.0 h. The brain was then trimmed into a 6 mm block surrounding the injection site, and stored in a solution containing 20% sucrose, 0.1% sodium azide and 0.01% bacitracin in PB for 24 h at 4°C. The tissue block was then transferred to a solution containing 20% glycerol and 2% dimethyl sulfoxide dissolved in 0.1 M sodium phosphate buffer, and stored at 4°C until it was sectioned. Serial coronal sections (40 µm) were cut and five series of sections at 0.2 mm intervals were obtained for histological analysis using 1) cresyl violet, 2) tau-2, 3) Alz-50, and 4) GFAP. The first series was immediately mounted on slides, dried, and stained with cresyl violet. The other series were placed in an ethylene glycol cryoprotectant and stored at -20°C until used for immunohistochemistry.

Histology

1) Cresyl violet: The mounted sections (40 µm) from one series were defatted in xylene and hydrated using ethyl alcohol and H₂O. Staining was performed for 20 min in a solution containing 200 ml of 0.2 M acetic acid, 133 ml 0.2 M sodium acetate and 67 ml of 0.1% cresyl violet acetate. The sections then were dehydrated in an ethyl alcohol series and cleared in xylene. The tissue was subsequently coverslipped using DePeX mounting medium.

2) Tau-2: A series of 40 µm sections were removed from the cryoprotectant and washed overnight in phosphate buffered saline (PBS; pH 7.4) at 4°C. Sections were subsequently placed in 0.3% H₂O₂ in Tris buffered saline (TBS; pH 7.6) for 30 min, and then washed 3 x 10 min in 0.3% Triton X-100 in TBS. The sections then were incubated in primary antibody tau-2 (Sigma) at a 1:500 dilution for 24 h at room temperature. The antibody diluent contained 2.0% Triton X-100, 0.1 % sodium azide, 0.01% bacitracin, 2% bovine serum albumin, and 10% normal horse serum in TBS. Subsequently, the tissue was washed 3 x 10 min in 0.3% Triton X-100 in PBS, and then incubated for 1.0 h in

biotinylated anti-mouse immunoglobulin (Ig) G secondary antibody (Vectastain ABC Elite kit, Vector Laboratories, Burlingame, CA) diluted 1:2000 in 0.3% Triton X-100 in PBS. Following two washes in 0.3% Triton X-100 in PBS for a total of 15 min, the tissue then was incubated for 1.0 h in avidin horseradish peroxidase (Vector) diluted 1:2000 in 0.3% Triton X-100 in PBS. The sections were washed in PBS for 1.0 h, and sodium acetate buffer (0.2 M, pH 6.0) for 15 min, and then reacted in 3,3'-diaminobenzidine tetrahydrochloride (DAB) with nickel ammonium sulfate intensification (35 mg DAB, 2.5 g nickel ammonium sulfate per 100 ml sodium acetate buffer with 0.3% H₂O₂ added in 10 µl increments). Tissue sections then were placed in sodium acetate buffer, transferred to cold PBS and left at 4°C overnight. Subsequently, the tissue was mounted on slides, dried, defatted and cover slipped. According to product specifications, the biotinylated anti-mouse IgG (Vector) has 25% cross-reactivity with rat IgG. We were able to reduce this non-specific staining in the omit sections by diluting this secondary antibody. Immunolabelled cells in the omit sections were subtracted accordingly to establish a baseline.

3) Alz-50: Performed as above, except that 10% normal goat serum was used in the primary antibody diluent instead of normal horse serum. Alz-50 (courtesy of Dr. L. I. Binder) was used at a 1:1000 dilution, and the secondary antibody was a peroxidase-conjugated goat anti-mouse IgM (Boehringer Mannheim, Indianapolis, IN), diluted to 1:200.

4) GFAP: Performed the same way as tau-2 staining, except that 10% normal goat serum was used in the primary antibody diluent instead of normal horse serum. The GFAP antibody (Dako, Denmark) was used at a 1:500 dilution. The secondary antibody was a goat anti-rabbit IgG (Vector) diluted 1:1333.

Experimental Design

Experiment 1: Effects of A β 25-35 at 8 days postoperatively.

Group#	n	Drug (dose), right amygdala
1	9	VEH (10.0 nmol TFA/3.0 μ l H ₂ O)
2	9	A β 25-35 (5.0 nmol/3.0 μ l H ₂ O)

Methods: Cresyl violet, tau-2, Alz-50 and GFAP staining.

Both cresyl violet and tau-2 staining were performed on series from all the rats. Because of limited amounts of the Alz-50 antibody, we were not able to stain all series. Alz-50 staining was performed on a series of sections from two A β 25-35 treated rats that showed intense tau-2 IR, and on the same number of VEH treated rats. GFAP staining was performed on a series from eight VEH treated rats and five A β 25-35 treated rats.

Experiment 2: Effects of A β 25-35 at 32 days postoperatively.

Group#	n	Drug (dose), right amygdala
1	3	VEH (10.0 nmol TFA/3.0 μ l H ₂ O)
2	4	A β 25-35 (5.0 nmol/3.0 μ l H ₂ O)

Methods: Cresyl violet, tau-2, Alz-50 and GFAP staining.

Cresyl violet, tau-2 and GFAP staining were performed on a series of sections from all the rats. Alz-50 staining was performed on a series from two of the VEH treated rats and all of the A β 25-35 treated rats. The Alz-50 and GFAP staining were performed simultaneously on sections from the rats sacrificed 8 days postoperatively.

In a separate experiment, we injected the same dose of the reverse peptide (A β 35-25) into the rat amygdala and examined GFAP and tau-2 IR at 8 days and 32 days postoperatively (n = 2-3). The same VEH (n = 2-3) was used for comparison.

Data Analysis

Tau-2 IR cells were counted from 12 coronal sections (40 μ m) surrounding the cannula track. The number of tau-2 IR cells in distinct brain areas in the VEH and A β 25-35 treated animals were analyzed using a t-test (SIGMASTAT, version 1.01; Jandel, San Rafael, CA). Reactive astrocytosis in the ipsilateral hippocampus was rated on a scale of 0-2+. An animal was considered positive if it exhibited $\geq 1+$ staining. The GFAP staining was analyzed using a one-tailed Fisher exact test (SIGMASTAT). The rating of the GFAP sections was based on the complexity of astrocytic branching within the hippocampus (0 = resting astrocytes, few processes; 1+ = reactive astrocytes, moderate branching; 2+ = reactive astrocytes, extensive branching).

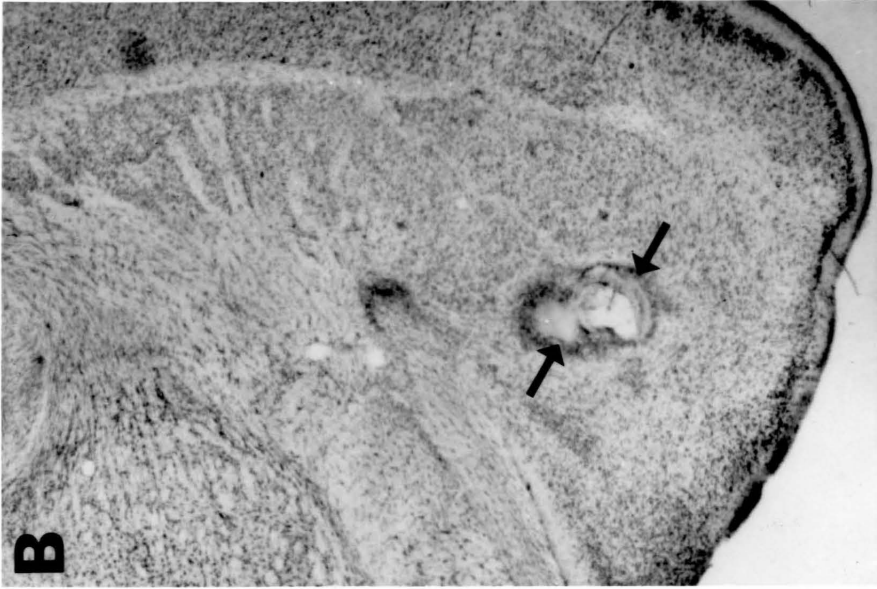
Results

Experiment 1: Effects of A β 25-35 at 8 Days Postoperatively.

Cresyl violet:

No difference was seen in cresyl violet stained sections between VEH and A β 25-35 treated rats except for proteinaceous deposits in the amygdala of A β 25-35 rats (Figure 3A-B). These deposits were identical to the Congo red positive deposits that we have observed following A β 25-35 injections into the ventral pallidum/substantia innominata (VP/SI) (314). Proteinaceous deposits did not form at the site of injection in rats treated with the reverse peptide. Sections from the latter group of rats did not appear to differ from the VEH treated rats.

Figure 3. Cresyl violet staining at 8 days postinjection. Coronal sections through VEH (A) and A β 25-35 (B) injection sites. The cannula track and the tip of the injection are seen in the VEH treated rat (A; arrowheads). Note the proteinaceous deposit (arrows) within the cavitation in B. No other histological differences were discerned between the VEH and A β 25-35 groups. Scale bar = 0.5 mm.



Tau-2:

A β 25-35 significantly increased tau-2 IR in the neuronal perikarya and processes ipsilaterally in the amygdala [A β 25-35: (mean \pm SEM) 226 \pm 95 IR cells; VEH: 10 \pm 7, p < 0.001], cingulate cortex [A β 25-35: 94 \pm 30; VEH: 0, p < 0.01] and hippocampus [A β 25-35: 251 \pm 78; VEH: 5 \pm 4, p < 0.001] (Figures 4-6). IR cells were also seen in other brain areas such as the parietal and pyriform cortices, hypothalamus, thalamus, globus pallidus, claustrum, substantia nigra, VP/SI, and the entorhinal cortex. No contralateral staining was observed except in the hypothalamus and occasionally in the cingulate cortex. Sections from rats treated with the reverse peptide did not appear to differ from the VEH treated rats.

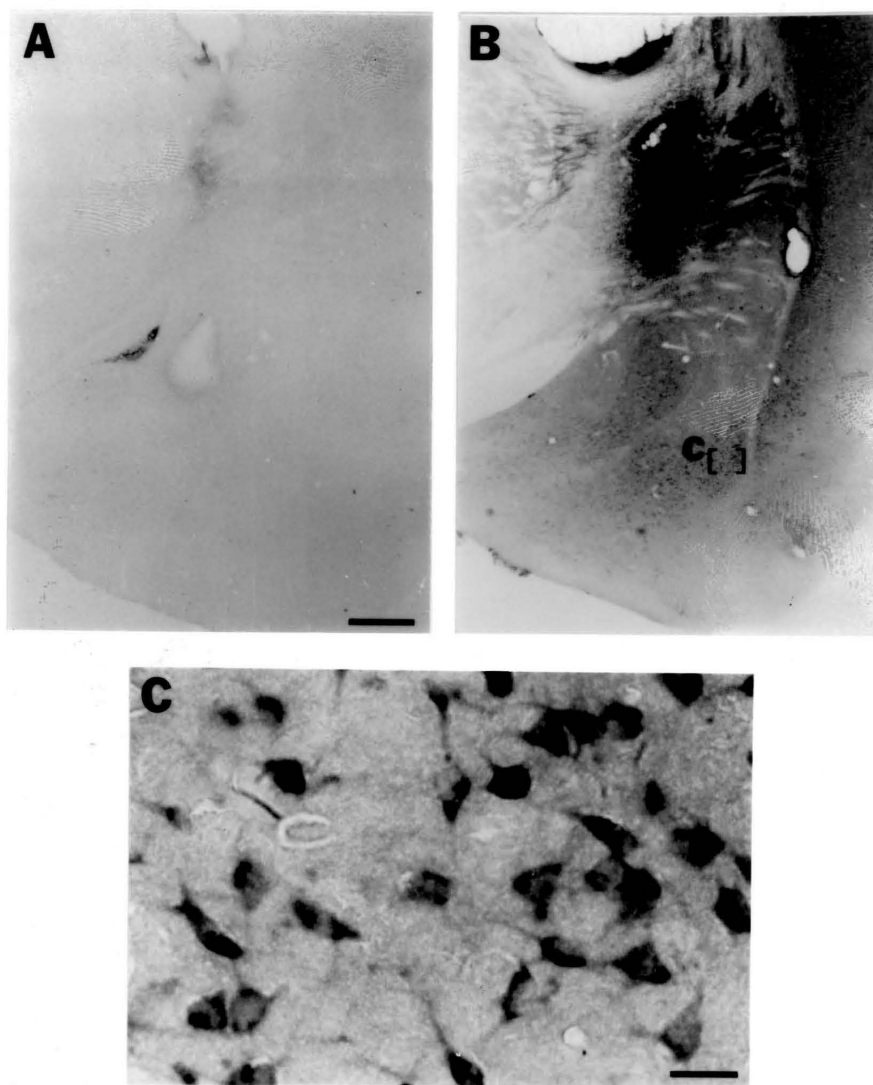


Figure 4. Tau-2 IR at 8 days postinjection. Coronal sections adjacent to VEH (A) and A β 25-35 (B, C) injection sites. C is a magnification of the area bracketed in B. Virtually no tau-2 IR is observed in the VEH treated rat (A). A β 25-35 induces neuronal cell body and processes tau-2 IR in the amygdala (B, C). Scale bar (A) = 0.5 mm. Scale bar (C) = 20 μ m.

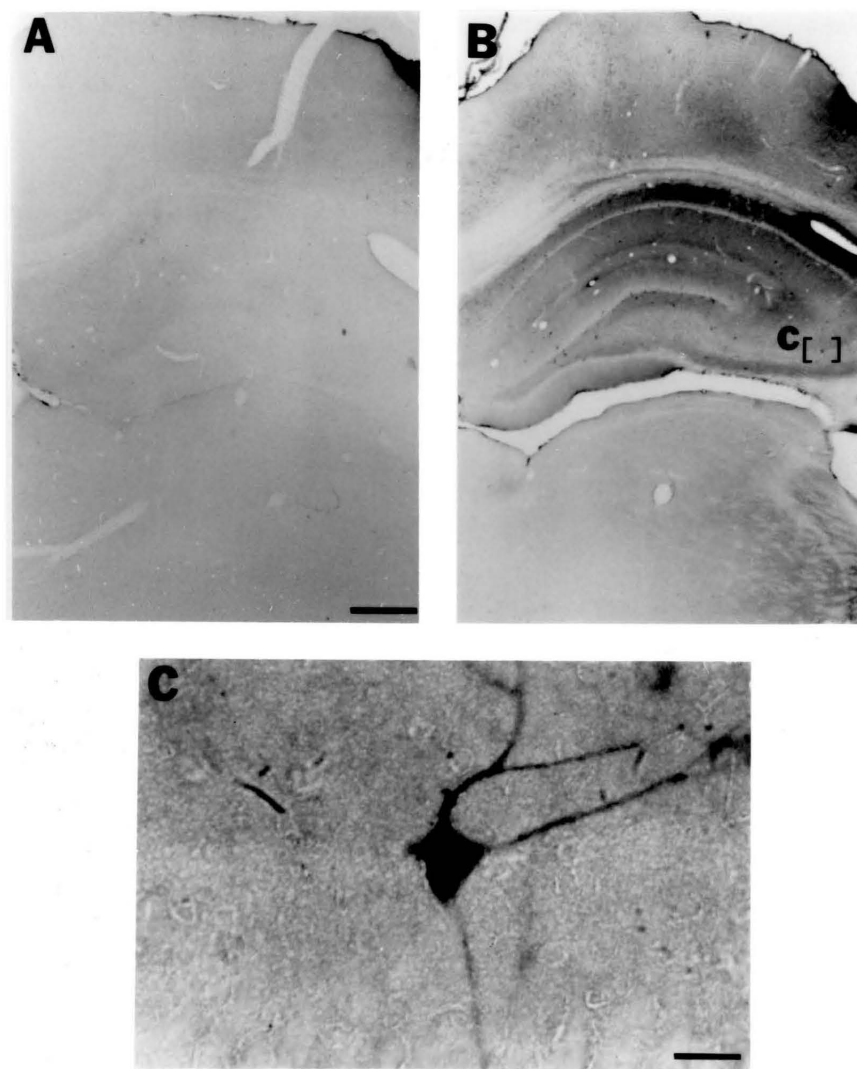


Figure 5. Tau-2 IR at 8 days postinjection. Coronal sections adjacent to VEH (A) and A β 25-35 (B, C) injection sites. C is a magnification of the area bracketed in B. Virtually no tau-2 IR is observed in the VEH treated rat (A). A β 25-35 induces neuronal cell body and processes tau-2 IR in the hippocampus (B, C), and cortical areas (B). Scale bar (A) = 0.5 mm. Scale bar (C) = 20 μ m.

Alz-50:

An increase in Alz-50 IR was observed in the amygdala of the A β 25-35 treated animals. Several beaded fibers and an occasional neuronal perikarya were visualized with Alz-50 in the ipsilateral amygdala and to a lesser extent in the contralateral amygdala. Interestingly, no Alz-50 IR was observed in the basolateral amygdala. Moderate staining of similar morphology also was observed ipsilaterally in the VP/Sl and there was faint staining ipsilaterally in the hippocampus. In addition, hypothalamic cell bodies and fibers were observed bilaterally in both VEH and A β 25-35 treated rats. Hypothalamic IR in normal rats has been observed by others (32).

GFAP:

Reactive astrocytosis was observed in the ipsilateral amygdala but there did not appear to be differences between A β 25-35 and VEH treated animals. However, reactive astrocytosis was seen in the ipsilateral hippocampus of all the A β 25-35 treated rats (5/5) but only in 50% of the VEH treated rats (4/8; $p=0.105$). No reactive astrocytosis was observed in rats treated with the reverse peptide.

Experiment 2: Effects of A β 25-35 at 32 Days Postoperatively.

Cresyl violet:

Microscopic analysis of the ipsi- and contralateral amygdala appeared to reveal neuronal shrinkage within the right amygdala (injected site) of A β 25-35 treated rats when compared to the left amygdala. This finding, however, requires confirmation by quantitative analysis in a larger number of animals. Proteinaceous deposits were observed 32 days postinjection in the right amygdala of A β 25-35 treated rats. However, proteinaceous

deposits did not form at the site of injection in rats treated with the reverse peptide.

Sections from these rats did not differ from the VEH treated rats.

Tau-2:

A β 25-35 significantly increased tau-2 IR ipsilaterally in the amygdala (A β 25-35: 721 \pm 194 IR cells; VEH: 48 \pm 24, $p < 0.05$) and hippocampus (A β 25-35: 938 \pm 84; VEH: 310 \pm 161, $p < 0.05$) in rats 32 days postoperatively (Figure 6). As at 8 days postoperatively, IR cell bodies and processes were also seen in other brain areas such as the parietal and pyriform cortices, hypothalamus, thalamus, globus pallidus, claustrum, substantia nigra, VP/SI, and the entorhinal cortex. Contralateral staining was only observed in the hypothalamus and occasionally in the cingulate cortex. The staining appeared to be more intense than at 8 days postoperatively but a similar anatomical distribution was noted. Sections from rats treated with the reverse peptide did not appear to differ from the VEH treated rats.

Alz-50:

The pattern and morphology of Alz-50 staining was similar to that observed at 8 days postoperatively but the intensity in the A β 25-35 treated rats appeared to be greater at 32 days postoperatively (Figure 7).

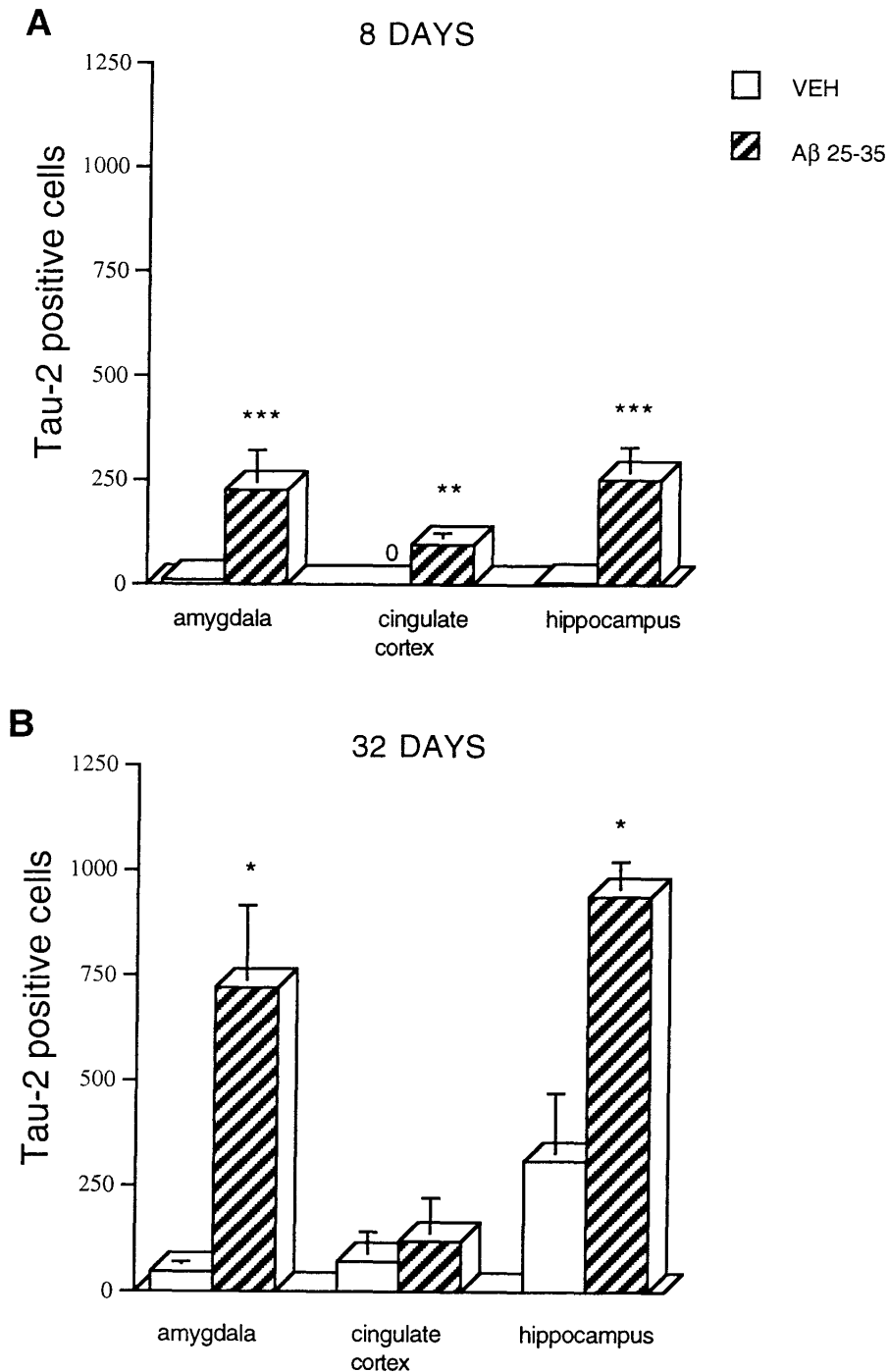


Figure 6. Quantitation of tau-2 IR cells at 8 days and 32 days postinjection. Following unilateral intra-amygdaloid injection, there was a significant increase in ipsilateral tau-2 IR cells in the amygdala, cingulate cortex and hippocampus in Aβ 25-35 treated rats 8 days postoperatively (A), and in the amygdala and hippocampus 32 days postoperatively (B) when compared to VEH treated rats. Each bar represents the mean + SEM of tau-2 IR cells from 12 sections (40 μm) surrounding the cannula track. (A) ** $p < 0.01$; *** $p < 0.001$; (B) * $p < 0.05$.

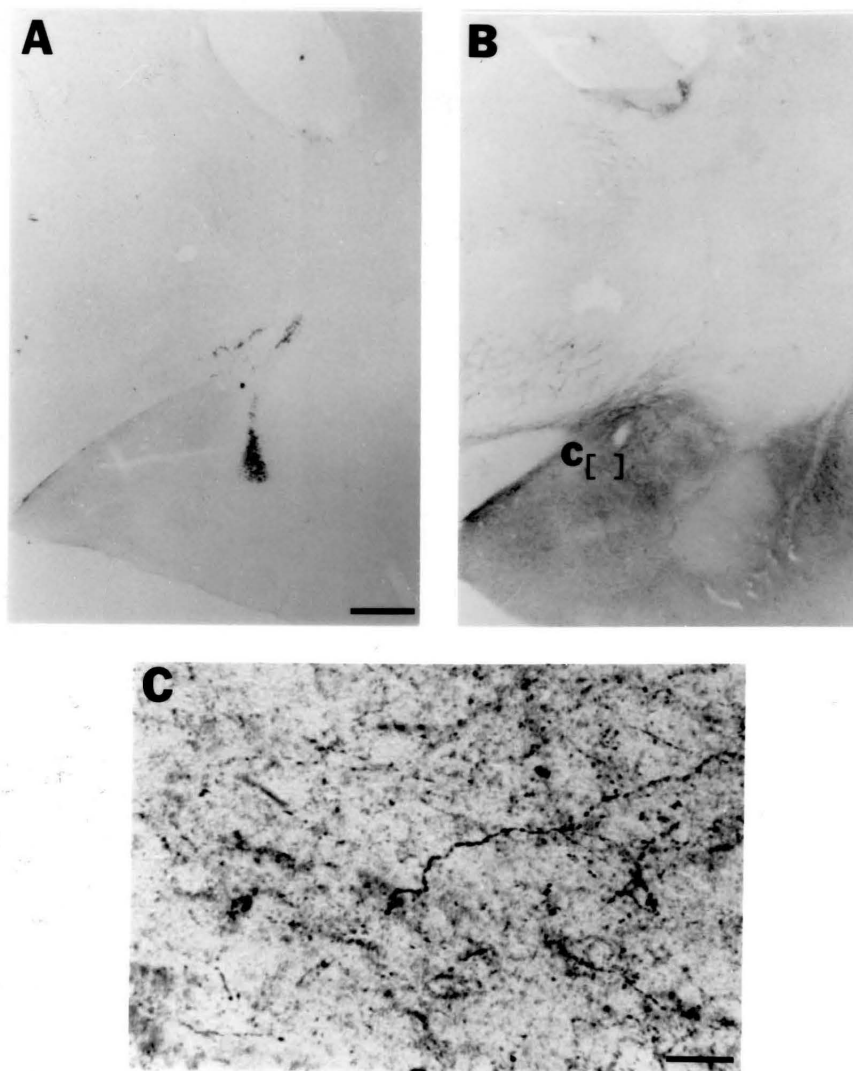


Figure 7. Alz-50 IR at 32 days postinjection. Coronal sections through VEH (A) and adjacent to A β 25-35 (B, C) injection sites. C is a magnification of the area bracketed in B. Virtually no staining is observed in the VEH treated rat (A), but collection of red blood cells are seen at the tip of the injection site. Several beaded fibers and an occasional neuronal perikarya are visualized with Alz-50 in the amygdala of the A β 25-35 treated rat (B, C). Note the lack of staining in the basolateral amygdala. Scale bar (A) = 0.5 mm. Scale bar (C) = 20 μ m.

GFAP:

At 32 days, no reactive astrocytosis was observed in the VEH treated animals. Reactive astrocytosis in the A β 25-35 treated rats was predominantly observed within the right hemisphere. These histological changes were seen in areas such as the amygdala, hypothalamus and cortical regions but were seen most consistently within the hippocampus. Reactive astrocytosis was observed in the ipsilateral hippocampus (Figure 8) of all the A β 25-35 treated rats (4/4) but not in the VEH treated rats (0/3; $p=0.029$). No evidence of reactive astrocytosis was observed in rats treated with the reverse peptide.

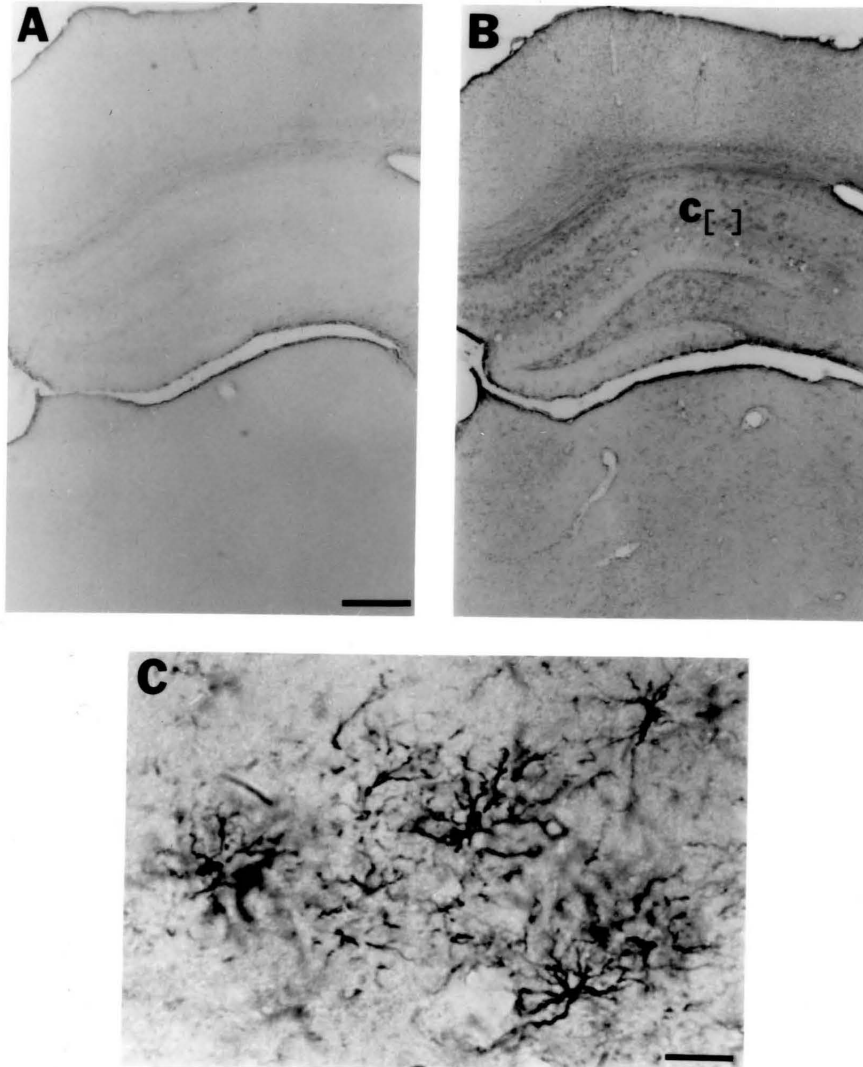


Figure 8. GFAP IR 32 days postinjection. Coronal sections adjacent to VEH (A) and A β 25-35 (B, C) injection sites. C is a magnification of the area bracketed in B. Virtually no GFAP IR is observed in the VEH treated rat (A). In the A β 25-35 treated rat a reactive astrocytosis is predominantly observed in the ipsilateral hippocampus (B, C; $p=0.015$). Scale bar (A)=0.5 mm. Scale bar (C)=20 μ m.

Discussion

We have demonstrated that a unilateral intra-amygdaloid injection of A β 25-35 in the rat induces the appearance of abnormal tau proteins both within the ipsilateral amygdala as well as at distant sites as recognized by the tau-2 and Alz-50 antibodies. These cytoskeletal changes appeared to be progressive and associated with reactive astrocytosis. Studies have reported local effects immediately surrounding the injection site of A β injections into rat cerebral cortex and hippocampus (91,178,180), but there are no reports on A β injections into the rat amygdala, and their distal effects.

The tau-2 antibody recognizes tau proteins in both the phosphorylated and non-phosphorylated form. This antibody does not discriminate between normal tau and hyperphosphorylated Alzheimer's tau in unfixed tissue, but recognizes only the Alzheimer's tau in fixed tissue (259). The epitope that tau-2 recognizes has been localized to the alanine 95 through alanine 108 sequence, in particular, amino acid 101 (346). On immunoblots, tau-2 has a higher affinity for bovine tau, that has serine in position 101, than human, mouse or rat tau, that all have proline in position 101. It has been suggested that the tau comprising paired helical filaments has a serine 101 peptide-like conformation similar to that seen for bovine tau (346). Therefore, the increase in tau-2 IR suggests that A β 25-35 may be causing a conformational change in tau proteins. Tau-2 IR cells were seen consistently in several brain areas ipsilateral to the injection site of A β 25-35 treated rats at 8 and 32 days postoperatively. The anatomical distribution of senile plaques and neurofibrillary tangles in AD suggests that A β may act on nerve terminals to cause cytoskeletal alterations in axons, which ultimately lead to tangle formation within the perikarya (265). Therefore, the appearance of abnormal tau IR following intra-amygdaloid injections of A β 25-35 can be expected in brain regions that project to the amygdala (Figure 9). Our results support this view. The hippocampus and cortical areas have prominent bidirectional connections with

the amygdala but the corpus striatum is one of only a few brain regions that receives amygdaloid fibers but does not project back to the amygdala (276). The observation of tau-2 IR cells in the hippocampus and cortical areas and relative lack of reactive cells in the neostriatum supports the hypothesis that A β 25-35 acts on nerve terminals to induce the appearance of abnormal tau proteins in brain regions that have efferent projections to the amygdala. It is unlikely that these distant effects are due to diffusion of the peptide from the site of injection into the ventricles, because A β deposits were not observed outside the site of injection. In addition, induced tau IR and reactive astrocytosis were not observed in the ependymal lining of the ventricles.

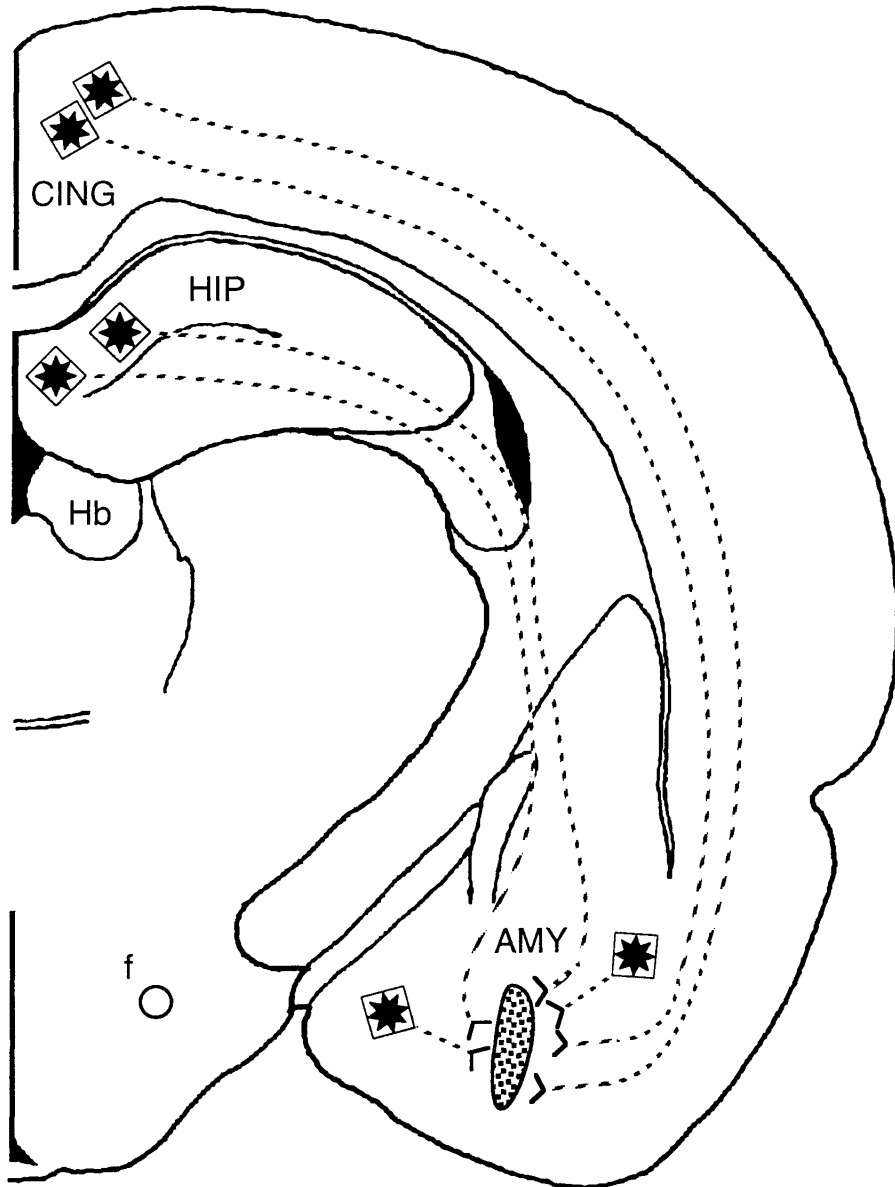


Figure 9. Schematic diagram of the right hemisphere of a coronal section through the A β 25-35 injection site. A β 25-35 in its β -pleated sheet conformation (stippled area in the amygdala) acts on nerve terminals to induce the appearance of abnormal tau proteins in brain regions that have efferent projections to the amygdala. The cingulate cortex and the hippocampus are examples of brain regions that have prominent efferent connections (dashed lines) with the amygdala. Amygdaloid interneurons are also shown projecting (dashed lines) towards the A β 25-35 deposit. Tau-2 positive cell bodies are represented by black stars within white boxes. Abbreviations: CING: cingulate cortex; HIP: hippocampus; AMY: amygdala; Hb: habenula; f: fornix.

The Alz-50 antibody in immunocytochemical studies stains AD brain tissue (55) but its IR in normal brain tissue appears to depend on the method used (293). It demonstrates early changes in AD by recognizing abnormally phosphorylated tau protein (337). The location and nature of the epitope recognized by Alz-50 remains controversial. It has been reported to recognize an acid phosphatase sensitive phosphorylated epitope of tau that is localized within the 14-amino acid carboxy-terminal to the tubulin-binding domain of tau (337). However, the epitope also has been mapped to the amino-terminal region of tau proteins (105,182). Although the epitope that Alz-50 recognizes may not be phosphorylated, the overall peptide conformation recognized by the antibody may be phosphorylation dependent. In the present study, the morphology and distribution of the Alz-50 staining differed from that of tau-2. Beaded fibers, but only an occasional perikarya, were visualized with Alz-50 whereas tau-2 IR was observed in cell bodies and processes. Alz-50 staining was predominantly observed in the ipsilateral amygdala, to a lesser extent in the contralateral amygdala, and ipsilaterally in the VP/Sl and hippocampus. At present, there is no obvious explanation for the lack of IR in the basolateral amygdala. The ipsi- and contralateral amygdala are connected through the anterior commissure (276), which may explain the IR observed in the contralateral amygdala. In addition, the IR in the ipsilateral VP/Sl and hippocampus can be explained by prominent anatomical connections between these brain regions and the amygdala (276). We did not attempt to quantify the effects of A β 25-35 on Alz-50 IR because of the morphology of staining. Immunohistochemistry was performed simultaneously on sections from rats sacrificed 8 and 32 days postoperatively. As with tau-2, staining appeared to be substantially more intense at 32 days postoperatively but the pattern was similar to that observed 8 days postoperatively. This supports the observation that A β 25-35 induced effects on the cytoskeleton gradually increase up to 32 days postoperatively. The A β 25-35 induction in Alz-50 staining suggests that the peptide alters the conformation of tau proteins possibly through an increase in tau phosphorylation.

We have recently found (unpublished observation) that A β 25-35 increases Alz-50 IR on Western blots 8 days postoperatively.

There is no obvious explanation for the differences in distribution and morphology between Alz-50 and tau-2 staining. These two antibodies recognize different conformation dependent epitopes on tau proteins. A β 25-35 may be inducing multiple conformational changes in tau proteins, which are differently stained using the two antibodies. The nature and extent of these conformational changes may be time dependent, brain region specific, and differ within the neuronal structure.

It can be argued that the A β 25-35 induction in tau-2 and Alz-50 IR does not arise from conformational change but rather is due to increased synthesis of tau proteins. We have performed Western blot analysis on the amygdala of rats sacrificed 8 days postinjection using the same experimental protocol as in this study. By using the tau-1 antibody that reacts only with normal and unphosphorylated tau (16), no differences were observed in the molecular weights of tau-1 IR bands or their density when A β 25-35 treated rats were compared to VEH treated rats (unpublished observation). This finding suggests that the A β 25-35 induction in abnormal tau IR is not the result of an increased synthesis of tau proteins.

The effects of A β on tau IR may be mediated through an increase in intracellular calcium. A β has been shown to increase intracellular calcium (7,218), and calcium influx in cultured rat hippocampal neurons caused by glutamate induces tau IR as recognized by the antibodies Alz-50 and 5E2 (216). Protein kinases are generally activated by increases in intracellular calcium and several of those have been shown to phosphorylate different sites on tau proteins (238). Therefore, A β may increase the phosphorylation of tau proteins through an activation of kinases mediated by an increase in intracellular calcium. The activities of some phosphatases that may dephosphorylate tau proteins have been shown to

be decreased in AD (111,311). Therefore, A β 25-35 may also be decreasing the dephosphorylation of tau proteins through an inhibition of phosphatases.

The proteinaceous deposits observed at the site of injection, both at 8 and 32 days postinjection, were identical to those we have observed following injection of A β 25-35 into the VP/SI (314). Those deposits were Congo red positive with birefringence under polarized light, suggesting that they were most likely composed of fibrillar A β because the dye reacts with the peptide in its β -pleated sheet conformation. Therefore, these findings further support the notion that A β 25-35 is not readily degraded *in vivo*, and suggest that its toxic effects may gradually increase as long as the peptide is present in its toxic conformation (β -pleated sheets).

GFAP immunohistochemistry was performed in order to determine 1) if A β 25-35 increases reactive astrocytosis, like that seen surrounding senile plaques in AD; and, 2) if there is a correlation between the location and severity of abnormal tau and GFAP IR. Following stab wounds of the rodent cerebrum reactive gliosis reaches maximum intensity 3-7 days postoperatively (253). The contralateral hemisphere is rarely affected and the glial reaction is transient in nature and declines to nearly normal appearance by 3 weeks. Therefore, the non-specific damage caused by the cannula placement may explain the similar amygdaloid GFAP IR in A β 25-35 and VEH treated rats at 8 days postoperatively. This injury related effect may also explain the reactive gliosis in the ipsilateral hippocampus of some of the VEH treated rats and thereby the lack of a significant effect of A β 25-35 at 8 days postoperatively ($p=0.105$). Microscopic analysis of cresyl violet stained sections did not reveal any hippocampal neuronal loss. However, numerous tau-2 IR cells were observed in the ipsilateral hippocampus at this timepoint, suggesting an association between neuronal cytoskeletal changes and reactive astrocytosis. The transient nature of the glial reaction caused by the cannula placement is supported by the lack of reactive astrocytosis in the VEH treated rats 32 days postoperatively. Reactive astrocytosis was consistently observed

in the ipsilateral hippocampus of the A β 25-35 treated rats at this timepoint ($p = 0.029$).

These observations suggest a long lasting effect of A β 25-35 on astrocytic reactivity in a brain region that has prominent efferent connections with the amygdala.

In a separate experiment, we injected the same dose of the reverse peptide (A β 35-25) into the rat amygdala and performed cresyl violet, tau-2 and GFAP staining at 8 and 32 days postoperatively. No difference was seen between rats treated with VEH and the reverse peptide. It did not form proteinaceous deposits at the site of injection and did not induce significant tau-2 IR or reactive astrocytosis. Therefore, the histopathological effects of A β 25-35 are specifically caused by that particular amino acid sequence. The effects of A β 25-35 in present study, furthermore, are not caused by its greater acidity (pH 3.5-3.9) than the VEH solution (pH 5.9-6.0), as the acidity (pH 3.6) of the same dose of the reverse peptide, was similar to that of A β 25-35.

Animal models can be evaluated in terms of construct validity, face validity and predictive validity. We believe that this model has construct validity because we are injecting a fragment of a peptide, that may play a prominent role in the etiology of AD, into a brain region that is affected early in the disease. The most appropriate face validity of an animal model of AD would be the demonstration of senile plaques associated with reactive astrocytes, neurofibrillary tangles, and neuronal cell loss in the same brain regions as observed in AD. It is unlikely, however, that this effect can be obtained using a single injection of A β into rat brain, but this approach may demonstrate the early histopathological changes in AD. In our opinion, the present rat model has a relatively high face validity because of the induction of abnormal tau proteins and reactive astrocytes in brain regions where the primary and early histopathological changes in AD are observed. Currently, no definitive transgenic animal models are available that resemble all aspects of AD, although plaque-like A β deposits have been observed (98). The predictive validity of the present rat

model, as well as future transgenic models, will ultimately determine their usefulness in screening potential drugs for therapy.

In conclusion, these data suggest that injection of A β 25-35 into the right amygdala of young rats induces progressive transsynaptic cytoskeletal and astroglial reactions that gradually spread from the amygdala to brain regions that have prominent efferent connections with that area. These findings also suggest a direct association between plaque and tangle formation in AD, and support the use of this rat model to screen drugs that may attenuate or enhance the initial pathological events associated with AD.

CHAPTER IV

LATERALITY IN THE HISTOLOGICAL EFFECTS OF INJECTIONS OF AMYLOID- β 25-35 INTO THE AMYGDALA OF YOUNG MALE FISCHER RATS

Abstract

We have observed that single amyloid- β 25-35 ($A\beta$) injections (5.0 nmol) into the right amygdala of rats produce progressive cytoskeletal and astrogliotic reactions not only within the amygdala, but also in distal brain regions that project to the amygdala. To determine if these effects are potentiated by bilateral injections, we injected $A\beta$ (5.0 nmol) into the left and right amygdala of young male Fischer rats. Animals were sacrificed at 32 days postoperatively. Bilateral infusions of $A\beta$ induced significant neuronal shrinkage, tau-2 neuronal staining and reactive astrocytosis within the right amygdala and/or hippocampus, compared to vehicle treated rats. Surprisingly, the same brain regions within the left hemisphere were significantly less affected even though no differences were observed between the left and right amygdala in the size of Congo red positive $A\beta$ deposits. Unilateral injections of $A\beta$ into the left amygdala led to significant histological changes in the right amygdala and hippocampus but not in the same brain regions within the left hemisphere. These results suggest a laterality in the histopathological effects of $A\beta$ in male Fischer rats. Identification of the cause for the lateralized effect of $A\beta$ may prove valuable for understanding the etiology of Alzheimer's disease and provide possible therapeutic strategies designed to slow the progression of the disease.

Introduction

The histopathological characteristics of Alzheimer's disease (AD) include senile plaques, reactive astrocytes, neurofibrillary tangles, and neuronal cell loss in several brain regions. Senile plaques consist predominantly of amyloid- β ($A\beta$) 1-42 (103,214,233,285), which is derived from a large membrane spanning protein, the amyloid- β precursor protein (APP) (166). Mutations in APP in some forms of familial AD are associated with an elevated production of $A\beta$ (33,39,331). APP is overexpressed in Down's syndrome (248,291), and individuals with this disease invariably develop the neuropathological hallmarks of AD (23,187). The proposed role for $A\beta$ in the pathogenesis of AD is further supported by the neurotoxicity of $A\beta$ (369,370), that includes amino acids 25-35 of the peptide (370). $A\beta$ toxicity depends on its aggregation state (269,273), and requires the assembly of $A\beta$ into amyloid fibrils composed of a β -pleated sheet structure (203). Other amyloidogenic peptides also are toxic to neurons *in vitro*, including amylin, serum amyloid P component, and a peptide derived from the prion protein (87,202,222,338). These findings suggest that the structure of the fibril, rather than its amino acid sequence, is responsible for its toxicity. The discovery of the association of AD with inherited APP mutations led to the development of transgenic mouse models containing these mutations. Recently, two mouse models have been described that contain age dependent congophilic $A\beta$ plaques similar to those observed in AD (98,145), and in one of these models these changes are associated with behavioral impairments (145).

The main component of neurofibrillary tangles is paired helical filaments (168,335), which consist largely of the microtubule associated protein tau in an abnormal state of phosphorylation (171,182,355,356). Only recently have a few studies demonstrated a direct association between plaque and tangle formation using *in vitro* and *in vivo* models. *In*

vitro studies have demonstrated that A β increases tau protein kinase I (TPK I) activity (332), induces tau immunoreactivity (IR) (26,207), and that the neuronal death caused by A β can be prevented with TPK I antisense oligonucleotides (332). *In vivo* studies have reported that A β can induce tau IR in the vicinity of the injection site (91,178,180,317), as well as at distal sites (317). Also, one report indicates that injection of hyperphosphorylated tau into rat brain induces A β IR (312).

In the AD brain, reactive astrocytes are found in high abundance surrounding senile plaques (70). Glial fibrillary acidic protein (GFAP) (77) is a component of the glial intermediate filaments that form part of the cytoskeleton, and is found predominantly in astrocytes. GFAP levels in AD brains are increased 8 to 16 fold compared to control brains (21,60). Recent *in vitro* (34,141,271) and *in vivo* (317) findings suggest that A β induces reactive astrocytosis.

The major pathological changes in AD are found in regions of the medial temporal lobe, including the amygdala (265). Previously, we observed that single A β 25-35 injections (5.0 nmol) into the right amygdala of rats produce progressive (8 vs. 32 days) cytoskeletal and astroglial reactions not only within the amygdala, but also in distal brain regions that project to the amygdala (317). To determine if these effects are potentiated by bilateral injections of A β , we injected A β 25-35 (5.0 nmol) into the left and right amygdala of young male Fischer-344 rats. The present study suggests that there is a laterality in the histological effects of A β .

Materials and Methods

Animals

Male Fischer-344 rats were obtained from the NIA colony at Harlan Sprague-Dawley (Indianapolis, IN). At the time of arrival, the rats weighed 250-300 g and were 3-4 months of age. The animals were housed individually, maintained on a 12 h light-dark cycle (lights on at 07:00 h) in a AAALAC approved facilities, had access to food and water *ad libitum*, and were habituated to their new environment for 2-3 weeks prior to surgery.

Drugs

A β 25-35 (BACHEM, Torrance, CA) was supplied as a trifluoroacetic acid (TFA) salt. At the time of surgery, information was not available from the supplier regarding the amount of TFA per mg of the salt of the peptide. According to the supplier, there is not a direct stoichiometric relationship between the content of A β 25-35 and TFA, in other words it is not known how many mol of TFA there are in each mol of the TFA salt of A β 25-35. The peptide content was 77% (\pm 3%) with the remaining 23% consisting of TFA and H₂O, and the purity of the peptide was >98%. We assumed that there are 2 nmol of TFA per 1 nmol of A β 25-35, that is TFA content of 16.7% per mg of the salt. Recent information from the supplier indicates that the TFA content is 9.7%. The peptide and its respective vehicle (VEH; TFA, sodium salt; Sigma) were dissolved in Nanopure[®] water (H₂O) immediately before use and stored at 4°C between injections.

Surgery

Surgery was performed as described previously (317). Briefly, the animals received bilateral injections of 5.0 nmol/3.0 μ l (n = 20), or its respective VEH (n = 13), into the amygdala. The rats were either injected first into the right amygdala and subsequently into

the left amygdala ($A\beta$ rats = 10; VEH rats = 7), or injected simultaneously into the right and left amygdala ($A\beta$ rats = 10; VEH rats = 6). In addition, a few rats ($A\beta$ rats = 4; VEH rats = 2) received unilateral injections of $A\beta$ 25-35 (5.0 nmol/3.0 μ l) into the left amygdala. A Kopf stereotaxic instrument was used with the incisor bar set at 3.3 mm below the interaural line. Injection coordinates measured from the bregma and the surface of the skull (AP - 3.0, ML \pm 4.6, DV - 8.8) were empirically determined based on the atlas of Paxinos and Watson (261).

Animal Sacrifice, Tissue Preparation and Histology

The animals were anesthetized with sodium pentobarbital (100 mg/kg, intraperitoneally) and perfused transaortically 32 days postoperatively, as previously described (317). Serial coronal sections (40 μ m) were cut with five series of sections at 0.2 mm intervals saved for histological analysis of 1) cresyl violet, 2) tau-2, 3) GFAP, and 4) Congo red staining. Immunohistochemistry was performed as previously described (317). Briefly, sections (40 μ m) were incubated in tau-2 (Sigma, St. Louis, MO) primary antibody at a 1:500 dilution for 24 h at room temperature. An anti-mouse immunoglobulin (Ig) G secondary antibody (Vectastain ABC Elite kit, Vector Laboratories, Burlingame, CA) was used at a 1:2000 dilution. GFAP staining was performed the same way as the tau-2 staining. The GFAP antibody (Dako, Denmark) was used at a 1:500 dilution. The secondary antibody was a goat anti-rabbit IgG (Vector) diluted 1:1333. Omit sections for tau-2 and GFAP were obtained by omitting the primary antibody. According to product specifications, the biotinylated anti-mouse IgG (Vector) has 25% cross-reactivity with rat IgG. We were able to reduce the intensity of this non-specific staining by diluting the secondary antibody. The staining intensity was always substantially less in the omit sections than in sections treated with the primary tau-2 antibody. Immunolabelled neurons in the omit sections from the same animal were subtracted accordingly to establish a

baseline. In the VEH treated animals, the number of cells in the omit sections, regardless of the intensity of staining, was 43% of the total cell number in the primary antibody sections. In the A β treated rats, the number of cells in the omit sections was 23% of the total cell number in the primary antibody sections. This percentage (23%) is in accordance with the 25% cross-reactivity of the secondary antibody. There was relatively more non-specific staining in the VEH treated rats (i.e. 43% of total staining) than might be expected but this may be due to the fact that few VEH treated animals had tau-2 positive cells (31%), and there was a low number of positive cells in those animals.

Data Analysis

The A β deposits, neuronal shrinkage and tau-2 staining were analyzed quantitatively. The size of the deposits and the neuronal perikarya were measured, and tau-2 IR neurons were counted. Reactive astrogliosis was analyzed semi-quantitatively by using a rating scale.

An image analysis system (NIH Image 1.49) was used to determine the size of the A β deposits and neuronal shrinkage within the left and right amygdala. The area of the A β deposits was measured at 0.2 mm intervals. These data were analyzed using a t-test (SIGMASTAT, version 1.01; Jandel, San Rafael, CA) for comparison of the deposit area in the left vs. right amygdala. The basolateral nucleus within the amygdala can be divided into parvocellular and magnocellular subnuclei based on the cytoarchitecture of the neurons. The cells within these subnuclei have a relatively uniform appearance and their boundaries are easily identified. The magnocellular division is located mainly rostral and medial to the parvocellular division. The area of 10 of the largest magnocellular cells (X400 magnification) within the left and right basolateral amygdala was measured in one cresyl violet stained section per animal slightly rostral to the injection site, and we carefully chose sections at a similar coronal level. The average area of these 10 cells was calculated and the data were

analyzed by a t-test for the unilateral A β injections, and a two-way analysis of variance (ANOVA; SIGMASTAT) for the bilateral injections, followed by a Newman-Keuls' multiple range test for *post hoc* comparisons. Tau-2 IR neurons were counted in the left and right amygdala in six sections surrounding the injection site, and in six hippocampal sections including and caudal to the injection site. Tau-2 IR neurons were also counted in omit sections and subtracted accordingly. These data were analyzed using a two-way ANOVA for the amygdala and hippocampus separately, followed by a Newman-Keuls' multiple range test for *post hoc* comparisons. When the tau-2 data failed a normality test, it was analyzed by a two-way ANOVA on ranks. The correlation between the number of tau-2 positive neurons and neuronal cell size within the left and right amygdala, as well as the correlation between the number of tau-2 positive neurons within the amygdala and hippocampus, was analyzed using the Pearson product-moment correlation (SIGMASTAT). Reactive astrocytosis in the left and right hippocampus was rated on a scale of 0-2+. An animal was considered positive if it exhibited $\geq 1+$ staining. These data were analyzed using a Fisher exact test, one-tail (SIGMASTAT). The rating of the GFAP sections was based on the complexity of astrocytic branching within the hippocampus (0 = resting astrocytes, few processes; 1+ = reactive astrocytes, moderate branching; 2+ = reactive astrocytes, extensive branching). The observers did not know which rat numbers corresponded to which treatment. However, the A β treated animals were easily identifiable because of the proteinaceous deposits within the amygdala.

No statistical difference was discerned, in any of the parameters analyzed, between rats injected first into the right amygdala and subsequently into the left amygdala, and animals injected simultaneously into the left and right amygdala, so they were combined in the subsequent analyses.

Results

Bilateral Injections into the Amygdala

A β Deposits

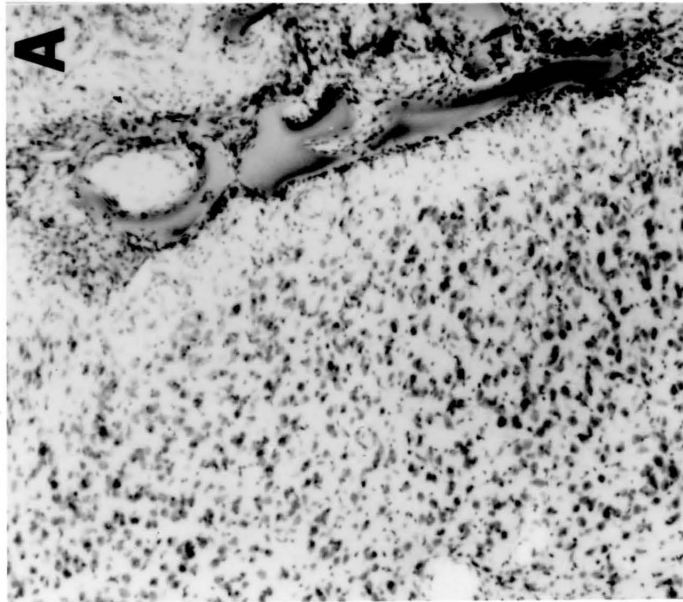
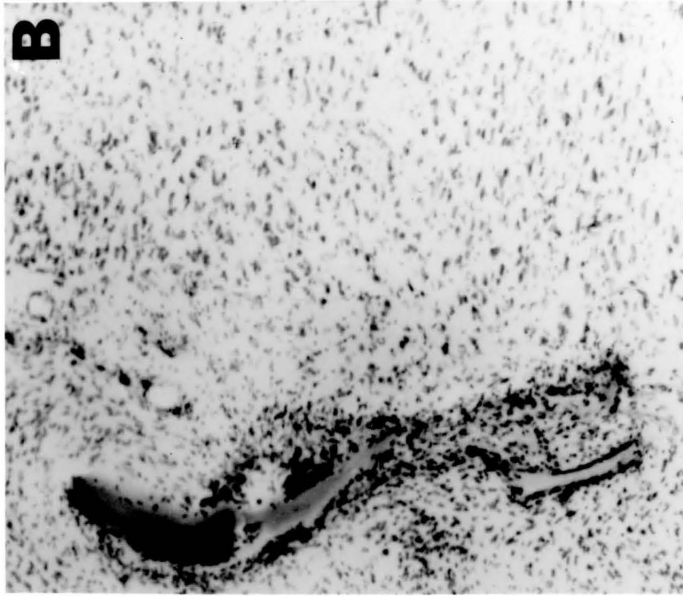
Proteinaceous deposits were observed bilaterally in the amygdala of the A β 25-35 treated rats (Figures 10A, B; 11; 14A). The location of the deposits did not vary between the left and right amygdala. The deposits were found consistently medial to the basolateral nucleus at the injection site, and their size appeared to be less than that of the basolateral nucleus. These deposits were Congo red positive (apple-green birefringence under polarized light; Figure 11), similar to those we observed following A β 25-35 injections into the ventral pallidum/substantia innominata (VP/SI) (314). Of the 20 rats injected bilaterally with A β 25-35, deposits were observed bilaterally in 18 rats, and unilaterally in 2 rats. Analysis of the area of these deposits within the left vs. the right amygdala revealed no significant differences (Figure 14A).

Cresyl Violet

Analysis of the areas of 10 of the largest magnocellular cells within the left and right basolateral amygdala revealed a treatment effect of A β 25-35 [$F(1, 62) = 18.649$, $p < 0.001$]. Laterality was also observed [$F(1,62) = 31.981$, $p < 0.001$], and there was a significant treatment x laterality interaction [$F(1,62) = 9.469$, $p = 0.003$]. *Post hoc* analysis revealed that bilateral intra-amygdaloid injections of A β 25-35 caused neuronal shrinkage within the right amygdala [cell area = $1433 \pm 82 \mu\text{m}^2$ (SEM); $p < 0.01$], compared to VEH injections [cell area = $2040 \pm 84 \mu\text{m}^2$; Figure 14B]. The left amygdala in the A β treated rats [cell area = $2150 \pm 71 \mu\text{m}^2$] was significantly less affected than the right amygdala ($p < 0.01$; Figure 14B). There was no significant difference between the cell area of the left [cell

area = $2252 \pm 80 \mu\text{m}^2$] and the right [cell area = $2040 \pm 84 \mu\text{m}^2$] amygdala in the VEH treated rats. All nuclei within the right amygdala appeared to be equally affected but the shrinkage was most obvious in the large neurons within the basolateral amygdala (Figure 10A, B). The neuronal atrophy appeared to extend into other brain regions within the right hemisphere, such as cortical areas. Cell bodies within the hippocampus overlapped and, therefore, analysis of cell shrinkage was not performed in that brain region.

Figure 10. Neuronal shrinkage within the right amygdala. Cresyl violet stained coronal section (X63) through the left (A) and right (B) amygdala in a bilaterally injected A β rat. A β deposits are seen bilaterally adjacent to the basolateral nuclei. Note the neuronal shrinkage within the right (B) but not the left basolateral nucleus (A). In this animal, the average area of 10 of the largest magnocellular cells was $1986 \pm 187 \mu\text{m}^2$ (SD) in the left nucleus, and $1016 \pm 178 \mu\text{m}^2$ in the right nucleus.



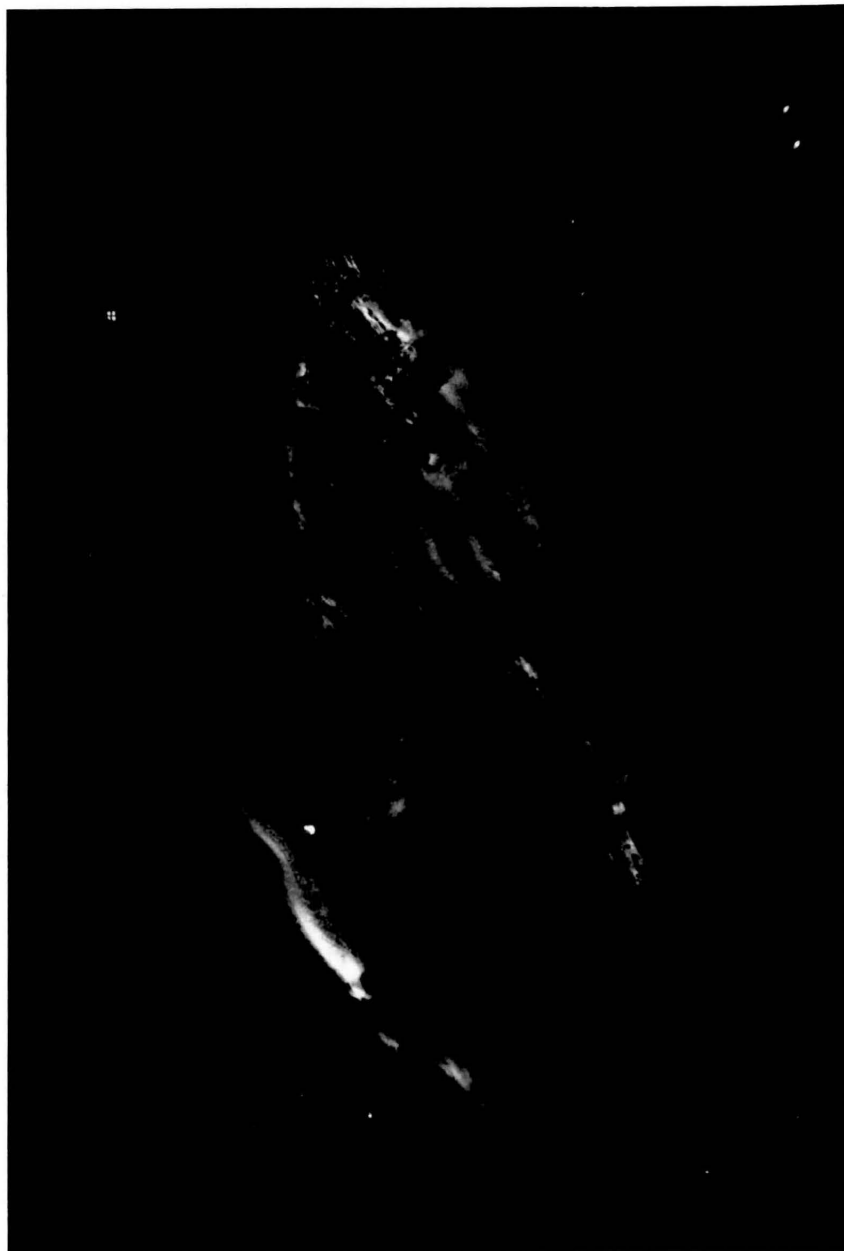


Figure 11. Congo red positive A β deposit. Congo red stained coronal section (X63) through the injection site within the left amygdala in a bilaterally injected A β rat. Note the birefringence of the A β deposit under polarized light that indicates a β -pleated sheet structure.

Tau-2

There was a treatment effect of A β 25-35 in the induction of specific neuronal tau-2 staining within the amygdala [$F(1,60) = 22.150, p < 0.001$] and the hippocampus [$F(1,60) = 34.513, p < 0.001$] (Figure 14C, D). Laterality was observed in the amygdala [$F(1,60) = 31.782, p < 0.001$] and the hippocampus [$F(1,60) = 9.266, p = 0.003$] (Figure 12; 14C, D). There was also a significant treatment x laterality interaction within the amygdala [$F(1,60) = 8.198, p = 0.006$], but not within the hippocampus [$F(1,60) = 3.096, p = 0.084$]. *Post hoc* analysis for the treatment effect revealed a significant increase in the number of tau-2 IR neurons in the A β treated rats within the right amygdala ($p < 0.01$) and the right hippocampus ($p < 0.01$), compared to the same brain regions in the VEH treated rats. Interestingly, there was also a significant increase in the number of tau-2 positive neurons within the left hippocampus in the A β treated rats ($p < 0.05$), compared to VEH treated rats. *Post hoc* analysis for the laterality effect revealed a significant increase in the number of tau-2 IR neurons in the right amygdala ($p < 0.01$) and the right hippocampus ($p < 0.01$), compared to the same brain regions within the left hemisphere in the A β treated rats. There also appeared to be an increase in tau-2 IR neurons in other brain areas, predominantly on the right side, including the cingulate, parietal and pyriform cortices, hypothalamus, thalamus, globus pallidus, claustrum, substantia nigra, VP/SI, and the entorhinal cortex (data not shown). Within individual animals, there was a significant positive correlation between the number of tau-2 IR neurons within the amygdala and hippocampus ($r = 0.833, p < 0.001$). There was also a significant negative correlation between the number of tau-2 positive cells and cell size within the left and right amygdala ($r = -0.67, p < 0.001$).

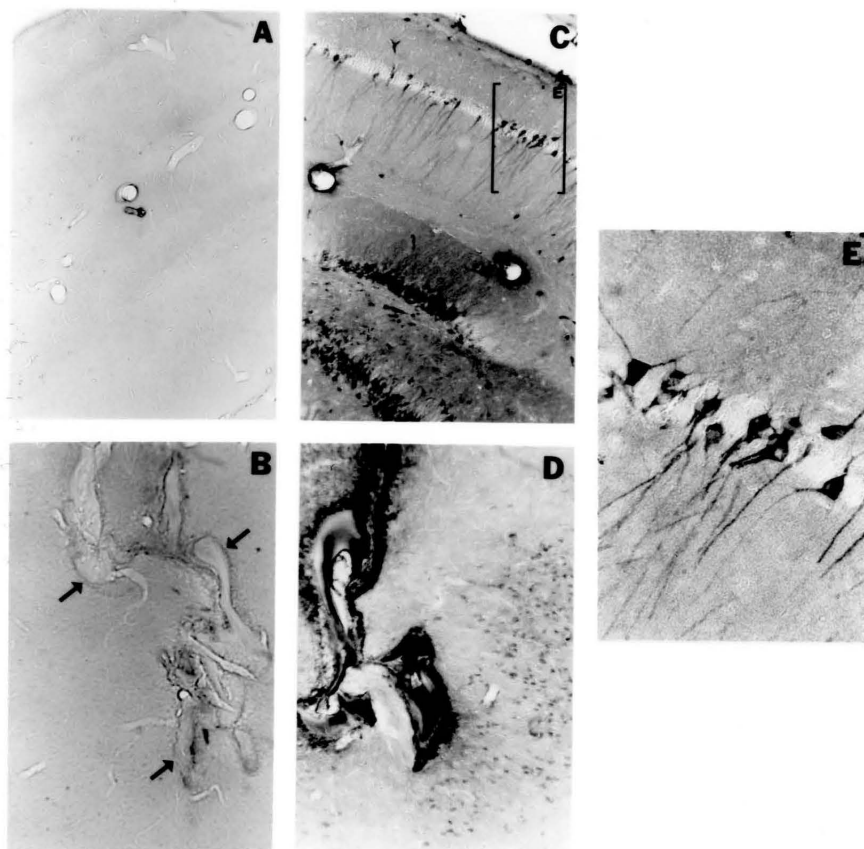
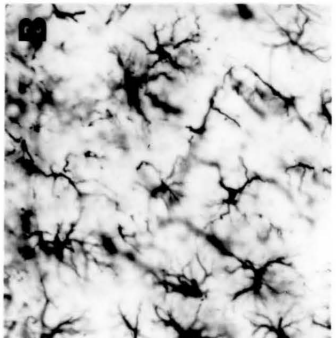
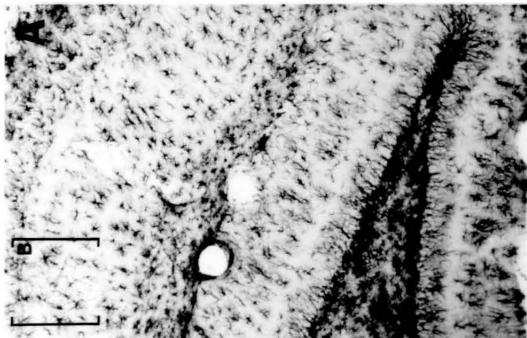
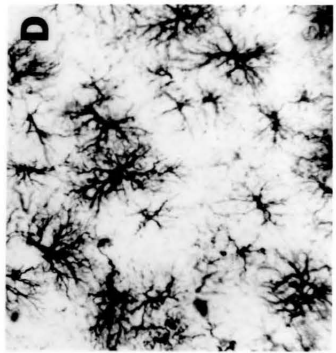
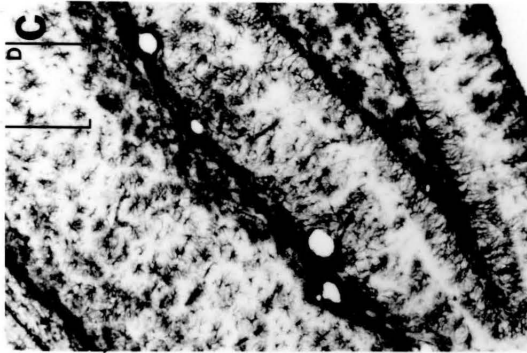
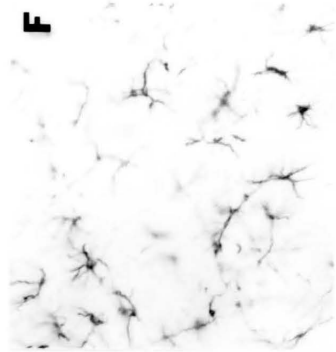
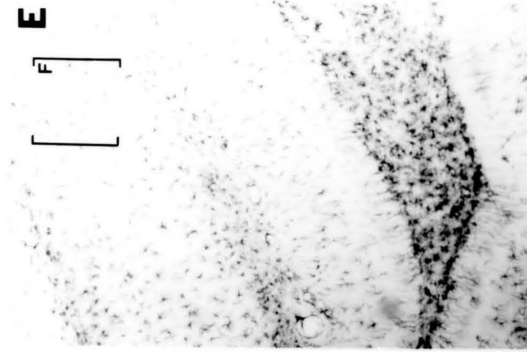


Figure 12. Laterality in tau-2 IR. Tau-2 stained coronal section through the left (A) and right (C) hippocampus (X63), and the left (B) and right (D) amygdala (X63) in a bilaterally injected A β rat. E (X250) is a magnification of the area bracketed in C. No tau-2 IR is observed within the left hippocampus (A) or the left amygdala (B) although an A β deposit is visible (arrows). Note the neuronal tau-2 IR within the right hippocampus (C, E) and the right amygdala (D) in this same animal.

GFAP

Reactive astrocytosis was observed predominantly within the right hippocampus in A β treated rats ($p < 0.001$), compared to VEH treated rats (Figures 13C-F; 14E). The left hippocampus was significantly less affected ($p < 0.001$; Figure 14E). These histological changes were seen most consistently within the right hippocampus although other areas of the right hemisphere appeared to be also affected. However, it should be noted that the left hippocampus had occasionally moderate reactive astrocytosis (Figure 13A, B) in rats with the most severe gliosis in the right hippocampus (Figure 13C, D). Reactive astrocytes appeared to be also associated with the A β deposits, and with the cannula track in both treatment groups.

Figure 13. Laterality in GFAP staining. GFAP stained coronal section through the left (A, B) and right (C, D) hippocampus in a bilaterally injected A β rat, and through the right (E, F) hippocampus in a bilaterally treated VEH rat. Reactive astrocytosis is moderate in the left hippocampus (A, B), whereas prominent reactive astrocytosis is observed in the right hippocampus (C, D). No effect is observed in the VEH treated rat (E, F). B, D and F (X250) are magnifications of the areas bracketed in A, C and E (X63), respectively. The A β infused rat represents a rating of 1+ in the left hippocampus and a rating of 2+ in the right hippocampus. The VEH injected rat represents a rating of 0 in the right hippocampus.



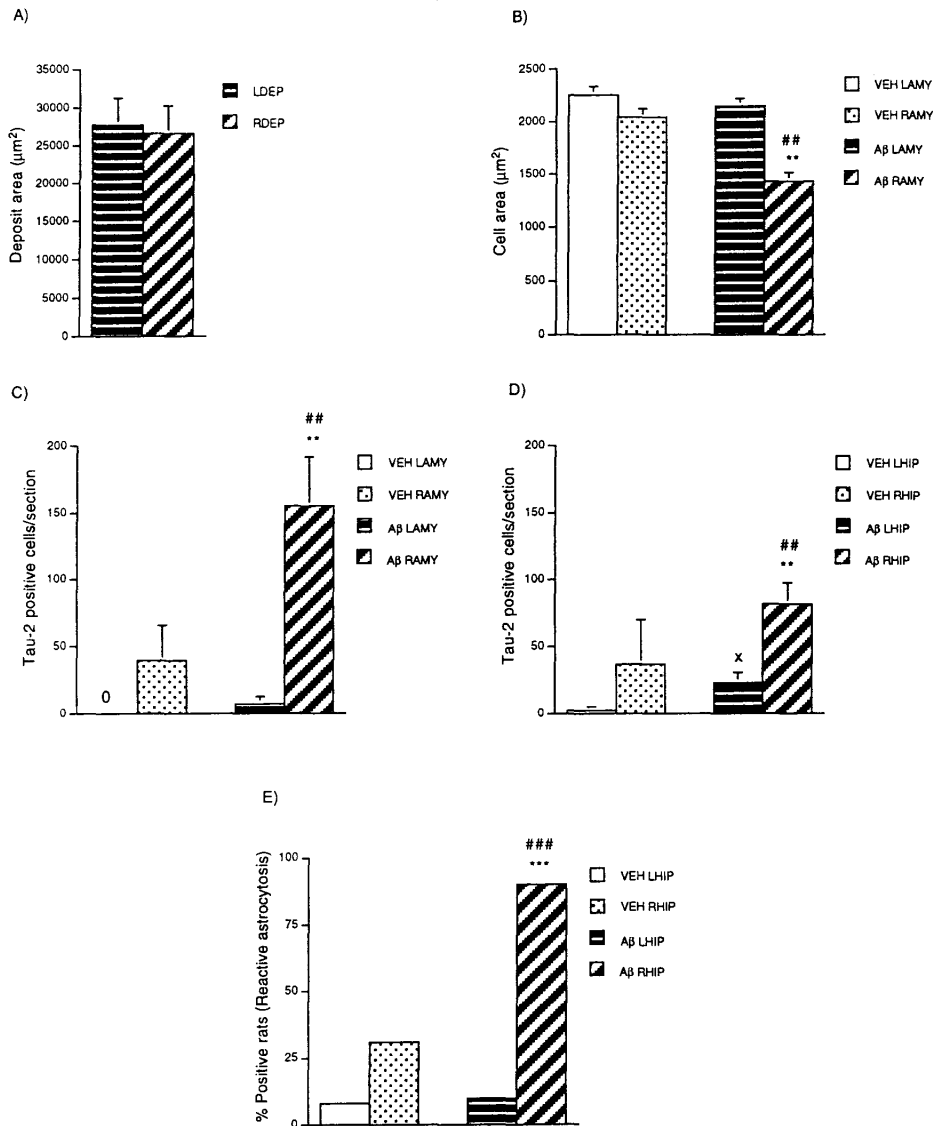


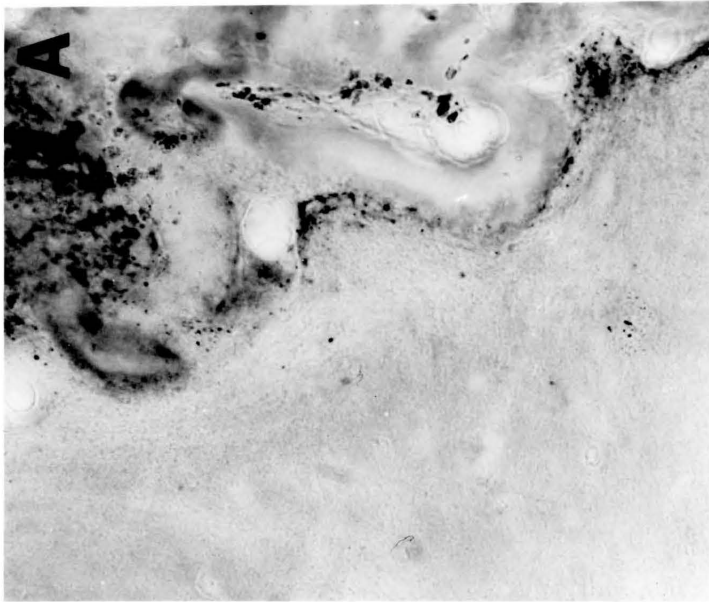
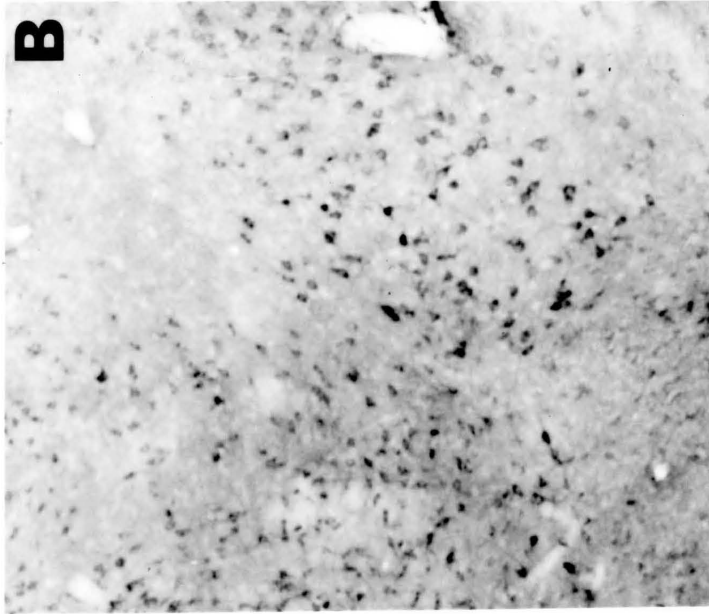
Figure 14. A β deposits, neuronal shrinkage, tau-2 and GFAP staining. A quantitative analysis of the size of the A β deposits (A) and neuronal shrinkage (B) within the right amygdala vs. the left amygdala. Each bar represents the mean + SEM of $n = 13-20$ rats. No significant difference was seen between the left and right amygdala in the size of the A β deposits. A quantitative analysis of neuronal tau-2 IR within the left and right amygdala and hippocampus is shown in C and D, respectively. Each bar represents the mean + SEM of $n = 13-19$ rats. A semi-quantitative analysis of reactive astrogliosis within the left and right hippocampus is illustrated in E. The data are presented as the percentage of positive rats (rating of ≥ 1) of total rats ($n = 13-20$) analyzed.

*** $p < 0.001$ [A β RHIP vs. VEH RHIP]; ### $p < 0.001$ [A β RHIP vs. A β LHIP]; ** $p < 0.01$ [A β RAMY or RHIP vs. VEH RAMY or RHIP]; ## $p < 0.01$ [A β RAMY or RHIP vs. A β LAMY or LHIP]; x $p < 0.05$ [A β LHIP vs. VEH LHIP]. Abbreviations: LHIP: left hippocampus; RHIP: right hippocampus; LAMY: left amygdala; RAMY: right amygdala; LDEP: A β deposits, left amygdala; RDEP: A β deposits, right amygdala.

Unilateral Injections into the Left Amygdala

Analysis of the areas of 10 of the largest magnocellular cells within the left and right basolateral amygdala in the A β treated rats revealed a significant difference [$t = 3.472$, $df = 6$, $p = 0.013$] between the left [cell area = $2309 \pm 92 \mu\text{m}^2$ (SEM)] and right amygdala [cell area = $1535 \pm 203 \mu\text{m}^2$]. There was a treatment effect of A β 25-35 in the induction of specific neuronal tau-2 staining within the amygdala [$F(1,8) = 6.122$, $p = 0.038$], but not within the hippocampus. Laterality in tau-2 neuronal staining was also observed in the amygdala [$F(1,8) = 55.102$, $p < 0.001$] (Figure 15A, B), but not in the hippocampus. *Post hoc* analysis revealed a significant increase in the number of tau-2 IR neurons within the right amygdala in the A β treated rats (267 ± 95) compared to the right amygdala in the VEH treated rats (78 ± 10 , $p < 0.05$). There was also a significant increase in the number of tau-2 IR neurons in the right amygdala vs. the left amygdala in the A β (right = 267 ± 95 ; left = 1 ± 1 , $p < 0.01$) and the VEH treated rats (right = 78 ± 10 ; left = 0 , $p < 0.05$), respectively. In all 4 rats injected with A β 25-35 into the left amygdala, reactive astrocytosis was observed in the right hippocampus but not the left hippocampus ($p = 0.014$). The regional distribution of these histological changes appeared similar to that observed following unilateral injections into the right amygdala (317), as well as following bilateral infusions.

Figure 15. Tau-2 IR within the right amygdala following injection of A β 25-35 into the left amygdala. Tau-2 stained coronal section (X63) through the left (A) and right (B) amygdala in an A β treated rat injected only into the left amygdala. No tau-2 IR is observed in the left amygdala (A), although an A β deposit is visible. Note the induction of neuronal tau-2 IR within the right amygdala (B) in this same animal.



Discussion

We have confirmed our previous finding (317) that injection of A β 25-35 into the right amygdala induces neuronal cytoskeletal changes and reactive astrocytosis within the amygdala, as well as at distal sites within the right hemisphere. Surprisingly, following bilateral injections, these changes were predominantly observed within the right amygdala and hippocampus whereas the same brain regions in the left hemisphere were significantly less affected. To our knowledge, this is the first report demonstrating a laterality in the histological effects of A β injected intracerebrally.

The reproducibility of A β toxicity *in vivo* has been inconsistent (42,91,99,101,102,178,180,314,317,320,354). This may be due to variations in: 1) the conformational state (25,269,273), dose, and sequence of A β ; 2) method of administration; 3) pathological endpoints measured; 4) what brain region and/or hemisphere is injected (present study); 5) postoperative interval; and, 6) species and/or strain used.

The anatomical distribution of senile plaques and neurofibrillary tangles in AD suggests that A β may act on nerve terminals to cause cytoskeletal alterations in axons, which ultimately lead to tangle formation within the perikarya (265). This notion is supported by the observation that the APP is predominantly located in the synaptic zone of neurons (301). Therefore, deposition of A β fibrils and their initial toxic effects would primarily occur near their site of generation, namely at the nerve terminals. These effects then would gradually spread to distal brain regions that send axons to the area of initial deposition. Our findings support this view.

As discussed previously (317), the increase in tau-2 IR suggests that A β 25-35 is causing a conformational change in tau proteins. These cytoskeletal changes are associated with neuronal shrinkage and reactive astrocytosis, and this may simulate the initial

histopathological changes that occur in AD. Reactive astrocytosis appears to be a more sensitive marker of toxicity than tau-2 IR and neuronal shrinkage, but the A β 25-35 effects are comparable using these three different markers (Figure 14). There appeared to be a good correlation within individual rats between the extent and regional distribution of reactive astrocytosis, cytoskeletal changes, and neuronal shrinkage.

Congo red positive (apple-green birefringence under polarized light) A β deposits were consistently observed at the site of injection. This indicates that the deposits were composed of a β -pleated sheet structure, the prominent conformation of A β in senile plaques. It can be argued that although the aggregation state of the peptide can be revealed by Congo red, A β immunostaining is necessary to prove the identity of the peptide. Unfortunately, there is no antibody commercially available that specifically detects A β 25-35. However, the characteristic apple-green birefringence was not observed in VEH treated rats but always in A β treated rats with proteinaceous deposits. The consistency and persistence of A β deposits within the brain likely depends on several factors, such as the method of administration, solvent, dose, volume, sequence of A β , and brain region injected. The presence of heparan sulfate proteoglycans has been shown to be important for consistent *in vivo* deposition of A β 1-40, and persistence of fibrillar A β in the rat hippocampus (321). Furthermore, A β 25-35 deposits within the rat nucleus basalis are degraded more rapidly than A β 1-40 deposits (102). A β *in vitro* develops protease resistance to degradation when polymerized into fibrils (252), and acetylcholinesterase (AChE) has been shown to promote the formation of and/or stabilize A β fibrils (150). Since the basolateral amygdala, adjacent to the injection site, contains very high levels of AChE (261), this proposed role of AChE may explain the consistency and persistence of the A β fibrils in the present study. Importantly, no hemispheric differences were observed in the size of the A β deposits (Figure 14A), indicating that the laterality in the histological effects

of A β 25-35 can not be explained by variations in fibril formation and/or degradation between the left and right amygdala.

Previously, we have injected the same dose of the reverse peptide (A β 35-25) into the right amygdala and performed cresyl violet, tau-2 and GFAP staining at 8 and 32 days postoperatively (317). No difference was seen between rats treated with VEH and the reverse peptide. A β 35-25 did not form proteinaceous deposits at the site of injection and did not induce significant tau-2 IR or reactive astrocytosis. Therefore, the histopathological effects of A β 25-35 are specifically caused by that particular amino acid sequence.

We tried to exclude experimental artifacts by measuring three different cellular variables. Staining with antibodies for abnormal conformation of tau, for GFAP, and cresyl violet staining all suggested a laterality in the effects of A β 25-35. Also, because both the left and right amygdala were treated in exactly the same manner, each side served as an internal control for the other side. In addition, unilateral injections into the left amygdala alone caused histopathology only within the right amygdala and hippocampus. This observation indicates that surgical damage to the right hemisphere is not the principal source for the histopathological changes. The observed laterality effect, therefore, is unlikely to be due to an experimental artifact. We are currently investigating injections into other areas of brain, as well as different strains of rats to determine if the laterality effect of A β 25-35 is brain region and/or strain specific.

At present, there is no obvious explanation for the laterality effects of A β 25-35. In four rats, unilateral injections into the left amygdala caused an induction in tau-2 IR within the right amygdala but not the left amygdala ($p < 0.01$; Figure 15A, B). Also, reactive astrocytosis was observed within the right hippocampus in all 4 rats but not the left hippocampus ($p = 0.014$). The regional distribution of these histological changes within the right hemisphere appeared to be similar to that observed following bilateral infusions, as well as following unilateral injections into the right amygdala (317). Since the left and right

amygdala are connected through the anterior commissure (276), A β 25-35 may be affecting the efferent terminals of neurons whose cell bodies originate within the right amygdala, and the laterality may be explained by hemispheric differences in secondary responses such as immune functions (249).

Some investigators have demonstrated lateralization in the involvement of the rat amygdala in learning and memory (15,45-47), and lesions of various brain regions in rats (36,61,121,184,262,281,329,342) and mice (10) have asymmetrical effects. Ligation of the right middle cerebral artery has been shown to lead to hyperactivity and reductions in norepinephrine and dopamine, whereas ligation of the left middle cerebral artery has no behavioral or neurochemical effects (281). Also, occlusion of the left or right middle cerebral artery has different effects on mean arterial pressure, renal sympathetic nerve discharge, and plasma norepinephrine levels (121). Suction lesions of the right frontal cerebral cortex induce hyperactivity (61,262), that is accompanied by a bilateral decrease in norepinephrine concentrations (262). However, identical lesions of the left cortex do not produce hyperactivity (61,262) or a decrease in norepinephrine concentrations (262). Left cortical ablations affect mainly the activity of serotonergic inputs to the right neocortex, whereas ablations of the right cortex influence the activity of the catecholaminergic inputs to the left cortex (10). Ablations of the prefrontal or parietal cortices lead to lateralized brain immunomodulation (342). Kainic acid injections into the right frontal cortex produce a significantly greater hyperactivity than identical injections into the left hemisphere (184). Striatal lesions with 6-hydroxydopamine lead to greater dopamine depletion in right-lesioned rats than in left-lesioned rats (329). Also, left and right 6-hydroxydopamine lesions of the medial prefrontal cortex differentially alter subcortical dopamine utilization and the behavioral response to stress (36).

Asymmetries have been observed in the histopathological hallmarks (52,235), and in the reductions in choline acetyltransferase activity (235,287) in individual cases of AD, but

preferential involvement of either hemisphere has not been demonstrated in groups of AD patients. Interestingly, asymmetry in the density of senile plaques diminishes with increasing neuropathological severity (235), suggesting that laterality may be more prominent in the initial stages of the disease. In AD, there is an extensive neuronal loss and shrinkage in all subdivisions of the amygdala (340), but no left-right hemispheric differences were detected in total neuron numbers in a study of 9 AD cases (340). However, hemispheric laterality in cerebral metabolism and perfusion in AD has been demonstrated in several studies. In most of these reports, there is no left-right preference in this asymmetry (37,68,95,113,129-132,254). On the other hand, some findings indicate a preferential involvement of the left (197,306) or the right hemisphere (239). In addition, early onset cases of AD have been associated with a greater prevalence of a left (247,306) or right (148) hemispheric dysfunction compared to late onset AD cases. Other studies have found no correlation between a hemispheric dysfunction and the severity of the illness, suggesting that if there is a laterality in AD it reflects subtypes of the disease more than a generalized phenomena (197,239).

Overall, we have demonstrated reproducible histopathological effects of intra-amygdaloid injections of A β 25-35 that in young inbred male Fischer-344 rats are found primarily within the right amygdala and hippocampus. The same brain regions within the left hemisphere are significantly less affected. These findings support the use of this rat model as a reliable tool to screen drugs that may alter the initial pathological events associated with deposition of A β fibrils containing the same β -sheet structure that is observed in senile plaques in AD. It may serve as a relatively inexpensive and efficient tool to screen drugs that may interfere with the fibrillogenesis of A β , enhance its degradation, and/or attenuate its toxicity. Furthermore, identification of the cause for the lateralized effect of A β 25-35 may prove valuable for understanding the etiology of AD and provide possible therapeutic strategies designed to slow the progression of AD.

CHAPTER V

TIME COURSE OF THE HISTOPATHOLOGICAL EFFECTS OF INJECTIONS OF AMYLOID- β 25-35 INTO THE AMYGDALA OF YOUNG MALE FISCHER RATS

Abstract

To examine the time course of the histopathological effects of bilateral injections of amyloid- β 25-35 (A β) and to determine if these effects are associated with a reduction in choline acetyltransferase (ChAT) activity and behavioral impairments, we injected A β (5.0 nmol) into the amygdala of young male Fischer rats. Control rats received vehicle infusions. For histological analysis, animals were sacrificed at 8, 32, 64, 96 and 128 days postoperatively (n = 21-33 per timepoint). A β induced neuronal tau-2 staining in the right amygdala and hippocampus but not in the same brain regions within the left hemisphere. A β also induced reactive astrogliosis and neuronal shrinkage within the right hippocampus and amygdala, respectively. As with tau-2, the same brain regions within the left hemisphere in the A β treated rats were significantly less affected. In addition, A β appeared to induce microglial and neuronal interleukin-1 β staining. The histopathological effects of A β peaked at 32 days postoperatively. These effects were not associated with a reduction in amygdaloid ChAT activity at 32 days postinjection. In a separate experiment, behavioral effects of bilateral intra-amygdaloid injections of A β were analyzed at 34-52 days postoperatively. In the open field, the treatment groups differed only in the numbers of rears emitted. A β treated rats emitted significantly more rears than vehicle treated rats ($p = 0.016$). There was no effect of A β in the Morris water maze or in the acquisition and

retention of a one-way conditioned avoidance response. These data suggest a laterality in the histopathological effects of $A\beta$ and that the effects of single injections are in part transient. These findings also suggest a direct association between plaque and tangle formation in Alzheimer's disease (AD), and support the use of this rat model to screen drugs that may alter the initial pathological events associated with AD, that occur before the manifestations of extensive behavioral impairments.

Introduction

The histopathological characteristics of Alzheimer's disease (AD) include senile plaques, reactive astrocytes and microglia, neurofibrillary tangles, neuronal shrinkage and cell loss in several brain regions. Senile plaques consist predominantly of amyloid- β ($A\beta$) 1-42 (103,214,233,285). It is derived from a large membrane spanning protein, the amyloid- β precursor protein (APP) (166), and is thought to play an important role in the pathogenesis of AD. Mutations in APP in some forms of familial AD (104,242) are associated with an elevated production of $A\beta$ (33,39,331). APP is overexpressed in Down's syndrome (248,291) and individuals with this disease invariably develop the neuropathological hallmarks of AD (23,187). Senile plaques appear at a younger age than do neurofibrillary tangles in Down's syndrome (100,212,291,358), suggesting that $A\beta$ may have a role in tangle formation. The main component of neurofibrillary tangles is paired helical filaments (168,335), which consist largely of the microtubule associated protein tau in an abnormal state of phosphorylation (171,182,355,356). *In vitro* (26,207) and *in vivo* (91,178,180,315,317) studies have demonstrated that $A\beta$ induces abnormal tau immunoreactivity (IR), suggesting an association between plaque and tangle formation in AD. The distribution of plaques and tangles in AD is such that $A\beta$ deposits are often located at the nerve terminals of neurons that contain tangles. This suggests that $A\beta$ may act on nerve terminals to cause cytoskeletal alterations in axons that ultimately lead to tangle formation within the perikarya (265). This notion is supported by the observation that the APP is predominantly located in the synaptic zone of neurons (301).

The proposed role for $A\beta$ in the pathogenesis of AD is further supported by the neurotoxicity of $A\beta$ *in vitro* (369,370), that includes amino acids 25-35 of the peptide (370). $A\beta$ toxicity in cell culture (273,284,368-370) depends on its aggregation state (25,220,269,273), and requires the assembly of $A\beta$ into amyloid fibrils composed of a β -

pleated sheet structure (26,144,203). The reproducibility of A β toxicity *in vivo* has been inconsistent (42,91,99,101,102,178,180,314,315,317,320,354). This may be due to variations in: 1) the conformational state (25,269,273), dose, and sequence of A β ; 2) method of administration; 3) pathological endpoints measured; 4) what brain region and/or hemisphere is injected; 5) postoperative interval; and, 6) species and/or strain used.

The transformation of resting astrocytes to reactive astrocytes is one of the earliest and most predominant responses of the central nervous system (CNS) to tissue injury. In the AD brain, reactive astrocytes are found in high abundance surrounding senile plaques (70,126,128,250). They colocalize with plaques at a relatively early stage in AD and apparently prior to the appearance of plaque associated dystrophic neurites (270). Glial fibrillary acidic protein (GFAP) (77) is a component of the glial intermediate filaments that form part of the cytoskeleton, and is found predominantly in astrocytes. GFAP levels in AD brains are increased 8 to 16 fold compared to control brains (21,60). Recent reports suggest that A β induces reactive astrocytosis *in vitro* (34,141,271) and we have demonstrated a similar effect *in vivo* (315,317).

Microglia are the brain's representatives of the immune system and express many leukocyte surface antigens, which are upregulated in AD (227). In the AD brain, microglia are known to associate with plaques (122,155,228), and inflammatory cytokines found in senile plaque regions include interleukin (IL) 1, IL-6, and tumor necrosis factor (62,117,309). Microglia seems to be the major source of IL-1 within the CNS, but this cytokine is also found in astrocytes and neurons (300). In rat, mouse, human and other species, IL-1 exists in two forms, IL-1 α (199) and IL-1 β (9) that are the products of two separate genes (40,97). Human IL-1 α and IL-1 β have 25% homology and appear to have a similar biological activity (63). IL-1 β *in vitro* stimulates the APP promoter (64), induces APP mRNA (59,89,108), stimulates production of the secreted form of APP (31), and enhances A β cytotoxicity in PC12 cells (82). Conversely, A β *in vitro* induces IL-1 β mRNA in astroglial

cells (59), enhances astro- and microglial secretion of IL-1 (4), and stimulates the proliferation and morphological transformation of microglia (4).

Relatively few studies have investigated the effects of A β injections on behavior and the experimental procedures vary substantially (41,65,85,102,221,223,224,244,314,334,354). Most of these studies have shown that intracerebral injections of A β cause behavioral alterations, except a study using the rat A β (354) and a report where A β by itself had no effect but potentiated the behavioral impairments induced by ibotenic acid (65). We have also previously reported that injections of A β into the basal forebrain had no significant behavioral effects (314).

The major pathological changes in AD are in regions of the medial temporal lobe, including the hippocampus, amygdala, entorhinal cortex and parahippocampal gyrus (265). Among these brain regions, the number of senile plaques has been reported to be highest in the amygdala (8). Some reports indicate that the amygdala is affected earlier in the disease than the hippocampal or cortical areas (158,258). Previously, we have observed that single A β 25-35 injections (5.0 nmol) into the right amygdala of rats produce progressive (8 vs. 32 days) cytoskeletal and astrogliotic reactions within the amygdala, and at distant brain regions that project to the amygdala (317). We have also reported on the laterality in the histopathological effects of bilateral intra-amygdaloid injections of A β 25-35 at 32 days postoperatively (315). To examine the time course of the histopathological effects of bilateral injections of A β and to determine if these effects are associated with a reduction in choline acetyltransferase (ChAT) activity and behavioral impairments, we injected A β (5.0 nmol) bilaterally into the amygdala of young male Fischer-344 rats. The data for the A β deposits, tau-2 IR, reactive astrocytosis and neuronal shrinkage at 32 days postoperatively has been previously reported (315).

Materials and Methods

Animals

Male Fischer-344 rats were obtained from the NIA colony at Harlan Sprague-Dawley (Indianapolis, IN). At the time of arrival, the rats weighed 250-300 g and were 3-4 months of age. The animals were housed individually, maintained on a 12 h light-dark cycle (lights on at 07:00 h) in a AAALAC approved facilities, had access to food and water *ad libitum*, and were habituated to their new environment for 2-3 weeks prior to surgery.

Surgery

Surgery was performed under sodium pentobarbital (50 mg/kg, intraperitoneally (i.p.); Butler, Columbus, OH) anesthesia. Atropine sulfate (0.4 mg/kg; Sigma, St. Louis, MO) and ampicillin sodium salt (50 mg/kg; Sigma) were injected intramuscularly once the animals were anesthetized. The animals received a bilateral injection of 5.0 nmol into each amygdala. Some of the animals were injected first into the right amygdala and subsequently into the left amygdala, while others were injected simultaneously into the left and right amygdala. A Kopf stereotaxic instrument was used with the incisor bar set at 3.3 mm below the interaural line. Injection coordinates measured from the bregma and the surface of the skull (AP - 3.0, ML \pm 4.6, DV - 8.8) were empirically determined based on the atlas of Paxinos and Watson (261). A volume of 3.0 μ l was administered over 6 min (flow rate 0.5 μ l/min) using a CMA/100 microsyringe pump (Carnegie Medicin AD, Solna, Sweden). The cannula was left *in situ* for 2 min following injection, and then was slowly withdrawn. Following surgery the animals were placed on a heating pad until they regained their righting reflex.

Drugs

A β 25-35 and A β 35-25 (BACHEM, Torrance, CA) were supplied as trifluoroacetic acid (TFA) salts. At the time of surgery, information was not available from the supplier regarding the amount of TFA per mg of the salt of the peptide. According to the supplier, there is not a direct stoichiometric relationship between the content of A β 25-35 and TFA, in other words it is not known how many mol of TFA there are in each mol of the TFA salt of A β 25-35. The peptide content was 77% (\pm 3%) with the remaining 23% consisting of TFA and H₂O, and the purity of the peptide was >98%. We assumed that there are 2 nmol of TFA per 1 nmol of A β 25-35, that is TFA content of 16.7% per mg of the salt. Recent information from the supplier indicates that the TFA content is actually 9.7%. The peptide and its respective vehicle (VEH; TFA, sodium salt; Sigma) were dissolved in Nanopure[®] water (H₂O) immediately before use and stored at 4°C between injections.

Animal Sacrifice and Tissue Preparation

For histological analyses, animals were anesthetized with sodium pentobarbital (100 mg/kg, i.p.), perfused transaortically at 8, 32, 64, 96 or 128 days postoperatively and the brains processed as previously described (317). Serial coronal sections (40 μ m) were cut and five series of sections at 0.2 mm intervals were saved for histological analysis of 1) cresyl violet, 2) tau-2, and 3) GFAP staining. Also, selected series were stained with IL-1 β and Congo red. The first series was immediately mounted on slides, dried, and stained with cresyl violet. The other series were placed in ethylene glycol cryoprotectant and stored at -20°C until used for immunohistochemistry.

For neurochemical analysis (ChAT activity), the animals were sacrificed by decapitation between 09.00-15.00 h in an area outside the animal room. The brains were removed and dissected over ice using a modification of the method detailed by Heffner et al. (133). Accordingly, serial 2.0 mm coronal sections were obtained. The amygdaloid

complex (4.0 mm) was obtained, frozen on dry ice and stored at -80°C until assayed.

Extensive histological analysis was not performed on the rats that were tested behaviorally but appropriate cannula placement and A β deposition was verified in several animals.

Histology

Cresyl violet and Congo red: Mounted sections were defatted in xylene and hydrated in ethyl alcohol and water series. Cresyl violet staining was performed as previously described (317). Congo red staining was performed for 1 h in a 50% ethanol solution containing 1% Congo red. The sections were then dipped in saturated lithium carbonate for 15 sec and subsequently washed in running water for 15 min.

Counterstaining was performed in Harris hematoxylin for 2 min, the sections were then rinsed in running water, and differentiated in 1% acid alcohol. Subsequently, the sections were washed in running water, dipped in ammonia water, and again washed in running water. The sections were then dehydrated in ethyl alcohol series and cleared in xylene. The tissue was subsequently coverslipped using a DePeX mounting medium.

Tau-2 and GFAP: Staining was performed as previously described (317). Briefly, sections (40 μ m) were incubated in tau-2 (Sigma, St. Louis, MO) primary antibody at a 1:500 dilution for 24 h at room temperature. An anti-mouse immunoglobulin (Ig) G secondary antibody (Vectastain ABC Elite kit, Vector Laboratories, Burlingame, CA) was used at a 1:2000 dilution. GFAP staining was performed the same way as the tau-2 staining. The GFAP antibody (Dako, Denmark) was used at a 1:500 dilution. The secondary antibody was a goat anti-rabbit IgG (Vector) diluted 1:1333. Omit sections for tau-2 and GFAP were obtained by omitting the primary antibody. According to product specifications, the biotinylated anti-mouse IgG (Vector) has 25% cross-reactivity with rat IgG. We were able to reduce this non-specific staining by diluting the secondary antibody.

Immunolabelled neurons in the omit sections were subtracted accordingly to establish a baseline.

IL-1 β : Performed the same way as GFAP staining. The anti-rat IL-1 β (Endogen, Cambridge, MA) was used at a 1:250 dilution. The secondary antibody was a goat anti-rabbit IgG (Vector) diluted 1:1333.

Behavioral Analyses

Animals were handled daily beginning four days prior to the first behavioral experiment, and daily throughout the experiments.

Open Field Activity: The open field was used to measure a neophobic response and subsequent exploratory behavior. The dimensions of the open field were 100 cm x 100 cm x 40 cm high. The walls were composed of varnished plywood. The floor was painted flat white and divided by thin black lines into 25 squares (20 x 20 cm). Four equidistantly spaced holes (3.5 cm diameter) were located in the four corner squares of the central nine squares. The open field was located in a sound-attenuated dark room and was illuminated by two 15 W fluorescent tubes positioned adjacent to the chamber, as well as by a 25 W fluorescent tube located under the elevated (7.5 cm) floor of the chamber. The animals were placed in the open field for 12 min and their behavior analyzed by means of a video monitor. The following behaviors were quantified: (1) the time to leave the center squares, (2) the number of wall and center squares entered, (3) the number of rears, (4) the number of nose pokes, and (5) the number of fecal boli.

One-Way Conditioned Avoidance Response (CAR): One-way avoidance conditioning is a spatial (place) learning and memory task that is motivated by an aversive unconditional

stimulus. The chamber was comprised of two identical compartments (50 cm long, 24 cm wide, and 30 cm high) separated by a 7.0 cm high serrated metal hurdle (0.5 mm thick). The ceiling, rear, and end walls were composed of white opaque plastic (Perspex) whereas the front wall was made of transparent Perspex. The grid floor consisted of stainless steel rods (3.0 mm diameter) spaced 1.0 cm apart. Illumination was provided by a 25 W fluorescent tube mounted outside the rear wall. A Grason-Stadler control panel and shock generator were used to deliver scrambled continuous constant-current (0.8 mA) shock.

Each animal was placed in the apparatus, close to and facing the end wall of the "shock" compartment. After a delay of 5.0 sec, continuous shock was delivered until the rat crossed the hurdle and entered the opposite side of the apparatus (the "safe" compartment). If a rat failed to escape the shock within 15 sec, it was placed in the safe compartment. The animal was left undisturbed for 20 sec, unless it returned to the "shock" compartment. If so, shock was delivered until the rat re-entered the "safe" compartment. After spending 20 sec in the "safe" compartment, the rat was removed from the apparatus and placed in its home cage for 5.0 sec, before the start of the next trial. Crossing the hurdle within 5.0 sec after placement in the "shock" compartment was scored as an avoidance response. Response latency was measured automatically by an elapsed timer. Testing was continued until criterion (9 avoidance responses in 10 consecutive trials) was attained. If a rat returned within 20 sec to the "shock" compartment after having made a CAR, the preceding CAR was not included as one of the criterion trials. Failure to enter the "safe" compartment before shock was delivered and returns to the shock compartment were scored as errors. All the rats reached criterion in a single session.

Retention of the one-way CAR task was examined 2 weeks later. The rats were treated in the same manner as during the acquisition phase and tested until criterion was attained.

Morris Water Maze: Spatial learning and memory were tested in the Morris water maze task. The maze consisted of a circular plastic tub (152 cm in diameter and 74 cm deep), painted flat white. A platform (9 cm in diameter) was placed halfway between the center of the pool and the edge, 1.5 cm below the surface of the water. The water (56 cm deep) in the pool was made opaque by the addition of powdered milk, and its temperature was 19-21°C. Extra maze cues were plentiful and kept consistent throughout the entire experiment. Data was gathered with a video tracking system (Chromotrack 3.01a, San Diego Instruments, San Diego, CA). A small video camera linked to a computer was mounted directly over the center of the maze. A small black dot was painted on the animal's head with a non-toxic marker because the camera visualizes a dark object on a light field. The computer calculated the animal's path length to platform and the latency to find the platform.

The animals were given 4 trials a day for 5 consecutive days, or a total of 20 trials. On each trial the animal was placed into the pool close to the edge in the middle of a quadrant. The first 4 days, the platform was located in the same quadrant. The 5th day, the platform was moved to the opposite quadrant. On the first trial the animal was placed into the pool in a quadrant next to the platform. In the 3 subsequent trials the animals were placed into the pool in the adjacent quadrants in a clockwise manner. A trial continued until the animal climbed onto the platform, or until 60 sec had elapsed. It was left on the platform for 60 sec prior to the start of the next trial. Upon completion of all four trials the rat was removed from the maze, dried with a towel and returned to its cage.

Neurochemical Analysis

Frozen brain tissue (-80°C) was weighed, thawed at 4°C and homogenized in ice-cold sodium phosphate buffer (75 mM, pH 7.4). ChAT activity was measured using a modification of the method of Fonnum (86). Briefly, 10 µl of homogenate were added to 10

μl of buffer substrate mixture. The mixture contained 49 volumes of buffer substrate (sodium phosphate, 75 mM, pH 7.4; NaCl, 600 mM; MgCl_2 , 40 mM; eserine, 2.0 mM; bovine serum albumin, 0.05%; choline iodide, 10 mM; and acetyl-CoA, 0.87 mM) and 1 volume of [^3H]acetyl-CoA (200 mCi/mmol, 0.5 mCi/ml; Du Pont NEN®, Boston MA). The samples were incubated for 30 min at 37°C, and then placed on ice. Newly synthesized radiolabelled acetylcholine (ACh) was extracted into 150 μl of sodium tetraphenylboron solution (75 mg/ml in 3-heptanone). The tubes were vortexed and after centrifugation, 100 μl of the organic layer were taken to measure [^3H]ACh using liquid scintillation spectrometry. The amount of radioactivity extracted from buffer, incubated in parallel, without tissue, was subtracted as blank. Activities were measured in triplicates. Protein measurements, in duplicates, were performed according to Lowry et al. (204).

Data Analysis

An image analysis system (NIH Image 1.49) was used to determine the size of the A β deposits and neuronal shrinkage within the left and right amygdala at different timepoints. The area of the A β deposits was measured at 0.2 mm intervals. These data failed a normality test and were, therefore, analyzed by a two-way analysis of variance (ANOVA) on ranks (SIGMASTAT, version 1.01; Jandel, San Rafael, CA) followed by a Newman-Keuls' multiple range test for *post hoc* comparisons. Quantitative analysis was performed on the cresyl violet stained sections at 32 and 128 days postinjection. The basolateral nucleus within the amygdala can be divided into parvicellular and magnocellular subnuclei based on the cytoarchitecture of the neurons. The cells within these subnuclei have a relatively uniform appearance and their boundaries are easily identified. The magnocellular division is located mainly rostral and medial to the parvicellular division. The area of 10 of the largest magnocellular cells (X400 magnification) within the left and right basolateral amygdala was measured in one cresyl violet stained section per animal slightly

rostral to the injection site, and we carefully chose sections at a similar coronal level. The average area of these 10 cells was calculated. The data based on this average cell area failed a normality test and were, therefore, analyzed by a two-way ANOVA on ranks followed by a Newman-Keuls' multiple range test for *post hoc* comparisons. Neuronal tau-2 IR in the left and right amygdala and hippocampus, and reactive astrocytosis in the left and right hippocampus were rated on a scale of 0-2+. An animal was considered positive if it exhibited $\geq 1+$ staining. These data were analyzed using a Fisher exact test, one-tail (SIGMASTAT). No statistical difference was discerned between the VEH groups at each of the timepoints so they were combined in the subsequent analysis. The rating of the tau-2 sections was based on the number of IR cells (X400 magnification), relative to omit sections, within the amygdala or hippocampus in a section at the injection site (0 = 0-5 cells/section; 1+ = 6-50 cells/section; 2+ = > 50 cells/section). The brain region that had higher cell counts was used for analysis. We have previously demonstrated (315) that there is a significant correlation between the number of tau-2 IR neurons within the amygdala and hippocampus ($r=0.833$, $p<0.001$). The rating of the GFAP sections was based on the complexity of astrocytic branching within the hippocampus (0 = resting astrocytes, few processes; 1+ = reactive astrocytes, moderate branching; 2+ = reactive astrocytes, extensive branching). In addition, a more detailed analysis of tau-2 IR was performed at 32 and 128 days postoperatively. Tau-2 IR neurons were counted in the left and right amygdala in six sections surrounding the injection site, and in six hippocampal sections including and caudal to the injection site. Tau-2 IR neurons were also counted in omit sections and subtracted accordingly. These data failed a normality test and, therefore, were analyzed using a two-way ANOVA on ranks for the amygdala and hippocampus separately, followed by a Newman-Keuls' multiple range test for *post hoc* comparisons. No statistical difference was discerned, in any of the parameters analyzed, between rats injected first into the right and subsequently into the left amygdala, and animals injected simultaneously into

the left and right amygdala, so they were combined in the subsequent analyses. The open field and the CAR data were analyzed by a t-test or a Mann-Whitney rank sum test when the data failed a normality test (SIGMASTAT). The Morris water maze data, when the platform was in its original position, was analyzed by a two-way ANOVA with repeated measures on one factor (days) followed by a Newman-Keuls' *post hoc* test (SIGMASTAT). A t-test was used to analyze the water maze reversal data. The ChAT activity data was analyzed by a two-way ANOVA on ranks because the data failed a normality test.

Experimental Design

Experiment 1: Histological effects of A β 25-35 at 8, 32, 64, 96 and 128 days postoperatively. The rats were injected first into the right amygdala and subsequently into the left amygdala, or simultaneously into the left and right amygdala. The dose of A β 25-35 was 5.0 nmol/3.0 μ l H₂O (each side). VEH treated animals were injected with 10.0 nmol TFA/3.0 μ l H₂O (each side).

Group#	n	Days	Treatment
1	9	8	VEH
2	12	8	A β 25-35
3	13	32	VEH
4	20	32	A β 25-35
5	13	64	VEH
6	19	64	A β 25-35
7	11	96	VEH
8	16	96	A β 25-35
9	11	128	VEH
10	17	128	A β 25-35

Experiment 2: Behavioral effects of bilateral intra-amygdaloid injections of A β 25-35 at 34-52 days postoperatively. The same dose was used as in Experiment 1 (5.0 nmol/3.0 μ l).

Group#	n	Treatment
1	10	VEH
2	13	A β 25-35

Experiment 3: Effects of bilateral intra-amygdaloid injections of A β 25-35 (5.0 nmol/3.0 μ l) on ChAT activity in the amygdala at 32 days postinjection.

Group#	n	Treatment
1	5	VEH
2	5	A β 35-25
3	6	A β 25-35

Results

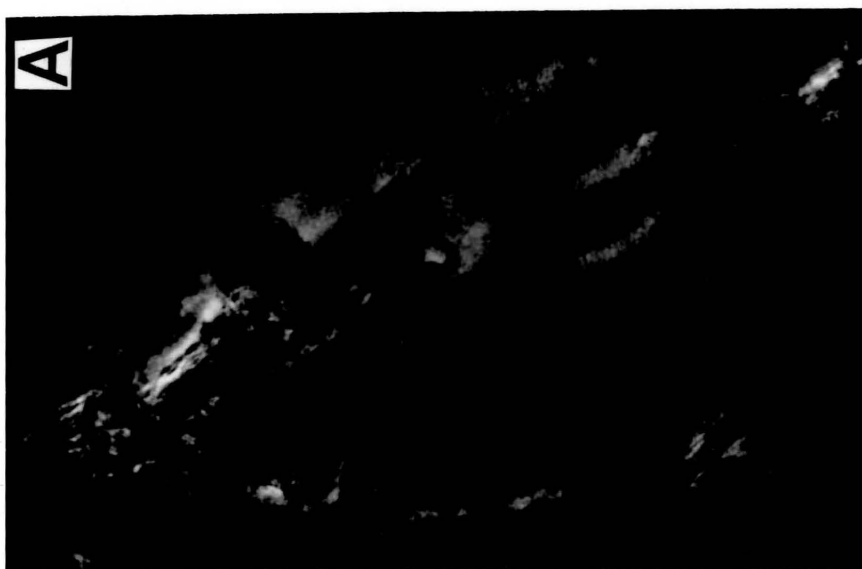
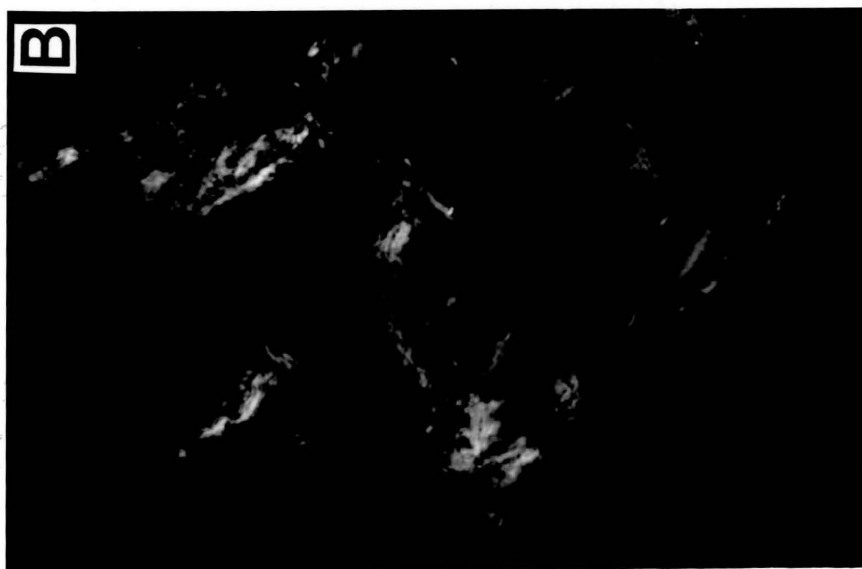
Experiment 1: Histological Effects of A β 25-35 at 8, 32, 64, 96 and 128 Days

Postoperatively.

A β deposits

Proteinaceous deposits were observed bilaterally in the amygdala of the A β 25-35 rats (Figures 16, 17). The location of the deposits did not vary between the left and right amygdala. The deposits were found consistently at the injection site immediately medial to the basolateral nucleus. The size of the deposits appeared to be less than the overall volume of the basolateral nucleus. These deposits were Congo red positive (apple-green birefringence under polarized light) similar to those we have observed following A β 25-35 injections into the ventral pallidum/substantia innominata (VP/SI) (314), and into the right amygdala (317). These deposits were seen in animals at all timepoints (8-128 days; Figure 17). Ninety percent of the injections resulted in A β deposits at the time of sacrifice. Two-way ANOVA of the area of these deposits within the left and right amygdala at different timepoints revealed a significant difference between the left and right amygdala [F(1, 158) = 5.261, p = 0.023] but there was no difference between timepoints [F(4, 158) = 1.774, p = 0.137], and no interaction between the two factors [F(4, 158) = 1.013, p = 0.402]. Also, *post hoc* pairwise comparisons between these two factors revealed no significant differences (Figure 17).

Figure 16. Congo red positive A β deposits at 32 and 128 days postoperatively. Congo red stained coronal sections (X160) through the left amygdala at the injection site in A β 25-35 treated rats at 32 days (A) and at 128 days (B) postoperatively. Note the Congo red positive birefringence under polarized light in the A β deposits at both 32 and 128 days postinjection.



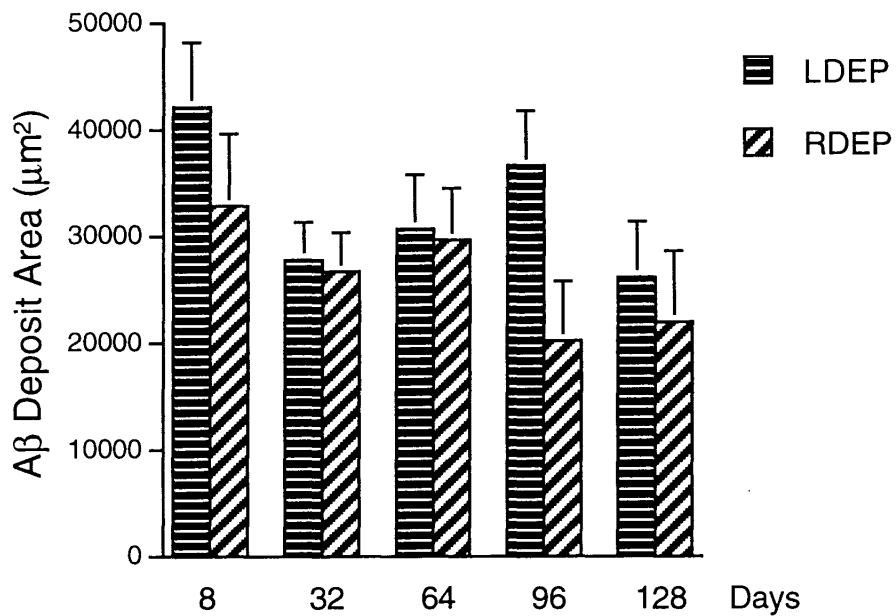


Figure 17. Size of the A β deposits within the left and right amygdala at 8, 32, 64, 96, and 128 days postoperatively. These deposits were Congo red positive (apple-green birefringence under polarized light). *Post hoc* analysis of the area of these deposits within the left and right amygdala at individual timepoints revealed no significant differences. Each bar represents the mean + SEM of n = 12-20 rats. LDEP: A β deposits, left amygdala; RDEP: A β deposits, right amygdala.

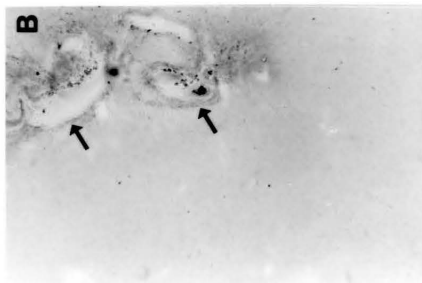
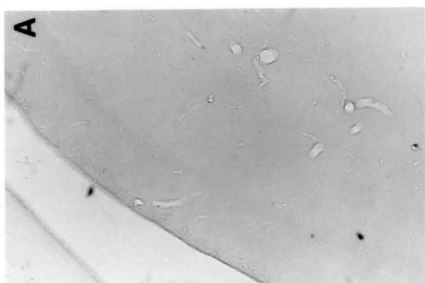
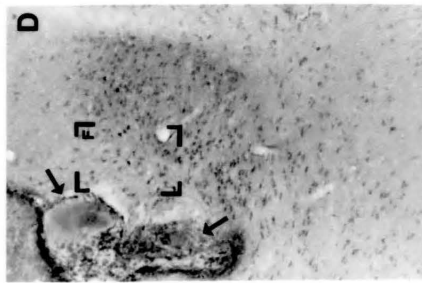
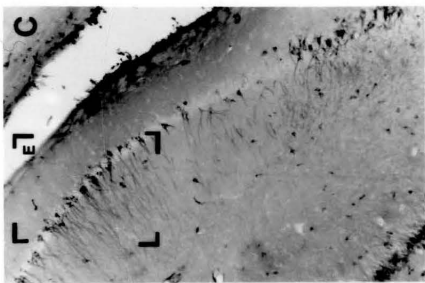
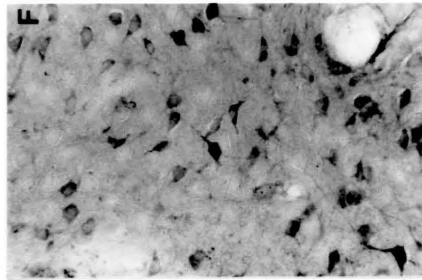
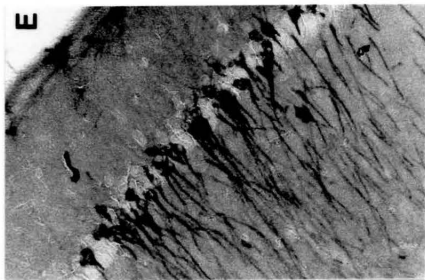
Tau-2

A semi-quantitative analysis revealed an increase in tau-2 staining that was observed predominantly within the right amygdala or hippocampus in the A β infused rats at 8 days ($p < 0.01$), 32 days ($p < 0.001$) and 64 days ($p < 0.01$) postinjection, compared to the VEH treated rats (Figures 18, 19). A β 25-35 increased tau-2 IR in neuronal perikarya and processes predominantly in the right amygdala and hippocampus. There also appeared to be an increase in tau-2 IR in other brain areas within the right hemisphere, such as the cingulate, parietal and pyriform cortices, hypothalamus, thalamus, globus pallidus, claustrum, substantia nigra, VP/SI, and the entorhinal cortex. These cytoskeletal changes peaked at 32 days postinjection (Figure 19). The left amygdala and hippocampus were significantly less affected in the VEH treated animals ($p < 0.01$), and the A β treated rats at 8 days ($p < 0.05$), 32 days ($p < 0.001$), and 64 days ($p < 0.01$) postoperatively.

A quantitative analysis at 32 and 128 days postoperatively revealed a similar effect as the semi-quantitative analysis. Two-way ANOVA for the amygdaloid tau-2 IR (Figure 20A) revealed a significant difference between rats sacrificed at 32 days vs. 128 days [$F(1, 112) = 6.195, p < 0.014$], and between treatments and/or hemispheres [$F(3, 112) = 19.234, p < 0.001$]. There was also a significant interaction between the two factors [$F(3, 112) = 5.306, p = 0.002$]. *Post hoc* pairwise comparisons between the two factors revealed a significant difference at 32 days between the left and right amygdala in the A β treated rats ($p < 0.01$) and in the right amygdala between the VEH and A β treated rats ($p < 0.01$). Also, in the A β infused rats the number of tau-2 IR neurons within the right amygdala differed at 32 days vs. 128 days postoperatively ($p < 0.01$). A similar pattern was observed within the hippocampus (Figure 20B). Two-way ANOVA for the hippocampal tau-2 IR revealed a significant difference between rats sacrificed at 32 days vs. 128 days [$F(1, 112) = 4.910, p < 0.029$], and between treatments and/or hemispheres [$F(3, 112) = 8.701, p < 0.001$]. There was also a significant interaction between the two factors [$F(3, 112) = 5.248,$

$p=0.002$]. *Post hoc* pairwise comparisons between the two factors revealed a significant difference at 32 days between the left and right hippocampus in the A β treated rats ($p<0.01$) and in the right hippocampus between the VEH and A β infused rats ($p<0.01$). Also, in the A β treated rats, the number of tau-2 IR neurons within the right hippocampus differed at 32 days vs. 128 days postoperatively ($p<0.01$).

Figure 18. Tau-2 IR at 32 days postinjection. Tau-2 stained coronal section through the left (A) and right (C) hippocampus (X63), and the left (B) and right (D) amygdala (X63) in a rat injected bilaterally with A β 25-35. E (X160) and F(X250) are magnifications of the areas bracketed in C and D, respectively. The hippocampal sections are substantially caudal (1.5 mm) to the injection site. The amygdaloid sections are at the injection site, where A β deposits (arrows in B and D) are visible. No tau-2 IR is observed within the left hippocampus (A) or the left amygdala (B). Note the neuronal tau-2 IR within the right hippocampus (C, E) and the right amygdala (D, F) in this same animal. This rat represents a rating of 0 in the left hippocampus and amygdala, and a rating of 1+ in the right hippocampus and amygdala.



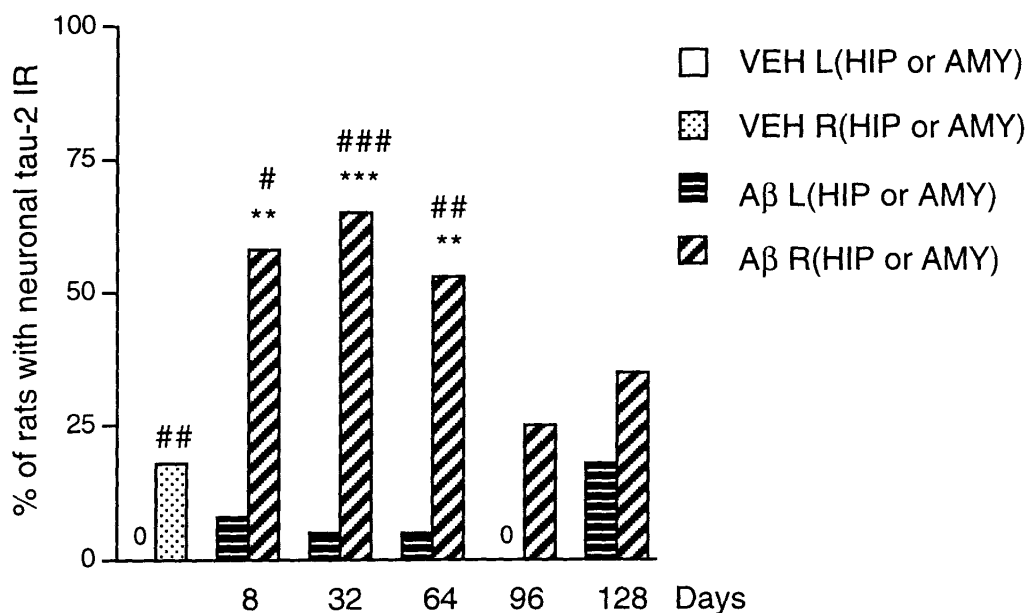


Figure 19. Time course of neuronal tau-2 IR within the left and right amygdala or hippocampus. Note the transient induction in tau-2 IR within the right amygdala or hippocampus in the A β treated rats. Note the lack of A β effect within the left hemisphere compared to the right hemisphere. No statistical difference was discerned between the VEH groups at each of the timepoints (n=9-13) so they were combined (n=58) in the subsequent analysis. The bars for the A β treated rats represent n=12-20. The data are presented as the percentage of positive rats (rating of $\geq 1+$) of total rats analyzed. Effects of A β in the right amygdala or hippocampus compared to VEH treated rats: ** $p < 0.01$; *** $p < 0.001$. Effects in the right amygdala or hippocampus compared to the left amygdala or hippocampus: # $p < 0.05$; ## $p < 0.01$; ### $p < 0.001$.

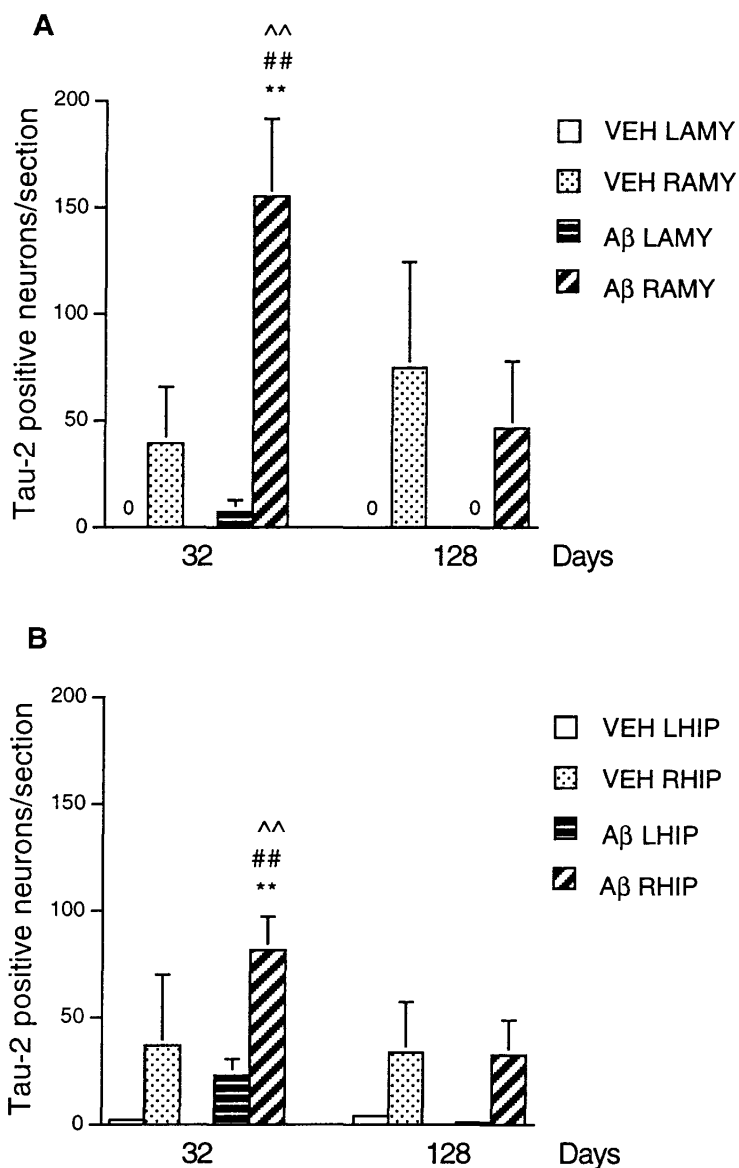


Figure 20. Neuronal tau-2 IR within the left and right amygdala (A) and hippocampus (B) at 32 and 128 days postinjection. Each bar represents the mean + SEM of tau-2 IR neurons from 6 sections (40 μ m). The bars for the VEH treated rats at 32 and 128 days represent $n = 13$ and 11, respectively. The bars for the A β treated rats at 32 and 128 days represent $n = 19$ and 17, respectively. Effects of A β at 32 days in the right amygdala or hippocampus compared to VEH treated rats: $**p < 0.01$. Effects of A β at 32 days in the right amygdala or hippocampus compared to the left amygdala or hippocampus: $##p < 0.01$. Effects of A β in the right amygdala or hippocampus at 32 vs. 128 days: $^^p < 0.01$.

GFAP

Reactive astrocytosis (Figures 21, 22) was observed predominantly within the right hippocampus in the A β treated rats at 8 days ($p < 0.001$), 32 days ($p < 0.001$), 64 days ($p < 0.01$), and 96 days ($p < 0.05$) postinjection, compared to VEH treated rats. The left hippocampus was significantly less affected in the VEH treated animals ($p < 0.01$), and the A β treated rats at 8 days ($p < 0.01$), 32 days ($p < 0.001$), and 64 days ($p < 0.01$) postoperatively. These histological changes peaked at 32 days postoperatively, and were seen most consistently within the right hippocampus although other areas of the right hemisphere appeared to be also affected.

Figure 21. GFAP IR at 32 and 128 days postinjection. GFAP stained coronal sections (X25) through the left (A) and right (B) hippocampus in a bilaterally injected A β 25-35 rat at 32 days postoperatively, and through the right hippocampus (C) in a bilaterally treated A β 25-35 rat at 128 days postinjection. D represents the right hippocampus in a VEH treated rat at 32 days postoperatively. E, F, G, and H are magnifications of the areas bracketed in A, B, C, and D, respectively. Reactive astrocytosis is moderate in the left hippocampus (A, E), whereas prominent reactive astrocytosis is observed in the right hippocampus (B, F). No effect is observed in the A β 25-35 treated rat at 128 days (C, G) or in the VEH treated rat (D, H). The A β 25-35 infused rat at 32 days postinjection represents a rating of 1+ in the left hippocampus and a rating of 2+ in the right hippocampus. The A β 25-35 treated rat at 128 days postinjection and the VEH injected rat at 32 days postoperatively represent a rating of 0 in the right hippocampus.

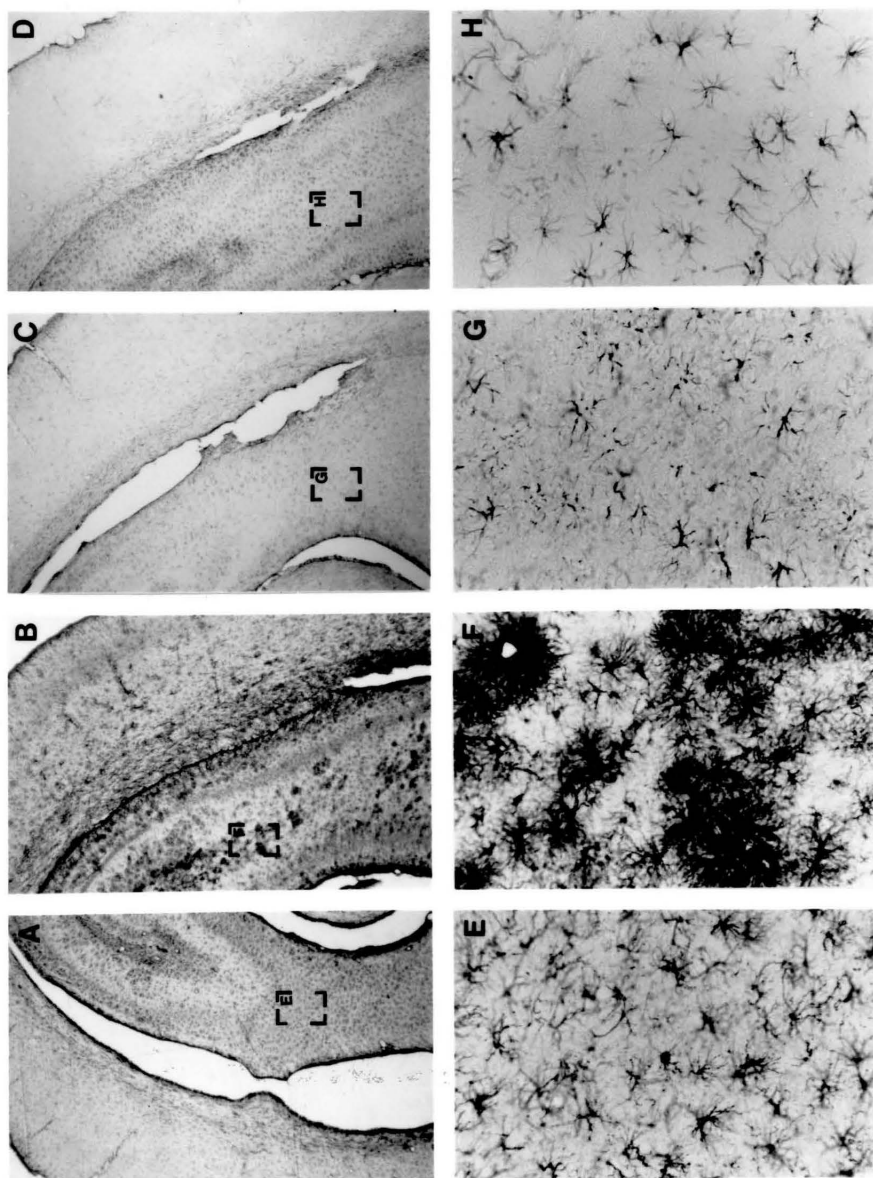


Figure 1. The hippocampus of the control group (A) and the hippocampus of the treated group (B) showing the granule cell layer (arrow) and the subgranular layer (arrowhead) of the hippocampus. The scale bars in the right column represent the magnification of the high-magnification photomicrographs (E-H).

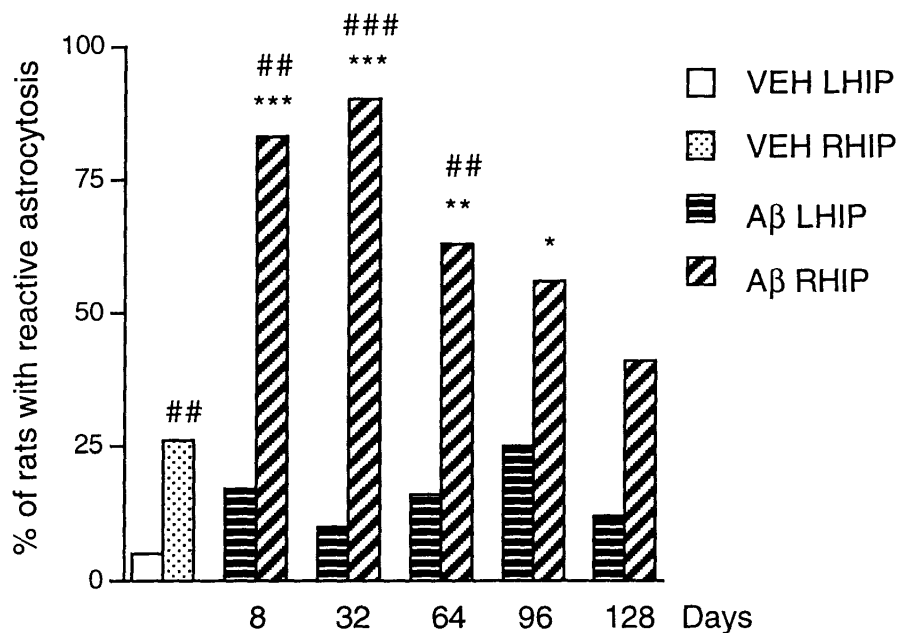


Figure 22. Time course of reactive astrocytosis within the left and right hippocampus. Note the transient induction in reactive astrocytosis within the right hippocampus in the A β treated rats. Note the lack of A β effect within the left hippocampus compared to the right hippocampus. No statistical difference was discerned between the VEH groups at each of the timepoints ($n=9-13$) so they were combined ($n=58$) in the subsequent analysis. The bars for the A β treated rats represent $n=12-20$. The data are presented as the percentage of positive rats (rating of $\geq 1+$) of total rats analyzed. Effects of A β in the right hippocampus compared to VEH treated rats: * $p < 0.05$; ** $p < 0.01$; *** $p < 0.001$. Effects in the right hippocampus compared to the left hippocampus: ## $p < 0.01$; ### $p < 0.001$.

Cresyl violet (CV)

All nuclei within the right amygdala appeared to be shrunken in the A β treated rats but the atrophy was most obvious in the large magnocellular neurons within the basolateral amygdala (Figure 23). A quantitative analysis was performed at 32 and 128 days postinjection of the area of 10 of the largest magnocellular cells within the basolateral amygdala (Figure 24). Two-way ANOVA revealed a significant difference between rats sacrificed at 32 days vs. 128 days [$F(1, 114) = 43.480, p < 0.001$], and between treatments and/or hemispheres [$F(3, 114) = 13.664, p < 0.001$]. There was not a significant interaction between the two factors [$F(3, 114) = 2.332, p < 0.078$]. *Post hoc* pairwise comparisons between the two factors revealed a significant difference at 32 days between the left and right amygdala in the A β treated rats ($p < 0.01$, 33% reduction in average cell area) and in the right amygdala between the VEH and A β treated rats ($p < 0.01$, 30% reduction). Also, in the A β treated rats the cell area at 32 days vs. 128 days differed in the left ($p < 0.01$) and right amygdala ($p < 0.01$). Furthermore, in the A β injected rats at 128 days the cell area within the right amygdala (13% reduction) differed from that in the left amygdala ($p < 0.05$). The neuronal atrophy appeared to extend into other brain regions within the right hemisphere, such as cortical areas. Cell bodies within the hippocampus overlapped and, therefore, analysis of cell shrinkage was not performed in that brain region. The A β induced neuronal shrinkage did not appear to be associated with extensive neuronal loss.

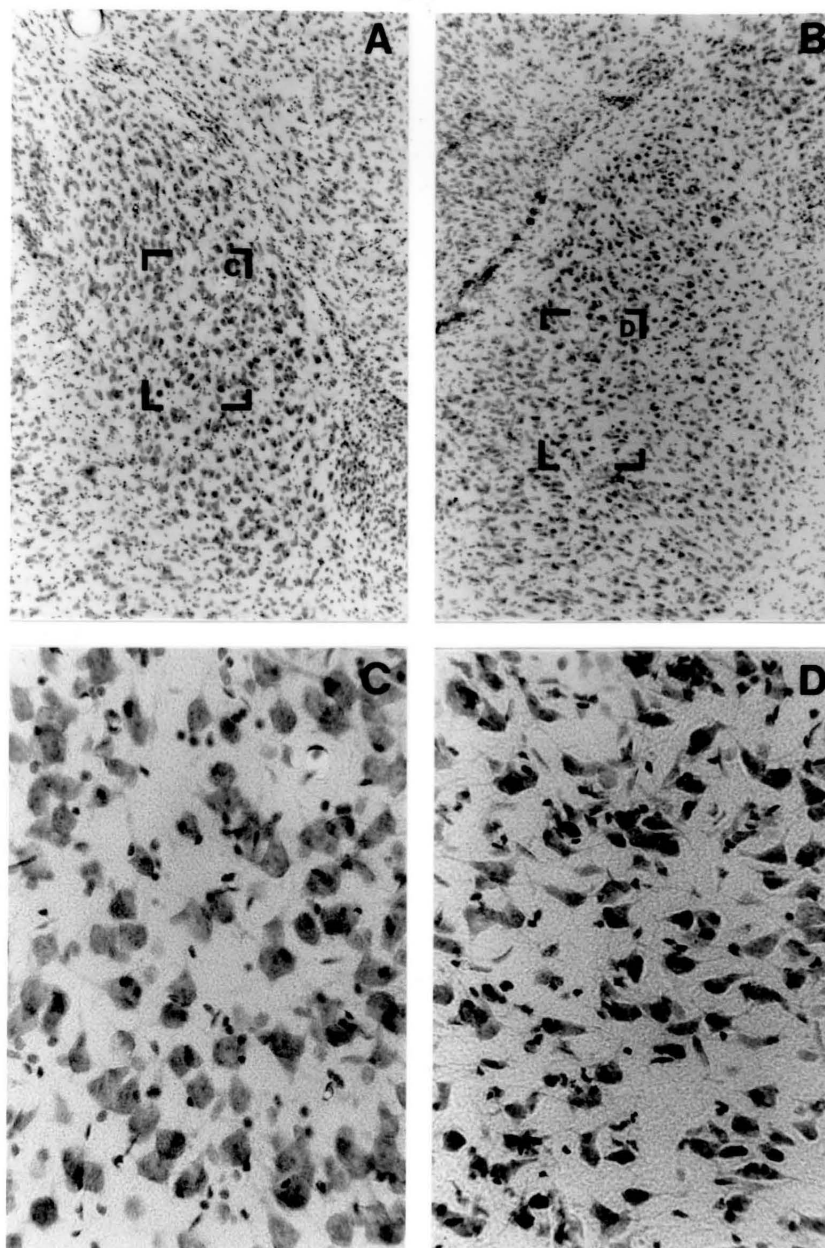


Figure 23. Cresyl violet staining at 32 days postinjection. Cresyl violet stained coronal section (X63) through the left (A) and right (B) amygdala slightly rostral to the injection site in a bilaterally injected A β rat, at the level of cell area measurements. C and D are magnification (X250) of the areas bracketed in A and B, respectively. Note the neuronal shrinkage within the right (B, D) as compared to the left basolateral nucleus (A, C). In this animal, the average area of 10 of the largest magnocellular cells was 1986 ± 187 (SD) in the left nucleus, and 1016 ± 178 in the right nucleus.

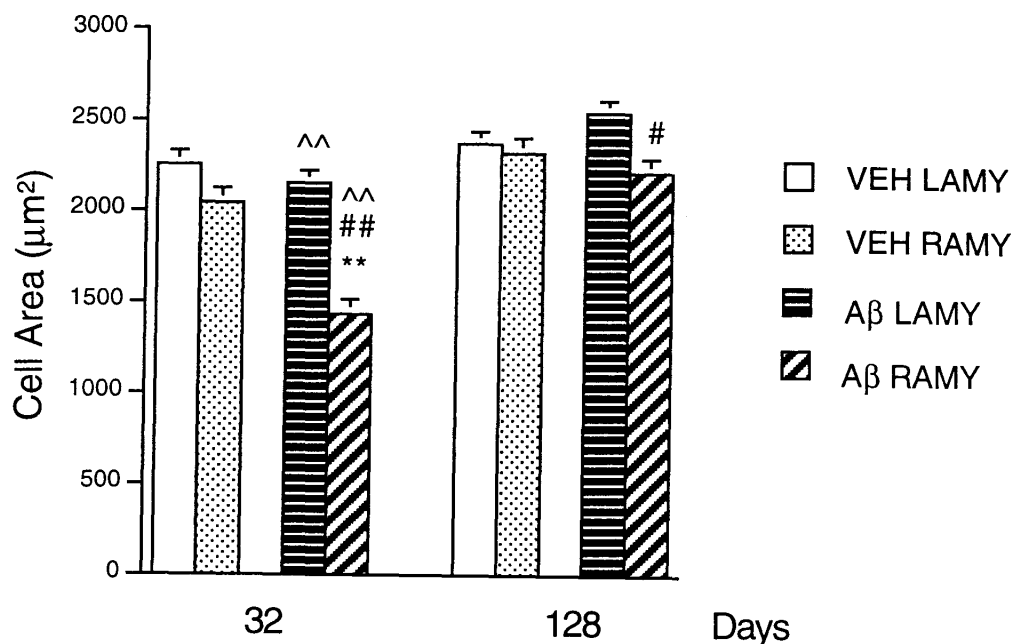


Figure 24. Neuronal shrinkage in cresyl violet stained sections within the right amygdala vs. the left amygdala at 32 and 128 days postoperatively. Each bar represents the mean + SEM. The bars for the VEH treated rats at 32 and 128 days represent $n = 13$ and 11 , respectively. The bars for the A β treated rats at 32 and 128 days represent $n = 20$ and 17 , respectively. Note the neuronal shrinkage within the right but not the left amygdala in the A β treated rats at 32 days and the partial reversibility of the effect of A β at 128 days postinjection. Effects of A β in the right amygdala compared to VEH treated rats: $**p < 0.01$. Effects of A β in the right amygdala compared to the left amygdala: $\#p < 0.05$; $\#\#p < 0.01$. Effects of A β in the left and right amygdala at 32 days vs. 128 days: $\wedge\wedge p < 0.01$.

IL-1 β

IL-1 β IR was predominantly observed in microglia but a less intense neuronal staining also was evident (Figure 25, 26). The microglia were seen in the vicinity of the cannula track, particularly at the injection site within the amygdala. Microglia were also prominent in the alveus and the molecular layer of the left hippocampus, and in the ependymal lining of the ventricles. In the A β injected rats, these microglia surrounded and infiltrated the A β deposits bilaterally in the amygdala. Reactive microglia appeared to be more prominent within the left than the right hippocampus at 8 and 32 days postoperatively in the A β treated animals. Laterality also was observed in neuronal IL-1 β staining. Neuronal staining appeared to be minimal in VEH treated rats. In A β treated rats, there appeared to be an evenly distributed induction in neuronal IL-1 β staining within the left amygdala and hippocampus. Minimal neuronal staining was observed within the right amygdala in the A β treated rats but several neuronal perikarya stained intensely within the right hippocampus. Further, the pattern of the most intensely IL-1 β stained neurons within the right hippocampus appeared to be similar to that of tau-2.

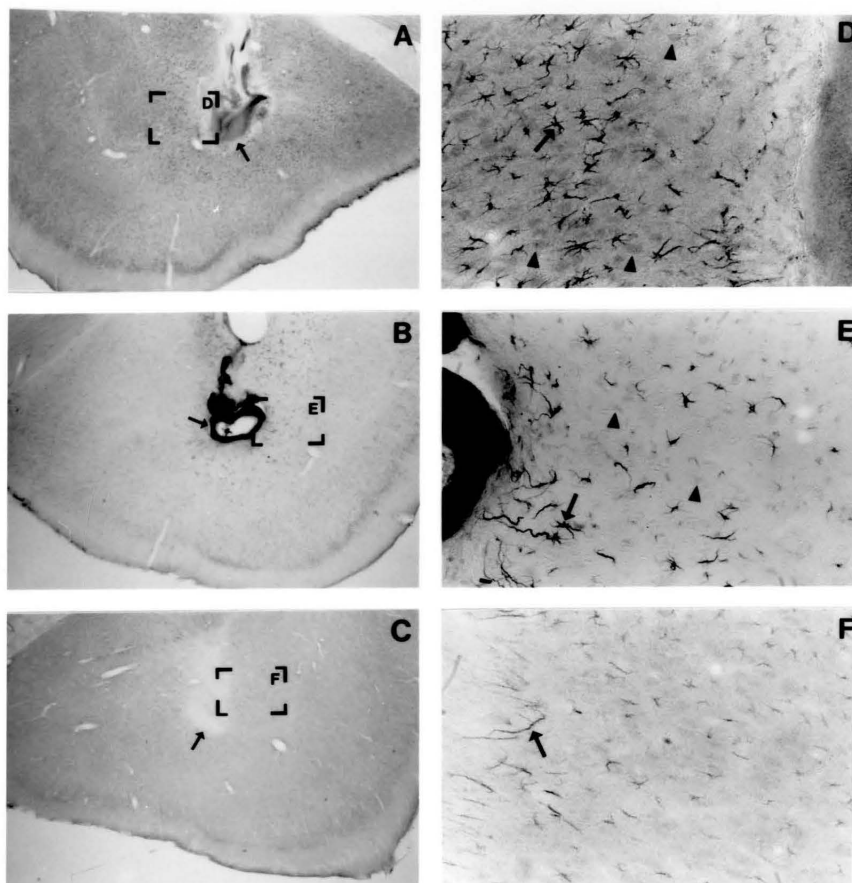


Figure 25. Amygdaloid IL-1 β IR at 32 days postinjection. Coronal sections (X25) through the injection site in the left (A) and right (B) amygdala in an A β 25-35 treated rat, and through the right amygdala in a VEH treated rat (C). A β deposits are visible in A and B (arrows), and the injection site in a VEH treated rat is visible in C (arrow). D, E, and F are magnifications (X160) of the areas bracketed in A, B, and C, respectively. Intense microglia-like IR (arrows in D and E) is observed surrounding and infiltrating the A β deposits both within the left (A, D) and right (B, E) amygdala. Note the more intense neuronal staining within the left amygdala (arrowheads in D), than in the right amygdala (arrowheads in E). Very little IL-1 β IR is observed in the VEH treated rat, except for a few microglia-like processes (arrow in F) at the tip of the injection site.

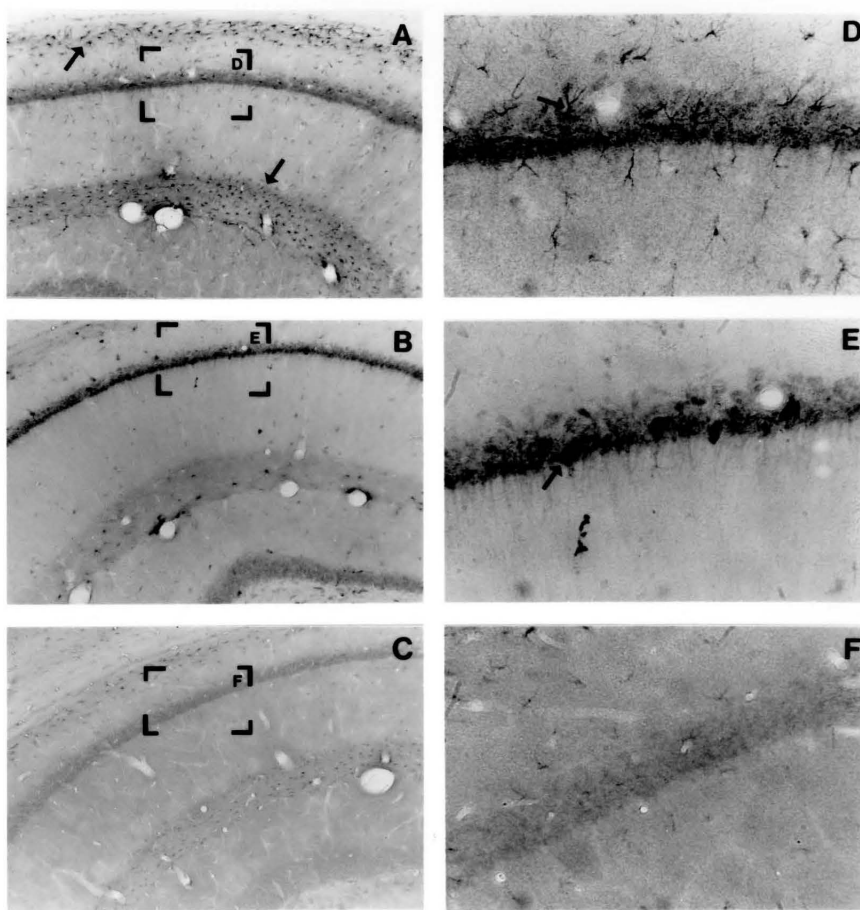


Figure 26. Hippocampal IL-1 β IR at 32 days postinjection. Coronal sections (X63) at the level of the injection site in the left (A) and right (B) hippocampus in an A β 25-35 treated rat, and in the right hippocampus in a VEH treated rat (C). D, E, and F are magnifications (X250) of the areas bracketed in A, B, and C, respectively. In the A β 25-35 treated rat, intense microglia-like IR (arrow in A) is observed in the alveus and the molecular layer of the left hippocampus (A) but not the right hippocampus (B). Also, moderate and evenly distributed induction in neuronal staining is observed within the left hippocampus (A, D) that is associated with microglia (arrow in D). More intense (arrow in E) unevenly distributed neuronal staining is observed within the right hippocampus (B, E). Minimal IL-1 β IR is observed in the VEH treated rat (C, F).

Experiment 2: Behavioral Effects of Bilateral Injections of A β 25-35 34-52 Days

Postoperatively.

Animals were injected bilaterally into the amygdala with A β 25-35 (5.0 nmol/3.0 μ l; n = 13) or its respective VEH (3.0 μ l; n = 10). Behavior in the open field (Figure 27A, B) and the acquisition of a one-way (spatial) CAR were analyzed 34-38 days postoperatively. Retention of the CAR was performed 2 weeks after initial testing (Table 1). In addition, the rats were tested in the Morris water maze 40-46 days postoperatively (Figure 28A, B). The animals were sacrificed at 58 days postinjection. Extensive histological analysis was not performed but appropriate cannula placement and the existence of A β deposits was verified in several animals.

There was no significant difference between the treatment groups in the number of center squares [VEH = 6.2 ± 1.4 (SEM); A β = 10.8 ± 2.2 ; $p = 0.119$], wall squares [VEH = 46.1 ± 11.8 ; A β = 74.5 ± 12.0 ; $p = 0.112$], or total squares [VEH = 52.3 ± 12.9 ; A β = 85.4 ± 13.0 ; $p = 0.091$] entered. Also, no significant difference was observed in the time (sec) to leave the center squares [VEH = 41.0 ± 11.6 ; A β = 25.9 ± 6.8 ; $p > 0.1$], the number of nose pokes emitted [VEH = 4.9 ± 0.8 ; A β = 6.1 ± 1.1 ; $p = 0.419$], or the number of fecal boli [VEH = 2.1 ± 0.8 ; A β = 1.2 ± 0.3 ; $p = 0.532$]. However, there was a significant difference in the numbers of rears emitted [VEH = 12.8 ± 2.3 ; A β = 21.4 ± 2.3 ; $p = 0.016$].

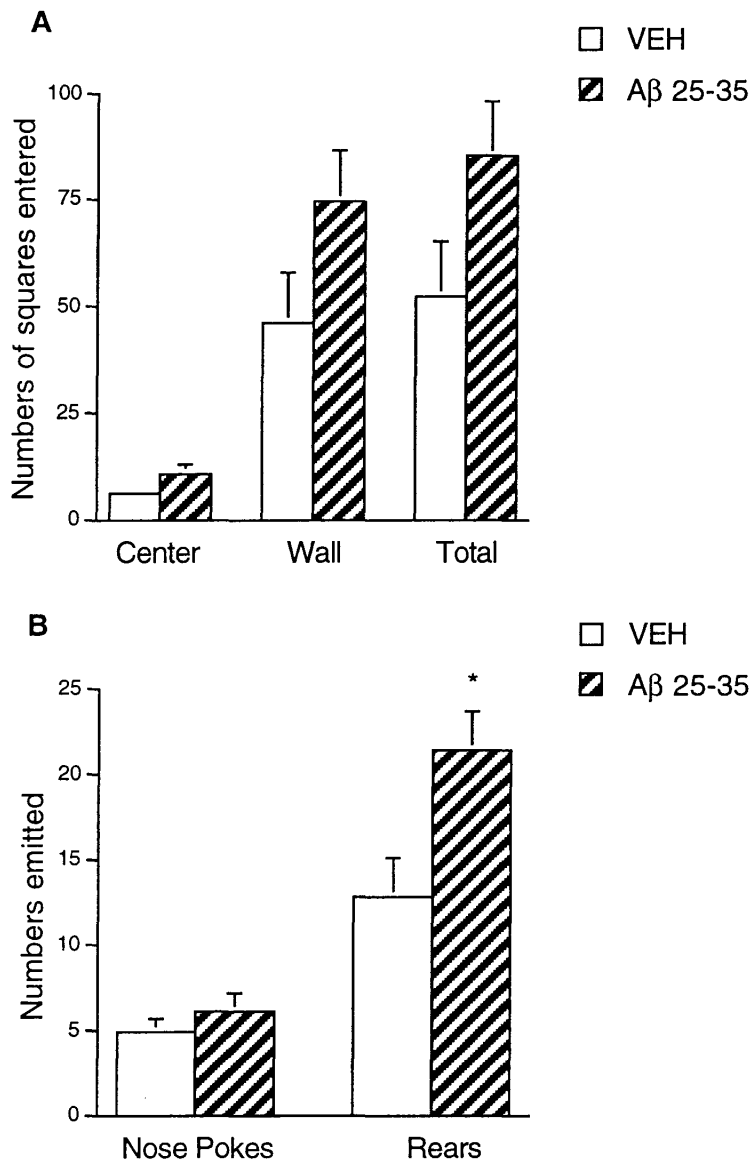


Figure 27. Behavior in the open field (12 min). Each bar represents the mean + SEM. (A) Bilateral injections of A β 25-35 (5.0 nmol) into the amygdala did not cause a significant difference in the number of center squares, wall squares, or total squares entered, when compared to VEH group. (B) There was a significant difference between the treatment groups in the numbers of rears emitted (* $p=0.016$), but not in the number of nose pokes emitted.

The one-way CAR acquisition did not reveal significant differences between the treatment groups in the latency (sec) of the first escape, in the number of trials required for the first CAR, in the number of trials to reach criterion, or in the number of errors committed (Table 1). Also, no treatment effect was observed in the retention of the one-way CAR.

<u>Treatment</u>	<u>Latency of the first escape (sec)</u>	<u>Trial number of the first CAR</u>	<u>Number of trials to reach criterion</u>	<u>Number of errors committed</u>
<u>Acquisition</u>				
VEH	4.8 ± 1.4	4.9 ± 0.5	15.0 ± 0.4	5.8 ± 0.3
A β 25-35	4.9 ± 0.9	3.8 ± 0.5	15.5 ± 0.7	5.7 ± 0.3
<u>Retention</u>				
VEH	2.9 ± 1.0	1.1 ± 0.1	10.9 ± 0.3	1.8 ± 0.2
A β 25-35	1.4 ± 0.2	1.2 ± 0.1	11.8 ± 1.0	1.9 ± 0.3

Table 1. One-way CAR acquisition and retention. The rats received bilateral intra-amygdaloid injections of A β 25-35 (5.0 nmol/3.0 μ l). Retention was examined two weeks following the acquisition. The data are presented as group means \pm SEM.

In the water maze there was no treatment effect. There was a time effect [time to find platform: $F(3, 60) = 49.505, p < 0.001$; distance swum to platform: $F(3, 60) = 39.088, p < 0.001$]. In addition, a treatment \times days interaction was close to being significant in the animals' path length swum to platform [$F(3, 60) = 2.708, p = 0.053$] but not in the animals' latency to find the platform [$F(3, 60) = 1.655, p = 0.186$]. No difference in swim speed was observed between the treatment groups (data not shown).

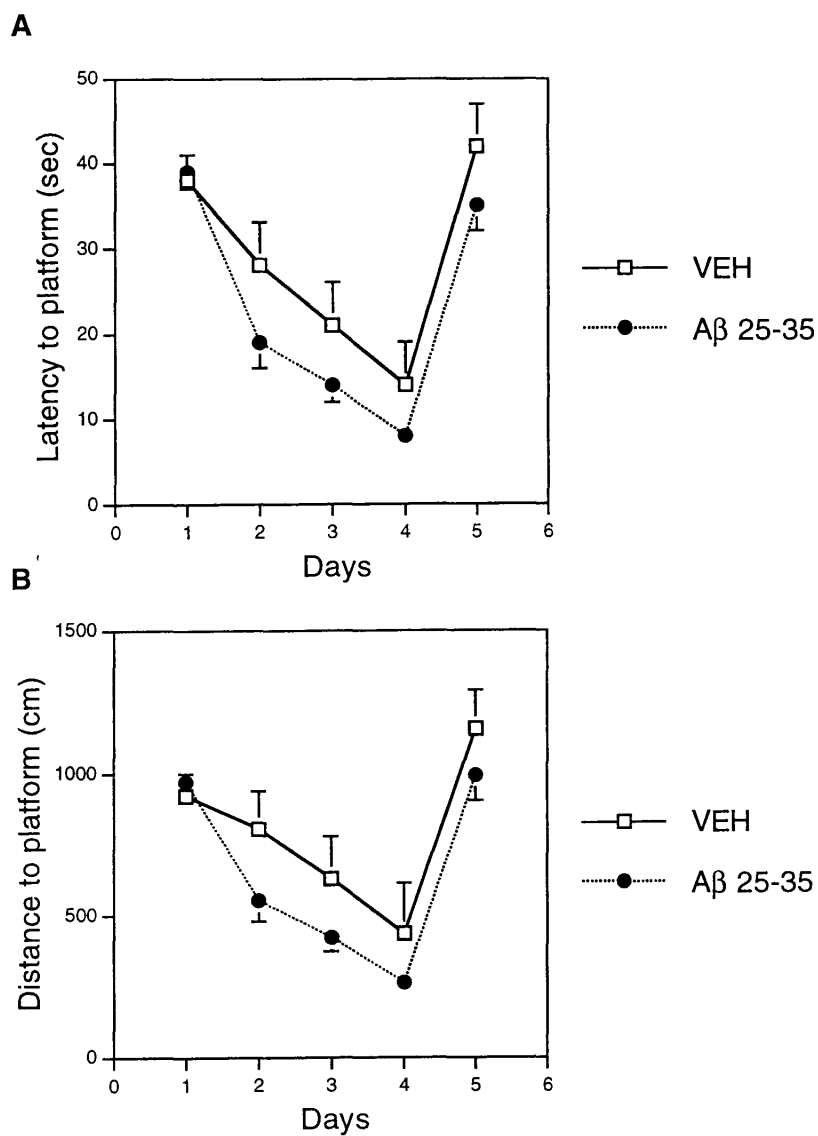


Figure 28. Behavior in the Morris water maze. Each point represents the mean + or -SEM of $n=10-13$. The first 4 days, the platform was located in the same quadrant. The 5th day, the platform was moved to the opposite quadrant. Bilateral injections of A β 25-35 (5.0 nmol) into the amygdala did not cause a significant difference in the latency to find the platform (A) or in distance traveled to the platform (B), when compared to VEH group.

Experiment 3: Effects of Bilateral Intra-Amygdaloid Injections of A β 25-35 (5.0 nmol/3.0 μ l) on ChAT Activity in the Amygdala at 32 Days Postoperatively.

Two-way ANOVA did not reveal significant differences in ChAT activity between treatment groups or hemispheres, or a significant interaction between the two factors (Table 2).

<u>Treatment</u>	<u>ChAT Activity (nmol ACh/h/mg protein)</u>	
	<u>Left Amygdala</u>	<u>Right Amygdala</u>
VEH	107.0 \pm 6.0	107.2 \pm 7.3
A β 35-25	110.1 \pm 5.8	109.0 \pm 4.0
A β 25-35	107.0 \pm 5.1	106.6 \pm 5.6

Table 2. Amygdaloid ChAT activity. The rats received bilateral intra-amygdaloid injections of A β 25-35 (5.0 nmol/3.0 μ l), A β 35-25 (5.0 nmol/3.0 μ l) or their respective vehicle, and were sacrificed 32 days postoperatively. The data are presented as group means \pm SEM.

Discussion

We have confirmed our previous finding (317), that intra-amygdaloid injection of A β 25-35 induces neuronal cytoskeletal changes and reactive astrocytosis within the amygdala as well as at distal sites. In addition, these changes were associated with neuronal shrinkage and alterations in IL-1 β IR. Furthermore, the histopathological effects of A β 25-35 were in part transient, and were predominantly observed within the right amygdala and hippocampus whereas the same brain regions in the left hemisphere were significantly less affected.

We have previously discussed the relevance of the distal histological effects of A β 25-35 to the etiology of AD (317). We have also elaborated previously on the correlation between the laterality effects of A β 25-35, and hemispheric asymmetries in the histopathological hallmarks, cerebral metabolism, and perfusion in AD (315).

The cytoskeletal changes observed following intra-amygdaloid injections of A β 25-35 were associated with neuronal shrinkage and reactive astrocytosis. This may simulate the initial histopathological changes that occur in AD, and suggests a direct association between plaque and tangle formation in AD. Reactive astrocytosis is a consistent response to neurotoxic insults, and has been observed to reveal dose, time, and region dependent patterns of neurotoxicity at toxicant dosages below those that cause light microscopic evidence of cell loss or damage (255). Our findings support this because reactive astrocytosis appeared to be a more sensitive marker of toxicity than tau-2 IR and neuronal shrinkage although the extent, regional distribution, and reversal of these histological effects appeared to be comparable using these three different markers.

Microglia appear to be the major source of IL-1 within the CNS, but this cytokine is also found in astrocytes and neurons (300). A β 25-35 *in vitro* induces IL-1 β mRNA in astroglial cells (59). A β 1-42 enhances *in vitro* astro- and microglial cell secretion of IL-1,

and stimulates the proliferation and morphological transformation of microglia (4). These *in vitro* findings are in accordance with the intense IL-1 β glial staining surrounding and infiltrating the A β deposits bilaterally within the amygdala. This observation correlates with the association of senile plaques in AD with IL-1 positive microglia (62,117,309). Laterality in IL-1 β IR was predominantly observed in neurons. Neuronal staining was minimal in VEH treated rats but in A β treated rats there appeared to be an induction in neuronal IL-1 β IR within the left hippocampus and amygdala that seemed to be rather evenly distributed within the neurons. In the right hemisphere in A β injected rats, intense neuronal IL-1 β IR was predominantly observed in hippocampal neuronal perikarya. Peptidergic neurotransmitters are always synthesized in the cell bodies and then transported to the nerve terminals. Inhibitors of axonal transport such as colchicine are often used to visualize peptide IR cell bodies in animal brains. Because A β 25-35 induces cytoskeletal changes it may attenuate the axonal transport of IL-1 β and presumably other peptides. This leads to accumulation of IL-1 β within neuronal cell bodies and a concomitant loss of staining in other neuronal compartments, which is what our results indicate within the right hippocampus. This hypothesis is supported by the observation that in adjacent sections from the same animal, the pattern of hippocampal neuronal IL-1 β and tau-2 staining appeared similar. However, double labeling of neurons with antibodies against IL-1 β and tau-2 would be necessary to verify this scenario. This presumed reduction in neuronal IL-1 β release may exacerbate A β toxicity because IL-1 β attenuates excitatory amino acid induced neurodegeneration *in vitro* (323), and A β potentiates *in vitro* neurotoxicity of excitatory amino acids (218). This scenario also suggests that the apparent induction in neuronal IL-1 β synthesis within the left amygdala and hippocampus may attenuate A β toxicity within these brain regions.

Congo red positive A β deposits were consistently observed at the site of injection, suggesting that these deposits retain their β -pleated sheet structure, the toxic conformation

of A β , several months following injection into the rat amygdala. The A β deposits were extremely resistant to degradation because volumetric analysis did not reveal significant reduction in their size up to 128 days postinjection (Figure 17). It has been demonstrated *in vitro*, that A β develops protease resistance to degradation when polymerized into fibrils (252). Microglia in culture scavenge A β (5) and microglia-like phagocytes have a role in A β clearance following intraventricular infusions of A β 1-40 (92). Microglial activation takes place in a rather stereotypic pattern where there is a transformation of resting microglia into activated cells, which in their end stage resemble phagocytic cells. We did not observe phagocytic IL-1 β positive microglia, supporting the findings from the quantitative measurements that the amygdaloid A β deposits are resistant to proteases that are necessary to cleave large peptide fragments for phagocytosis to occur. The consistency and persistence of A β deposits likely depends on several factors, such as the method of administration, solvent, dose, volume, sequence of A β , and brain region injected. The presence of heparan sulfate proteoglycans has been shown to be important for consistent *in vivo* deposition of A β 1-40 and persistence of fibrillar A β in the rat hippocampus (321). Furthermore, A β 25-35 deposits within the rat nucleus basalis have been reported to be degraded more rapidly than A β 1-40 deposits (102). Acetylcholinesterase (AChE) has been demonstrated to promote the formation of and/or stabilize A β fibrils (150). This proposed role of AChE may explain the consistency and persistence of the A β fibrils in the present study, because the basolateral amygdala adjacent to the injection site contains very high levels of AChE (261). Analysis of variance revealed that overall the size of the A β deposits was greater on the left than on the right side ($p=0.023$), suggesting that there may be hemispheric differences in the degradation and/or fibril formation of A β . However, *post hoc* comparison of the size of the deposits at each of the postoperative intervals investigated failed to reveal any significant differences. Therefore, these findings suggest that the

laterality and the partially transient effects of A β can not be explained by differences in the size of the A β deposits *per se* at any individual timepoint.

The histopathological effects of A β 25-35 peaked at 32 days postoperatively. This indicates that the effects of single injections are in part transient even though the A β deposits are resistant to degradation. Chemically induced gliosis has been shown to be often transient in nature with the time course of both the onset and decline in GFAP varying markedly from toxicant to toxicant (256). The A β deposits were always surrounded by reactive microglia and astrocytes. It is likely that this encapsulation renders the deposits biologically inert. The histological effects of A β are, therefore, likely to be initiated early following injection, and an inflammatory response triggered by glial activation in the vicinity of the deposits may have a role in A β induced pathology. However, it should be noted that reactive glia were also associated with the cannula scar in VEH treated rats. Lesion studies have demonstrated brain lateralization in immunomodulation (249). This asymmetry may in part explain laterality in the histological changes caused by A β , because the deposits may act as antigens to activate the immune system. It is possible that the histological effects of A β may not be as reversible in old animals that have compromised metabolic functions. However, these transient effects do not exclude the use of young animals injected with A β as a model for the initial pathological changes that occur in AD. Based on observations in Down's syndrome patients, the histopathology in AD is likely to begin at an early age and it is important to slow its progression in its infancy. An animal model using young rats in which the pathological changes peak within 2 months following injection may, therefore, serve as a relatively inexpensive and efficient tool to screen drugs that may interfere with the fibrillogenesis of A β , enhance its degradation, and/or attenuate its toxicity.

Electrolytic lesions of the amygdaloid complex (51,73,163,305), lesions of the central nucleus (118,160,350), or of the lateral and basal nuclei of the amygdala (159) enhance exploratory behavior of rats in the open field test. No significant difference was

observed between the treatment groups in any of the parameters examined in the open field, except that the A β treated rats emitted significantly more rears than their respective VEH group (Figure 27B; $p < 0.016$). Lesions of the amygdala have been shown to be associated with behavioral impairments in active avoidance learning (30,286), but do not appear to impair spatial learning in the Morris water maze (58,330). Lesions of the hippocampus severely disrupt spatial learning (257,278) and this impairment has been shown to be potentiated by amygdaloid lesions (1,267). Therefore, because intra-amygdaloid injections of A β induce histopathological changes not only within the amygdala but also at distal sites including the hippocampus, it was considered appropriate to use the water maze test. No behavioral differences were observed between the treatment groups in the one-way CAR (Table 1) or in the water maze (Figure 28 A,B). Overall, the lack of severe behavioral impairments in this study may be explained by the lack of extensive neuronal loss and/or by the laterality in the histopathological effects of A β . The left hemisphere may compensate for the impairments within the right hemisphere.

The amygdala receives a prominent cholinergic input from the nucleus basalis (35,363), and ChAT activity has been reported to be severely reduced within the amygdala in AD patients (258,287,288). Measurements of amygdaloid ChAT activity were performed to investigate if the cytoskeletal changes and neuronal shrinkage within the amygdala were associated with a reduction in ChAT activity. No differences were observed in amygdaloid ChAT activity between the treatment groups (Table 2). These data suggest that A β induced histopathological changes within the amygdala are not associated with a loss of cholinergic terminals projecting from the nucleus basalis. Alternatively, A β induced damage of cholinergic terminals within the amygdala may lead to compensatory increase in ChAT production within the cell bodies in the nucleus basalis. To investigate these possibilities, it would be necessary to analyze ChAT activity within the nucleus basalis and/or to stain for ChAT on brain sections.

Overall, we have demonstrated reproducible histopathological effects of intra-amygdaloid injections of A β , that may simulate the initial histopathological changes that occur in AD. Alternatively, this approach models the *in vivo* histopathological effects of deposition of A β fibrils containing the same β -sheet structure that is observed in senile plaques in AD. Furthermore, in young inbred male Fischer-344 rats these changes are in part transient, and are predominantly observed within the right amygdala and hippocampus. Identification of the cause for the lateralized effect of A β 25-35 may prove valuable by giving insight into possible therapeutic strategies to slow the progression of AD. These findings support the use of this rat model as a reliable tool to screen drugs that may alter the initial pathological events associated with AD, that occur before the manifestations of extensive behavioral impairments.

CHAPTER VI

GENERAL DISCUSSION

We have demonstrated that unilateral intra-amygdaloid injections of amyloid- β ($A\beta$) 25-35 in Fischer-344 rat induce the appearance of abnormal tau proteins both within the ipsilateral amygdala, as well as at distant sites as recognized by the tau-2 and Alz-50 antibodies (317). These cytoskeletal changes were progressive (8 vs. 32 days) and associated with reactive astrocytosis. Studies have reported local effects of $A\beta$ injections immediately surrounding the injection site in rat cerebral cortex and hippocampus (91,178,180), but this is the first report on $A\beta$ injections into the rat amygdala and their distal effects.

We also examined the time course of the histopathological effects of bilateral injections of $A\beta$ 25-35 and sought to determine if these effects were associated with a reduction in choline acetyltransferase (ChAT) activity and behavioral impairments (315,316). $A\beta$ 25-35 induced abnormal neuronal tau-2 and interleukin-1 β staining, and reactive astrocytosis within the amygdala, as well as at distal sites such as the hippocampus. These histological changes were associated with neuronal shrinkage within the amygdala. Surprisingly, these changes were predominantly observed within the right hemisphere with the left hemisphere significantly less affected. The effects of $A\beta$ 25-35 peaked at 32 days postoperatively. These histopathological effects were not associated with a reduction in amygdaloid ChAT activity at 32 days postinjection. This is the first report that demonstrates a laterality in the histopathological effects of $A\beta$, and it also shows that the effects of single intra-amygdaloid injections are in part transient.

In a separate experiment, behavioral effects of bilateral intra-amygdaloid injections of A β 25-35 were analyzed 34-52 days postoperatively. In the open field test, the treatment groups differed only in the numbers of rears emitted ($p=0.016$). There was no treatment effect in the Morris water maze or in the acquisition and retention of a one-way conditioned avoidance response. Thus, in young rats, A β induced histopathological changes are not accompanied by major behavioral deficits, perhaps because the pathology is restricted to the right hemisphere. The lack of extensive neuronal loss may also explain the lack of behavioral deficits.

Together, these findings suggest a direct association between plaque and tangle formation in Alzheimer's disease (AD), and support the use of this rat model to screen drugs that may alter the initial pathological events associated with AD, that occur before the manifestations of extensive behavioral impairments.

In an attempt to evaluate this model of the initial histopathological effects in AD, it is necessary to compare it to reports of other animal models of this disease. It is clear that the early animal models of AD (84,134,195), that attempted to mimic the loss of cholinergic neurons in the basal forebrain in AD (12,57,351), are of limited use as a model of AD, because they lacked the broad spectrum of pathological features of the disease. Neurons producing norepinephrine, serotonin, dopamine, glutamate, γ -aminobutyric acid, somatostatin, neuropeptide Y, corticotrophin releasing factor, substance P, and other neuromodulators are also affected in AD (54,56,157,177,288,327). Because of these broad deficits in neurotransmitter systems, it is unlikely that AD can be treated by transmitter replacement therapy alone. A more feasible approach is to develop compounds that interfere with neuritic plaque and tangle formation, the major histopathological hallmarks of the disease.

The discovery of A β as a major component of senile plaques and subsequent findings of its *in vitro* neurotoxicity led to reports examining the *in vivo* effects of A β by

microinjections of A β into the brains of rats and monkeys. The toxic effects of A β *in vivo* have been inconsistent (42,91,99,101,102,178,180,191,274,314-317,320,354). This may be due to variations in: 1) conformational state (25,269,273), dose, and sequence of A β ; 2) method of administration; 3) pathological endpoints measured; 4) what brain region and/or hemisphere is injected; 5) postoperative interval; and, 6) species and/or strain used. It can be argued that because A β 1-42 is the most prevalent form of A β in senile plaques, it is appropriate to use that peptide for injections into brain instead of A β 25-35. However, the main problem with using A β 1-42 is its insolubility in physiological solvents. Therefore, there is a risk of potentially toxic solvents interfering with the properties and effects of A β 1-42. On the other hand, A β 25-35 is readily soluble in H₂O and acquires the same β -pleated sheet conformation as A β 1-42, which is the toxic conformation of A β . In addition to injections of A β alone, coadministration of heparan sulfate proteoglycans has been shown to be important for consistent *in vivo* deposition and persistence of fibrillar A β in the rat hippocampus (321). Our studies represent the only comprehensive time course study that has been reported on the histopathological effects of A β , and shows in contrast to other studies (102,321) that A β deposits can be observed consistently without coadministration of other compounds and that these deposits are not degraded following intracerebral administration in the rat. The reason for these discrepancies may be due to variations in some of the experimental procedures mentioned above. For example, acetylcholinesterase (AChE) has been shown to promote the formation of and/or stabilization of A β fibrils (150), and the basolateral amygdala, that is adjacent to the injection site in our studies, has one of the highest levels of AChE of any brain structure (261).

Before our reports, a few *in vivo* studies had investigated the potential association between plaque and tangle formation in AD by examining the effects of A β injected into the brain on tau IR (42,91,99,178,180,274). Some of these studies indicated that A β can induce the appearance of abnormal tau proteins in the vicinity of the injection site (rat

cerebral cortex and hippocampus) (91,178,180). Other studies failed to show any effect (42,99,274). For the most part, these *in vivo* studies were only qualitative or descriptive in nature. Our reports are the first to attempt to quantify A β induced effects by counting neuronal tau IR cells, to demonstrate distal cytoskeletal and astrogliotic changes, and to investigate the time course of these histopathological effects of A β . Overall, these findings suggest an association between plaque and tangle formation in AD. It should be noted that the rodent brain does not spontaneously form senile plaques or neurofibrillary tangles (50), the main histopathological hallmarks of AD. Human and rodent A β differ in three amino acids. As a consequence, the rat A β is much less fibrillogenic than the human A β (72) and that may explain the lack of senile plaques in rodents. Rodent tau differs also from human tau (3) and that may explain the lack of tangles in rodents. Tangles are formed in several human neurodegenerative diseases besides AD (357) and may be a marker of specific form of cell injury, such as slow neurodegeneration, in some but not all mammals.

The effects of A β on tau IR may be mediated through an increase in intracellular calcium. A β has been shown to increase intracellular calcium (7,218), and calcium influx in cultured rat hippocampal neurons caused by glutamate induces tau IR as recognized by the antibodies Alz-50 and 5E2 (216). Protein kinases are generally activated by increases in intracellular calcium and several of those have been shown to phosphorylate different sites on tau proteins (238). Therefore, A β may increase the phosphorylation of tau proteins through an activation of kinases mediated by an increase in intracellular calcium. The activities of some phosphatases that may dephosphorylate tau proteins have been shown to be decreased in AD (111,311). Therefore, A β 25-35 may also be decreasing the dephosphorylation of tau proteins through an inhibition of phosphatases.

There have been reports on the effects of intracranial A β injections on behavior. These behavioral studies are difficult to compare because the experimental procedures varied substantially. Because of the nature of behavioral experiments it is necessary to

support alterations in behavior with neurochemical and/or histological findings. It is interesting to note that although several of these studies demonstrate behavioral impairments following A β injections, few of these reports investigated the time course of the histopathological and/or neurochemical changes caused by A β , to determine the most appropriate postoperative interval to perform behavioral testing. It is possible that the behavioral effects observed in some of these studies may be due to physical displacement of brain tissue by high doses of A β rather than actual histopathological effects. The behavioral effects obtained in our model were modest. In the three tests performed, there was a significant difference between the treatment groups only in the number of rears in the open field. These results were not surprising mostly because of the lateralized effects of A β . There is a consensus in the field of behavioral neuroscience that bilateral lesions are often necessary to obtain behavioral deficits, because of compensation by the unlesioned side.

Although there have been several reports on transgenic approaches to model AD (53,98,137-139,143,145,146,186,188,206,236,263,277,364) only two of these reports appear to be promising (98,145). These two mouse models contain age dependent compact congophilic A β plaques similar to those observed in AD, and in one of these models these changes are associated with behavioral impairments (145). The first of these models to be described overexpresses amyloid- β precursor protein (APP) containing the APP717 mutation that is associated with familial AD (98). These mice express 8-10 fold the normal level of APP and have large numbers of amyloid plaques in the hippocampus, corpus callosum, and cerebral cortex that first appear at 6-9 months of age. The majority of the plaques are associated with reactive astrocytes and dystrophic neurites. The neocortices of these mice exhibit diffuse synaptic and dendritic loss, and contain diffusely activated microglia. This histopathology is region specific and age dependent as in AD, despite expression of the APP transgene throughout the brain. These results suggest that region and/or cell type specific vulnerability of the aging brain may dictate the pattern of plaque formation. A significant

limitation of this model is the lack of neurofibrillary tangles, and their absence may reflect species variations in neuronal response to injury. Also, in this model there have been no reports of behavioral impairments associated with the histopathological changes.

The other promising transgenic mouse model (145) overexpresses a mutated form of APP695 that has been found in a Swedish family with early-onset AD (242). These mice express this human form at 5-6 fold the levels of endogenous mouse APP, that remains unchanged between 2 and 14 months of age. These mice demonstrate normal learning and memory in the Morris water maze and the Y maze at 3 months of age but are impaired by 9 to 10 months of age. A 5 fold increase in A β 1-40 and a 14 fold increase in A β 1-42 is associated with these behavioral deficits. Numerous Congo red positive A β plaques are present in mice with elevated A β levels. The distribution of the histopathological changes is reportedly similar to that observed by Games et al. (98). The authors indirectly control for impairments in motor performance but it is possible that the behavioral deficits may be caused by visual impairments. This possibility, overlooked by the investigators, is based on the impairment of the transgenic mice in swimming to a visible platform. Interestingly, other transgenic approaches that are not associated with AD-like histopathology (146,364), or that have only diffuse A β deposits that are not congophilic and lack neuritic involvement (139), have been reported to lead to deficits in spatial memory in the Morris water maze (236,364) and in the Y maze (146,236). As in the model by Hsiao et al. (145), both of the models tested in the water maze showed significant impairments in initial learning (236,364), suggesting that gene dosage effect or position effect of transgene integration but not the A β deposition *per se* may lead to behavioral deficits. Furthermore, as in the Hsiao model, the mice with the diffuse A β deposits (139) exhibited greater latency in locating a visible platform in the water maze (236). This observation further suggests that visual impairments may account for differences in performance. Interestingly, APP and A β are present at low levels in normal lenses and A β has toxic effects on lens epithelial cells

(94). APP is synthesized in retinal ganglion cells and transported into the optic nerve, in which C-terminal amyloidogenic fragments accumulate (237), and there is an increased APP IR in retinal ganglion cells of the elderly (198). Together, these findings emphasize the importance of investigating possible vision impairments in APP transgenic animals.

In contrast to other APP transgenic models, the expression of the APP variant in these two promising models (98,145) substantially exceeds those of the endogenous mouse APP gene. Because of the various proposed roles for APP, it is likely that a 5-10 fold increase in APP has several biological effects beside an increase in A β production and subsequent plaque formation. There is no compelling evidence that sporadic AD is associated with a global increase in APP expression (115). It is also possible that insertion of multiple copies of any gene construct may impair cognitive function, because inheritance of relatively small amounts of extra genomic DNA in human imbalanced translocation karyotypes results in mental retardation (364). The behavioral effects may also be due to position effect of transgene integration that may interfere with the expression of other genes.

Even though several *in vitro* studies have tested various hypotheses for the mechanism by which A β exerts its toxic effect, these hypotheses have not been adequately tested in *in vivo* situations. It is important to continue to explore the *in vivo* effects of A β by direct injections into brain. Findings from these studies may help elucidate the sequence of pathogenic events that ultimately lead to AD. In conjunction with transgenic models they may also distinguish between the biological effects of A β and elevated levels of APP, respectively.

Animal models can be evaluated in terms of construct validity, face validity and predictive validity. We believe that our model has construct validity because we are injecting a fragment of a peptide, that may play a prominent role in the etiology of AD, into a brain region that is affected early in the disease. The most appropriate face validity of an

animal model of AD would be the demonstration of senile plaques associated with reactive astrocytes, neurofibrillary tangles, and neuronal shrinkage and cell loss in the same brain regions as observed in AD. It is unlikely, however, that this effect can be obtained using a single injection of A β into rat brain, but this approach may demonstrate the early histopathological changes in AD. In my opinion, the present rat model has a relatively high face validity because of the neuronal shrinkage and the induction of abnormal tau proteins and reactive astrocytes in brain regions where the primary and early histopathological changes in AD are observed. Currently, no definitive transgenic animal models are available that resemble all aspects of AD, although plaque-like A β deposits have been observed (98,145), that in one model are associated with behavioral impairments (145). The predictive validity of the present rat model, as well as current transgenic models, will ultimately determine their usefulness in screening potential drugs for therapy.

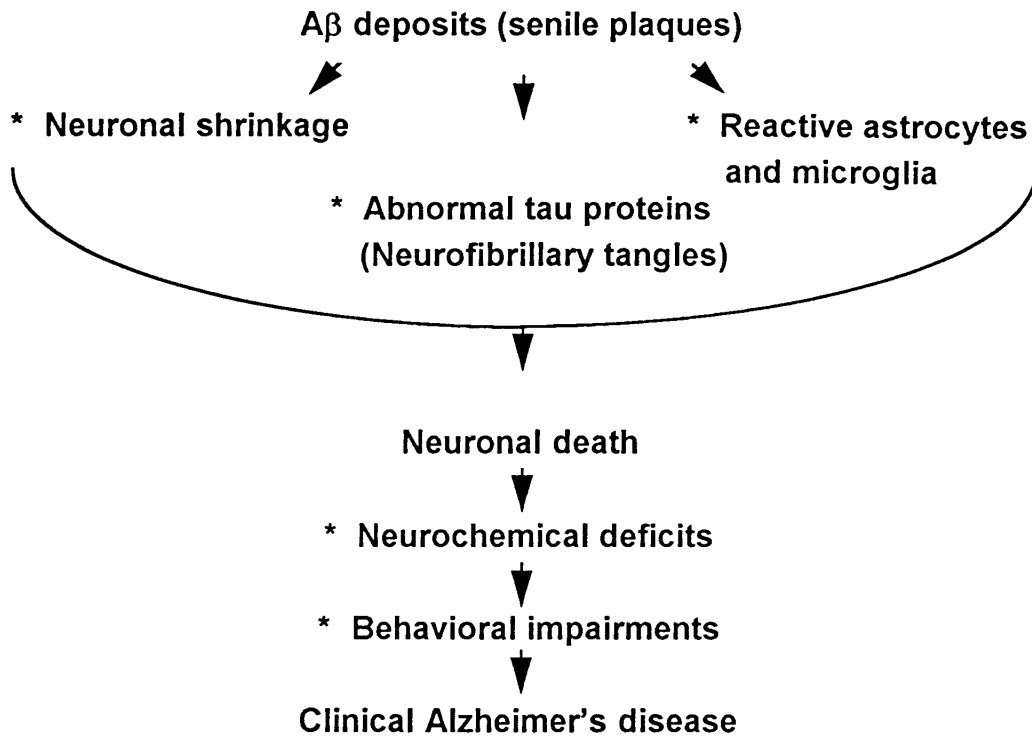


Figure 29. Pathological effects of A β . A flow diagram showing a proposed scenario for the pathological effects of A β . The star symbol (*) represents phenomena analyzed in rats in the present study. This figure represents an extremely simplified version of some of the pathological processes that may be involved in the progression of AD.

Future Directions

Because AD is an age related disorder it is necessary to investigate the effects of intracerebral injections of A β in old animals. A detailed histological analysis of the whole rat brain following intra-amygdaloid injections of A β will certainly be valuable. A comparison of the regional pattern of histopathology with efferent and afferent projections of the amygdala may provide insight into the mechanism of A β effects. However, a lack of pathology in a brain region that has prominent projections to the amygdala will not necessarily disprove the hypothesis that A β may be affecting nerve terminals. In AD there is a selective vulnerability of brain regions and the pathological process occurs over decades. It is possible that different regions and/or cell types of the brain have different kinetics and/or vulnerability for A β induced pathology. It would also be interesting to determine if multiple A β injections administered through implanted cannula could lead to more severe behavioral impairments than we observed following single injections. Behavioral testing using different behavioral paradigms and/or postoperative interval may also be useful. The laterality observed following bilateral intra-amygdaloid injections is a very surprising phenomenon. It is important to determine if the laterality in the effects of A β is specific for the amygdala, or if it can be observed following injections into other brain structures or following ventricular infusions. Injections of A β into other strains and species are necessary to determine if the histopathological effects and/or laterality are strain and/or species specific. Further investigations into the cause for the lateralized effects of A β are also warranted. In addition, injections of A β 1-40, A β 1-42, and other amyloidogenic peptides, co-injections of other plaque components, and even injections of senile plaque cores may provide clues on how prominent role the β -sheet structure of A β has in the process of AD histopathology. Finally, it would be interesting to determine if compounds that interfere with A β fibril formation and/or enhance fibril degradation *in vitro* could affect A β deposition and/or

accelerate the *in vivo* degradation of the deposits. Anti-inflammatory compounds that easily penetrate the blood-brain-barrier are also of potential interest to attenuate the histopathological effects of intracerebral injections of A β .

Conclusion

In summary, the present model has histopathological features that are likely to occur in the initial stages of AD but its predictive validity will ultimately determine its usefulness as an animal model for AD.

REFERENCES

1. Aggleton, J. P.; Blindt, H. S.; Rawlins, J. N. Effects of amygdaloid and amygdaloid-hippocampal lesions on object recognition and spatial working memory in rats. *Behavioral Neuroscience* 103:962-974; 1989.
2. Anderson, A. J.; Su, J. H.; Cotman, C. W. DNA damage and apoptosis in Alzheimers disease: Colocalization with c-jun immunoreactivity, relationship to brain area, and effect of postmortem delay. *Journal of Neuroscience* 16:1710-1719; 1996.
3. Andreadis, A.; Brown, W. M.; Kosik, K. S. Structure and novel exons of the human tau gene. *Biochemistry* 31:10626-10633; 1992.
4. Araujo, D. M.; Cotman, C. W. β -Amyloid stimulates glial cells in vitro to produce growth factors that accumulate in senile plaques in Alzheimer's disease. *Brain Research* 569:141-145; 1992.
5. Ard, M. D.; Cole, G. M.; Wei, J.; Mehrle, A. P.; Fratkin, J. D.; Scavenging of Alzheimers amyloid β -protein by microglia in culture. *Journal of Neuroscience Research* 43:190-202; 1996.
6. Arispe, N.; Pollard, H. B.; Rojas, E. Giant multilevel cation channels formed by Alzheimer disease amyloid beta-protein [$A\beta$ P-(1-40)] in bilayer membranes. *Proceedings of the National Academy of Sciences of the United States of America* 90:10573-10577; 1993.
7. Arispe, N.; Rojas, E.; Pollard, H. B. Alzheimer disease amyloid β protein forms calcium channels in bilayer membranes: Blockade by tromethamine and aluminum. *Proceedings of the National Academy of Sciences of the United States of America* 90:567-571; 1993.
8. Arriagada, P. V.; Growdon, J. H.; Hedley-Whyte, E. T.; Hyman, B. T. Neurofibrillary tangles but not senile plaques parallel duration and severity of Alzheimer's disease. *Neurology* 42:631-639; 1992.
9. Auron, P. E.; Webb, A. C.; Rosenwasser, L. J.; Mucci, S. F.; Rich, A.; Wolff, S. M.; Dinarello, C. A. Nucleotide sequence of human monocyte interleukin 1 precursor cDNA. *Proceedings of the National Academy of Sciences of the United States of America* 81:7907-7911; 1984.
10. Barneoud, P.; Le Moal, M.; Neveu, P. J. Asymmetrical effects of cortical ablation on brain monoamines in mice. *International Journal of Neuroscience* 56:283-294; 1991.
11. Barrow, C. J.; Yasuda, A.; Kenny, P. T.; Zagorski, M. G. Solution conformations and aggregational properties of synthetic amyloid β -peptides of Alzheimer's disease. Analysis of circular dichroism spectra. *Journal of Molecular Biology* 225:1075-1093; 1992.

12. Bartus, R. T.; Dean, R. L., 3d; Beer, B.; Lippa, A. S. The cholinergic hypothesis of geriatric memory dysfunction. [Review]. *Science* 217:408-414; 1982.
13. Behl, C.; Davis, J. B.; Klier, F. G.; Schubert, D. Amyloid β peptide induces necrosis rather than apoptosis. *Brain Research* 645:253-264; 1994.
14. Behl, C.; Davis, J. B.; Lesley, R.; Schubert, D. Hydrogen peroxide mediates amyloid β protein toxicity. *Cell* 77:817-827; 1994.
15. Belcheva, I.; Belcheva, S.; Petkov, V. V.; Petkov, V. D. Asymmetry in behavioral responses to cholecystokinin microinjected into rat nucleus accumbens and amygdala. *Neuropharmacology* 33:995-1002; 1994.
16. Binder, L. I.; Frankfurter, A.; Rebhun, L. I. The distribution of tau in the mammalian central nervous system. *Journal of Cell Biology* 101:1371-1378; 1985.
17. Blessed, G.; Tomlinson, B. E.; Roth, M. The association between quantitative measures of dementia and of senile change in the cerebral grey matter of elderly subjects. *British Journal of Psychiatry* 114:797-811; 1968.
18. Boland, K.; Behrens, M.; Choi, D.; Manias, K.; Perlmutter, D. H. The serpin-enzyme complex receptor recognizes soluble, nontoxic amyloid- β peptide but not aggregated, cytotoxic amyloid- β peptide. *Journal of Biological Chemistry* 271:18032-18044; 1996.
19. Boland, K.; Manias, K.; Perlmutter, D. H. Specificity in recognition of amyloid- β peptide by the serpin-enzyme complex receptor in hepatoma cells and neuronal cells. *Journal of Biological Chemistry* 270:28022-28028; 1995.
20. Breen, K. C.; Bruce, M.; Anderton, B. H. β -Amyloid precursor protein mediates neuronal cell-cell and cell-surface adhesion. *Journal of Neuroscience Research* 28:90-100; 1991.
21. Buee, L.; Laine, A.; Delacourte, A.; Flament, S.; Han, K. K. Qualitative and quantitative comparison of brain proteins in Alzheimer's disease. *Biological Chemistry Hoppe-Seyler* 370:1229-1234; 1989.
22. Burdick, D.; Soreghan, B.; Kwon, M.; Kosmoski, J.; Knauer, M.; Henschen, A.; Yates, J.; Cotman, C.; Glabe, C. Assembly and aggregation properties of synthetic Alzheimer's A4/ β amyloid peptide analogs. *Journal of Biological Chemistry* 267:546-554; 1992.
23. Burger, P. C.; Vogel, F. S. The development of the pathologic changes of Alzheimer's disease and senile dementia in patients with Down's syndrome. *American Journal of Pathology* 73:457-476; 1973.
24. Busciglio, J.; Gabuzda, D. H.; Matsudaira, P.; Yankner, B. A. Generation of β -amyloid in the secretory pathway in neuronal and nonneuronal cells. *Proceedings of the National Academy of Sciences of the United States of America* 90:2092-2096; 1993.
25. Busciglio, J.; Lorenzo, A.; Yankner, B. A. Methodological variables in the assessment of β amyloid neurotoxicity. [Review]. *Neurobiology of Aging* 13:609-612; 1992.
26. Busciglio, J.; Lorenzo, A.; Yeh, J.; Yankner, B. A. β -Amyloid fibrils induce tau phosphorylation and loss of microtubule binding. *Neuron* 14:879-888; 1995.

27. Busciglio, J.; Yankner, B. A. Apoptosis and increased generation of reactive oxygen species in Down's syndrome neurons in vitro. *Nature* 378:776-779; 1995.
28. Busciglio, J.; Yeh, J.; Yankner, B. A. β -Amyloid neurotoxicity in human cortical culture is not mediated by excitotoxins. *Journal of Neurochemistry* 61:1565-1568; 1993.
29. Bush, A. I.; Pettingell, W. H.; Multhaup, G.; d Paradis, M.; Vonsattel, J. P.; Gusella, J. F.; Beyreuther, K.; Masters, C. L.; Tanzi, R. E. Rapid induction of Alzheimer A β amyloid formation by zinc [see comments]. *Science* 265:1464-1467; 1994.
30. Bush, D. F.; Lovely, R. H.; Pagano, R. R. Injection of ACTH induces recovery from shuttle-box avoidance deficits in rats with amygdaloid lesions. *Journal of Comparative & Physiological Psychology* 83:168-172; 1973.
31. Buxbaum, J. D.; Oishi, M.; Chen, H. I.; Pinkas-Kramarski, R.; Jaffe, E. A.; Gandy, S. E.; Greengard, P. Cholinergic agonists and interleukin 1 regulate processing and secretion of the Alzheimer β /A4 amyloid protein precursor. *Proceedings of the National Academy of Sciences of the United States of America* 89:10075-10078; 1992.
32. Byne, W.; Mattiace, L.; Kress, Y.; Davies, P. Alz-50 immunoreactivity in the hypothalamus of the normal and Alzheimer human and the rat. *Journal of Comparative Neurology* 306:602-612; 1991.
33. Cai, X. D.; Golde, T. E.; Younkin, S. G. Release of excess amyloid β protein from a mutant amyloid β protein precursor [see comments]. *Science* 259:514-516; 1993.
34. Canning, D. R.; McKeon, R. J.; DeWitt, D. A.; Perry, G.; Wujek, J. R.; Frederickson, R. C.; Silver, J. β -Amyloid of Alzheimer's disease induces reactive gliosis that inhibits axonal outgrowth. *Experimental Neurology* 124:289-298; 1993.
35. Carlsen, J.; Zaborszky, L.; Heimer, L. Cholinergic projections from the basal forebrain to the basolateral amygdaloid complex: A combined retrograde fluorescent and immunohistochemical study. *Journal of Comparative Neurology* 234:155-167; 1985.
36. Carlson, J. N.; Visker, K. E.; Keller, R. W.; Glick, S. D.; Left and right 6-hydroxydopamine lesions of the medial prefrontal cortex differentially alter subcortical dopamine utilization and the behavioral response to stress. *Brain Research* 711:1-9; 1996.
37. Chase, T. N.; Foster, N. L.; Fedio, P.; Brooks, R.; Mansi, L.; Di Chiro, G. Regional cortical dysfunction in Alzheimer's disease as determined by positron emission tomography. *Annals of Neurology* 15 Suppl:S170-S174; 1984.
38. Chen, M.; Yankner, B. A. An antibody to β amyloid and the amyloid precursor protein inhibits cell-substratum adhesion in many mammalian cell types. *Neuroscience Letters* 125:223-226; 1991.
39. Citron, M.; Oltersdorf, T.; Haass, C.; McConlogue, L.; Hung, A. Y.; Seubert, P.; Lieberburg, I.; Selkoe, D. J. Mutation of the β -amyloid precursor protein in familial Alzheimer's disease increases β -protein production. *Nature* 360:672-674; 1992.

40. Clark, B. D.; Collins, K. L.; Gandy, M. S.; Webb, A. C.; Auron, P. E. Genomic sequence for human prointerleukin 1 β : Possible evolution from a reverse transcribed prointerleukin 1 α gene [published erratum appears in *Nucleic Acids Res* 1987 Jan 26;15(2): 868]. *Nucleic Acids Research* 14:7897-7914; 1986.
41. Cleary, J.; Hittner, J. M.; Semotuk, M.; Mantyh, P.; O'Hare, E. β -Amyloid(1-40) effects on behavior and memory. *Brain Research* 682:69-74; 1995.
42. Clemens, J. A.; Stephenson, D. T. Implants containing β -amyloid protein are not neurotoxic to young and old rat brain. *Neurobiology of Aging* 13:581-586; 1992.
43. Cleveland, D. W.; Hwo, S. Y.; Kirschner, M. W. Purification of tau, a microtubule-associated protein that induces assembly of microtubules from purified tubulin. *Journal of Molecular Biology* 116:207-225; 1977.
44. Cole, G. M.; Bell, L.; Truong, Q. B.; Saitoh, T. An endosomal-lysosomal pathway for degradation of amyloid precursor protein. *Annals of the New York Academy of Sciences* 674:103-117; 1992.
45. Coleman-Mesches, K.; McGaugh, J. L. Differential effects of pretraining inactivation of the right or left amygdala on retention of inhibitory avoidance training. *Behavioral Neuroscience* 109:642-647; 1995.
46. Coleman-Mesches, K.; McGaugh, J. L. Differential involvement of the right and left amygdalae in expression of memory for aversively motivated training. *Brain Research* 670:75-81; 1995.
47. Coleman-Mesches, K.; McGaugh, J. L. Muscimol injected into the right or left amygdaloid complex differentially affects retention performance following aversively motivated training. *Brain Research* 676:183-188; 1995.
48. Copani, A.; Koh, J. Y.; Cotman, C. W. β -Amyloid increases neuronal susceptibility to injury by glucose deprivation [see comments]. *Neuroreport* 2:763-765; 1991.
49. Corder, E. H.; Saunders, A. M.; Risch, N. J.; Strittmatter, W. J.; Schmechel, D. E.; Gaskell, P. C., Jr.; Rimmler, J. B.; Locke, P. A.; Conneally, P. M.; Schmechel, K. E.; et al. Protective effect of apolipoprotein E type 2 allele for late onset Alzheimer disease. *Nature Genetics* 7:180-184; 1994.
50. Cork, L. C.; Powers, R. E.; Selkoe, D. J.; Davies, P.; Geyer, J. J.; Price, D. L. Neurofibrillary tangles and senile plaques in aged bears [published erratum appears in *J Neuropathol Exp Neurol* 1989 Jul; 48(4):497] [see comments]. *Journal of Neuropathology & Experimental Neurology* 47:629-641; 1988.
51. Corman, C. D.; Meyer, P. M.; Meyer, D. R. Open-field activity and exploration in rats with septal and amygdaloid lesions. *Brain Research* 5:469-476; 1967.
52. Crystal, H. A.; Horoupian, D. S.; Katzman, R.; Jotkowitz, S. Biopsy-proved Alzheimer disease presenting as a right parietal lobe syndrome. *Annals of Neurology* 12:186-188; 1981.

53. Czech, C.; Masters, C.; Beyreuther, K. Alzheimer's disease and transgenic mice. *Journal of Neural Transmission Supplementum*. 44:219-230; 1994.
54. D'Amato, R. J.; Zweig, R. M.; Whitehouse, P. J.; Wenk, G. L.; Singer, H. S.; Mayeux, R.; Price, D. L.; Snyder, S. H. Aminergic systems in Alzheimer's disease and Parkinson's disease. *Annals of Neurology* 22:229-236; 1987.
55. Davies, P. Alz 50 as a reagent to assess animal models of Alzheimer's disease. [Review]. *Neurobiology of Aging* 13:613-614; 1992.
56. Davies, P.; Katzman, R.; Terry, R. D. Reduced somatostatin-like immunoreactivity in cerebral cortex from cases of Alzheimer disease and Alzheimer senile dementia. *Nature* 288:279-280; 1980.
57. Davies, P.; Maloney, A. J. Selective loss of central cholinergic neurons in Alzheimer's disease [letter]. *Lancet* 2:1403; 1976.
58. Decker, M. W.; Curzon, P.; Brioni, J. D. Influence of separate and combined septal and amygdala lesions on memory, acoustic startle, anxiety, and locomotor activity in rats. *Neurobiology of Learning & Memory* 64:156-168; 1995.
59. Del Bo, R.; Angeretti, N.; Lucca, E.; De Simoni, M. G.; Forloni, G. Reciprocal control of inflammatory cytokines, IL-1 and IL-6, and β -amyloid production in cultures. *Neuroscience Letters* 188:70-74; 1995.
60. Delacourte, A. General and dramatic glial reaction in Alzheimer brains. *Neurology* 40:33-37; 1990.
61. Dewberry, R. G.; Lipsey, J. R.; Saad, K.; Moran, T. H.; Robinson, R. G. Lateralized response to cortical injury in the rat: Interhemispheric interaction. *Behavioral Neuroscience* 100:556-562; 1986.
62. Dickson, D. W.; Lee, S. C.; Mattiace, L. A.; Yen, S. H.; Brosnan, C. Microglia and cytokines in neurological disease, with special reference to AIDS and Alzheimer's disease. [Review]. *GLIA* 7:75-83; 1993.
63. Dinarello, C. A. Interleukin-1 and interleukin-1 antagonism. [Review]. *Blood* 77:1627-1652; 1991.
64. Donnelly, R. J.; Friedhoff, A. J.; Beer, B.; Blume, A. J.; Vitek, M. P. Interleukin-1 stimulates the β -amyloid precursor protein promoter. *Cellular & Molecular Neurobiology* 10:485-495; 1990.
65. Dornan, W. A.; Kang, D. E.; McCampbell, A.; Kang, E. E. Bilateral injections of β A(25-35) + IBO into the hippocampus disrupts acquisition of spatial learning in the rat. *Neuroreport* 5:165-168; 1993.
66. Drewes, G.; Mandelkow, E. M.; Baumann, K.; Goris, J.; Merlevede, W.; Mandelkow, E. Dephosphorylation of tau protein and Alzheimer paired helical filaments by calcineurin and phosphatase-2A. *FEBS Letters* 336:425-432; 1993.

67. Drewes, G.; Trinczek, B.; Illenberger, S.; Biernat, J.; Schmitt-Ulms, G.; Meyer, H.E.; Mandelkow, E. M.; Mandelkow, E. Microtubule-associated protein/microtubule affinity-regulating kinase (p110mark). A novel protein kinase that regulates tau-microtubule interactions and dynamic instability by phosphorylation at the Alzheimer-specific site serine 262. *Journal of Biological Chemistry* 270:7679-7688; 1995.
68. Duara, R.; Grady, C.; Haxby, J.; Sundaram, M.; Cutler, N. R.; Heston, L.; Moore, A.; Larson, S.; Rapoport, S. I. Positron emission tomography in Alzheimer's disease. *Neurology* 36:879-887; 1986.
69. Duff, K.; Eckman, C.; Zehr, C.; Yu, X.; Prada, C. M.; Pereztur, J.; Hutton, M.; Buee, L.; Harigaya, Y.; Yager, D.; Morgan, D.; Gordon, M. N.; Holcomb, L.; Refolo, L.; Zenk, B.; Hardy, J.; Younkin, S. Increased amyloid- β -42(43) in brains of mice expressing mutant presenilin 1. *Nature* 383:710-713; 1996.
70. Duffy, P. E.; Rapport, M.; Graf, L. Glial fibrillary acidic protein and Alzheimer-type senile dementia. *Neurology* 30:778-782; 1980.
71. Dyrks, T.; Dyrks, E.; Hartmann, T.; Masters, C.; Beyreuther, K. Amyloidogenicity of β A4 and β A4-bearing amyloid protein precursor fragments by metal-catalyzed oxidation. *Journal of Biological Chemistry* 267:18210-18217; 1992.
72. Dyrks, T.; Dyrks, E.; Masters, C. L.; Beyreuther, K. Amyloidogenicity of rodent and human β A4 sequences. *FEBS Letters* 324:231-236; 1993.
73. Eclancher, F.; Karli, P. Effects of early amygdaloid lesions on the development of reactivity in the rat. *Physiology & Behavior* 22:123-134; 1979.
74. Eikelenboom, P.; Hack, C. E.; Rozemuller, J. M.; Stam, F. C. Complement activation in amyloid plaques in Alzheimer's dementia. *Virchows Archiv B, Cell Pathology* 50:259-262; 1989.
75. Eikelenboom, P.; Stam, F. C. Immunoglobulins and complement factors in senile plaques. An immunoperoxidase study. *Acta Neuropathologica* 57:239-242; 1982.
76. El Khoury, J.; Hickman, S. E.; Thomas, C. A.; Cao, L.; Silverstein, S. C.; Loike, J. D. Scavenger receptor-mediated adhesion of microglia to β -amyloid fibrils [see comments]. *Nature* 382:716-719; 1996.
77. Eng, L. F.; Vanderhaeghen, J. J.; Bignami, A.; Gerstl, B. An acidic protein isolated from fibrous astrocytes. *Brain Research* 28:351-354; 1971.
78. Esch, F. S.; Keim, P. S.; Beattie, E. C.; Blacher, R. W.; Culwell, A. R.; Oltersdorf, T.; McClure, D.; Ward, P. J. Cleavage of amyloid β peptide during constitutive processing of its precursor. *Science* 248:1122-1124; 1990.
79. Esiri, M. M.; Pearson, R. C.; Powell, T. P. The cortex of the primary auditory area in Alzheimer's disease. *Brain Research* 366:385-387; 1986.
80. Estus, S.; Golde, T. E.; Kunishita, T.; Blades, D.; Lowery, D.; Eisen, M.; Usiak, M.; Qu, X. M.; Tabira, T.; Greenberg, B. D.; et al. Potentially amyloidogenic, carboxyl-terminal derivatives of the amyloid protein precursor [see comments]. *Science* 255:726-728; 1992.

81. Fabian, H.; Szendrei, G. I.; Mantsch, H. H.; Greenberg, B. D.; Otvos, L., Jr. Synthetic post-translationally modified human A β peptide exhibits a markedly increased tendency to form β -pleated sheets in vitro. *European Journal of Biochemistry* 221:959-964; 1994.
82. Fagarasan, M. O.; Aisen, P. S. IL-1 and anti-inflammatory drugs modulate A- β cytotoxicity in PC12 cells. *Brain Research* 723:231-234; 1996.
83. Fasman, G. D.; Perczel, A.; Moore, C. D. Solubilization of β -amyloid-(1-42)-peptide: Reversing the β -sheet conformation induced by aluminum with silicates. *Proceedings of the National Academy of Sciences of the United States of America* 92:369-371; 1995.
84. Flicker, C.; Dean, R. L.; Watkins, D. L.; Fisher, S. K.; Bartus, R. T. Behavioral and neurochemical effects following neurotoxic lesions of a major cholinergic input to the cerebral cortex in the rat. *Pharmacology, Biochemistry & Behavior* 18:973-981; 1983.
85. Flood, J. F.; Morley, J. E.; Roberts, E. Amnestic effects in mice of four synthetic peptides homologous to amyloid β protein from patients with Alzheimer disease. *Proceedings of the National Academy of Sciences of the United States of America* 88:3363-3366; 1991.
86. Fonnum, F. A rapid radiochemical method for the determination of choline acetyltransferase. *Journal of Neurochemistry* 24:407-409; 1975.
87. Forloni, G.; Angeretti, N.; Chiesa, R.; Monzani, E.; Salmona, M.; Bugiani, O. Neurotoxicity of a prion protein fragment. *Nature* 362:543-546; 1993.
88. Forloni, G.; Chiesa, R.; Smiroldo, S.; Verga, L.; Salmona, M.; Tagliavini, F. Apoptosis mediated neurotoxicity induced by chronic application of β amyloid fragment 25-35. *Neuroreport* 4:523-526; 1993.
89. Forloni, G.; Demicheli, F.; Giorgi, S.; Bendotti, C.; Angeretti, N. Expression of amyloid precursor protein mRNAs in endothelial, neuronal and glial cells: modulation by interleukin-1. *Brain Research Molecular Brain Research*:128-134; 1992.
90. Fraser, P. E.; Nguyen, J. T.; Chin, D. T.; Kirschner, D. A. Effects of sulfate ions on Alzheimer β /A4 peptide assemblies: implications for amyloid fibril-proteoglycan interactions. *Journal of Neurochemistry* 59:1531-1540; 1992.
91. Frautschy, S. A.; Baird, A.; Cole, G. M. Effects of injected Alzheimer β -amyloid cores in rat brain. *Proceedings of the National Academy of Sciences of the United States of America* 88:8362-8366; 1991.
92. Frautschy, S. A.; Yang, F. S.; Calderon, L.; Cole, G. M. Rodent models of Alzheimers disease: Rat A- β infusion approaches to amyloid deposits. *Neurobiology of Aging* 17:311-321; 1996.
93. Frederickson, R. C. Astroglia in Alzheimer's disease. [Review]. *Neurobiology of Aging* 13:239-253; 1992.
94. Frederikse, P. H.; Garland, D.; Zigler, J. S., Jr.; Piatigorsky, J. Oxidative stress increases production of β -amyloid precursor protein and β -amyloid (A β) in mammalian lenses, and A β

has toxic effects on lens epithelial cells. *Journal of Biological Chemistry* 271:10169-10174; 1996.

95. Friedland, R. P.; Budinger, T. F.; Koss, E.; Ober, B. A. Alzheimer's disease: Anterior-posterior and lateral hemispheric alterations in cortical glucose utilization. *Neuroscience Letters* 53:235-240; 1985.

96. Furukawa, K.; Barger, S. W.; Blalock, E. M.; Mattson, M. P. Activation of K⁺ channels and suppression of neuronal activity by secreted β -amyloid-precursor protein. *Nature* 379:74-78; 1996.

97. Furutani, Y.; Notake, M.; Fukui, T.; Ohue, M.; Nomura, H.; Yamada, M.; Nakamura, S. Complete nucleotide sequence of the gene for human interleukin 1 α [published erratum appears in *Nucleic Acids Res* 1986 Jun 25; 14(12):5124]. *Nucleic Acids Research* 14:3167-3179; 1986.

98. Games, D.; Adams, D.; Alessandrini, R.; Barbour, R.; Berthelette, P.; Blackwell, C.; Carr, T.; Clemens, J.; Donaldson, T.; Gillespie, F.; et al. Alzheimer-type neuropathology in transgenic mice overexpressing V717F β -amyloid precursor protein [see comments]. *Nature* 373:523-527; 1995.

99. Games, D.; Khan, K. M.; Soriano, F. G.; Keim, P. S.; Davis, D. L.; Bryant, K. Lack of Alzheimer pathology after β -amyloid protein injections in rat brain. *Neurobiology of Aging* 13:569-576; 1992.

100. Giaccone, G.; Tagliavini, F.; Linoli, G.; Bouras, C.; Frigerio, L.; Frangione, B.; Bugiani, O. Down patients: Extracellular preamyloid deposits precede neuritic degeneration and senile plaques. *Neuroscience Letters* 97:232-238; 1989.

101. Giordano, T.; Pan, J. B.; Monteggia, L. M.; Holzman, T. F.; Snyder, S. W.; Krafft, G.; Kowall, N. W. Similarities between β amyloid peptides 1-40 and 40-1: Effects on aggregation, toxicity in vitro, and injection in young and aged rats. *Experimental Neurology* 125:175-182; 1994.

102. Giovannelli, L.; Casamenti, F.; Scali, C.; Bartolini, L.; Pepeu, G. Differential effects of amyloid peptides β -(1-40) and β -(25-35) injections into the rat nucleus basalis. *Neuroscience* 66:781-792; 1995.

103. Glenner, G. G.; Wong, C. W. Alzheimer's disease: Initial report of the purification and characterization of a novel cerebrovascular amyloid protein. *Biochemical & Biophysical Research Communications* 120:885-890; 1984.

104. Goate, A.; Chartier-Harlin, M. C.; Mullan, M.; Brown, J.; Crawford, F.; Fidani, L.; Haynes, A.; Irving, N.; James, L.; et al. Segregation of a missense mutation in the amyloid precursor protein gene with familial Alzheimer's disease [see comments]. *Nature* 349:704-706; 1991.

105. Goedert, M.; Spillantini, M. G.; Jakes, R. Localization of the Alz-50 epitope in recombinant human microtubule-associated protein tau. *Neuroscience Letters* 126:149-154; 1991.

106. Goedert, M.; Spillantini, M. G.; Jakes, R.; Rutherford, D.; Crowther, R. A. Multiple isoforms of human microtubule-associated protein tau: Sequences and localization in neurofibrillary tangles of Alzheimer's disease. *Neuron* 3:519-526; 1989.
107. Golde, T. E.; Estus, S.; Younkin, L. H.; Selkoe, D. J.; Younkin, S. G. Processing of the amyloid protein precursor to potentially amyloidogenic derivatives [see comments]. *Science* 255:728-730; 1992.
108. Goldgaber, D.; Harris, H. W.; Hla, T.; Maciag, T.; Donnelly, R. J.; Jacobsen, J. S.; Vitek, M. P.; Gajdusek, D. C. Interleukin 1 regulates synthesis of amyloid β -protein precursor mRNA in human endothelial cells. *Proceedings of the National Academy of Sciences of the United States of America* 86:7606-7610; 1989.
109. Gong, C. X.; Grundke-Iqbal, I.; Damuni, Z.; Iqbal, K. Dephosphorylation of microtubule-associated protein tau by protein phosphatase-1 and -2C and its implication in Alzheimer disease. *FEBS Letters* 341:94-98; 1994.
110. Gong, C. X.; Shaikh, S.; Wang, J. Z.; Zaidi, T.; Grundke-Iqbal, I.; Iqbal, K. Phosphatase activity toward abnormally phosphorylated tau: Decrease in Alzheimer disease brain. *Journal of Neurochemistry* 65:732-738; 1995.
111. Gong, C. X.; Singh, T. J.; Grundke-Iqbal, I.; Iqbal, K. Phosphoprotein phosphatase activities in Alzheimer disease brain. *Journal of Neurochemistry* 61:921-927; 1993.
112. Gong, C. X.; Singh, T. J.; Grundke-Iqbal, I.; Iqbal, K. Alzheimer's disease abnormally phosphorylated tau is dephosphorylated by protein phosphatase-2B (calcineurin). *Journal of Neurochemistry* 62:803-806; 1994.
113. Grady, C. L.; Haxby, J. V.; Schlageter, N. L.; Berg, G.; Rapoport, S. I. Stability of metabolic and neuropsychological asymmetries in dementia of the Alzheimer type. *Neurology* 36:1390-1392; 1986.
114. Greenamyre, J. T.; Young, A. B. Excitatory amino acids and Alzheimer's disease. [Review]. *Neurobiology of Aging* 10:593-602; 1989.
115. Greenberg, B. D.; Kezdy, F. J.; Kisilevsky, R. Amyloidogenesis as a therapeutic target in Alzheimer's disease. *Annu. Rep. Med. Chem.* 26:229-238; 1991.
116. Greenberg, S. M.; Koo, E. H.; Selkoe, D. J.; Qiu, W. Q.; Kosik, K. S. Secreted β -amyloid precursor protein stimulates mitogen-activated protein kinase and enhances tau phosphorylation. *Proceedings of the National Academy of Sciences of the United States of America* 91:7104-7108; 1994.
117. Griffin, W. S.; Sheng, J. G.; Roberts, G. W.; Mrak, R. E. Interleukin-1 expression in different plaque types in Alzheimer's disease: Significance in plaque evolution. *Journal of Neuropathology & Experimental Neurology* 54:276-281; 1995.
118. Grijalva, C. V.; Levin, E. D.; Morgan, M.; Roland, B.; Martin, F. C. Contrasting effects of centromedial and basolateral amygdaloid lesions on stress-related responses in the rat. *Physiology & Behavior* 48:495-500; 1990.

119. Haass, C.; Koo, E. H.; Mellon, A.; Hung, A. Y.; Selkoe, D. J. Targeting of cell-surface β -amyloid precursor protein to lysosomes: Alternative processing into amyloid-bearing fragments. *Nature* 357:500-503; 1992.
120. Haass, C.; Schlossmacher, M. G.; Hung, A. Y.; Vigo-Pelfrey, C.; Mellon, A.; Ostaszewski, B. L.; Lieberburg, I.; Koo, E. H.; Schenk, D.; Teplow, D. B.; et al. Amyloid β -peptide is produced by cultured cells during normal metabolism [see comments]. *Nature* 359:322-325; 1992.
121. Hachinski, V. C.; Oppenheimer, S. M.; Wilson, J. X.; Guiraudon, C.; Cechetto, D. F. Asymmetry of sympathetic consequences of experimental stroke. *Archives of Neurology* 49:697-702; 1992.
122. Haga, S.; Akai, K.; Ishii, T. Demonstration of microglial cells in and around senile (neuritic) plaques in the Alzheimer brain. An immunohistochemical study using a novel monoclonal antibody. *Acta Neuropathologica* 77:569-575; 1989.
123. Haga, S.; Ikeda, K.; Sato, M.; Ishii, T. Synthetic Alzheimer amyloid β /A4 peptides enhance production of complement C3 component by cultured microglial cells. *Brain Research* 601:88-94; 1993.
124. Halverson, K.; Fraser, P. E.; Kirschner, D. A.; Lansbury, P. T., Jr. Molecular determinants of amyloid deposition in Alzheimer's disease: Conformational studies of synthetic β -protein fragments. *Biochemistry* 29:2639-2644; 1990.
125. Han, S. H.; Einstein, G.; Weisgraber, K. H.; Strittmatter, W. J.; Saunders, A. M.; Pericak-Vance, M.; Roses, A. D.; Schmechel, D. E. Apolipoprotein E is localized to the cytoplasm of human cortical neurons: A light and electron microscopic study. *Journal of Neuropathology & Experimental Neurology* 53:535-544; 1994.
126. Hansen, L. A.; Armstrong, D. M.; Terry, R. D. An immunohistochemical quantification of fibrous astrocytes in the aging human cerebral cortex. *Neurobiology of Aging* 8:1-6; 1987.
127. Harris, M. E.; Hensley, K.; Butterfield, D. A.; Leedle, R. A.; Carney, J. M. Direct evidence of oxidative injury produced by the Alzheimer's β -amyloid peptide (1-40) in cultured hippocampal neurons. *Experimental Neurology* 131:193-202; 1995.
128. Hatten, M. E.; Liem, R. K.; Shelanski, M. L.; Mason, C. A. Astroglia in CNS injury. [Review]. *GLIA* 4:233-243; 1991.
129. Haxby, J. V.; Duara, R.; Grady, C. L.; Cutler, N. R.; Rapoport, S. I. Relations between neuropsychological and cerebral metabolic asymmetries in early Alzheimer's disease. *Journal of Cerebral Blood Flow & Metabolism* 5:193-200; 1985.
130. Haxby, J. V.; Grady, C. L.; Duara, R.; Schlageter, N.; Berg, G.; Rapoport, S. I. Neocortical metabolic abnormalities precede nonmemory cognitive defects in early Alzheimer's-type dementia. *Archives of Neurology* 43:882-885; 1986.
131. Haxby, J. V.; Grady, C. L.; Friedland, R. P.; Rapoport, S. I. Neocortical metabolic abnormalities precede nonmemory cognitive impairments in early dementia of the Alzheimer

type: Longitudinal confirmation. *Journal of Neural Transmission Supplementum*. 24:49-53; 1987.

132. Haxby, J. V.; Grady, C. L.; Koss, E.; Horwitz, B.; Heston, L.; Schapiro, M.; Rapoport, S. I. Longitudinal study of cerebral metabolic asymmetries and associated neuropsychological patterns in early dementia of the Alzheimer type. *Archives of Neurology* 47:753-760; 1990.

133. Heffner, T. G.; Hartman, J. A.; Seiden, L. S. A rapid method for the regional dissection of the rat brain. *Pharmacology, Biochemistry & Behavior* 13:453-456; 1980.

134. Hepler, D. J.; Olton, D. S.; Wenk, G. L.; Coyle, J. T. Lesions in nucleus basalis magnocellularis and medial septal area of rats produce qualitatively similar memory impairments. *Journal of Neuroscience* 5:866-873; 1985.

135. Hertz, L.; Schousboe, A. Role of astrocytes in compartmentation of amino acid and energy metabolism. In: Fedoroff, S.; Vernadakis, A. eds. *Astrocytes*. New York: Academic Press; 1986:179-208.

136. Hertz, L.; Schousboe, A. Metabolism of glutamate and glutamine in neurons and astrocytes in primary cultures. In: Kvamme, E. ed. *Glutamine and glutamate in mammals*. Boca Raton, FL: CRC Press; 1988:39-55.

137. Higgins, L. S.; Catalano, R.; Quon, D.; Cordell, B. Transgenic mice expressing human β -APP751, but not mice expressing β -APP695, display early Alzheimer's disease-like histopathology. *Annals of the New York Academy of Sciences* 695:224-227; 1993.

138. Higgins, L. S.; Holtzman, D. M.; Rabin, J.; Mobley, W. C.; Cordell, B. Transgenic mouse brain histopathology resembles early Alzheimer's disease. *Annals of Neurology* 35:598-607; 1994.

139. Higgins, L. S.; Rodems, J. M.; Catalano, R.; Quon, D.; Cordell, B. Early Alzheimer disease-like histopathology increases in frequency with age in mice transgenic for β -APP751. *Proceedings of the National Academy of Sciences of the United States of America* 92:4402-4406; 1995.

140. Himmler, A.; Drechsel, D.; Kirschner, M. W.; Martin, D. W., Jr. Tau consists of a set of proteins with repeated C-terminal microtubule-binding domains and variable N-terminal domains. *Molecular & Cellular Biology* 9:1381-1388; 1989.

141. Hoke, A.; Canning, D. R.; Malemud, C. J.; Silver, J. Regional differences in reactive gliosis induced by substrate-bound β -amyloid. *Experimental Neurology* 130:56-66; 1994.

142. Hosli, E.; Schousboe, A.; Hosli, L. Amino acid uptake. In: Fedoroff, S.; Vernadakis, A. eds. *Astrocytes*. New York: Academic Press; 1986:133-153.

143. Howland, D. S.; Savage, M. J.; Huntress, F. A.; Wallace, R. E.; Schwartz, D. A.; Loh, T.; Melloni, R. H., Jr.; DeGennaro, L. J.; Greenberg, B. D.; Siman, R.; et al. Mutant and native human β -amyloid precursor proteins in transgenic mouse brain [see comments]. *Neurobiology of Aging* 16:685-699; 1995.

144. Howlett, D. R.; Jennings, K. H.; Lee, D. C.; Clark, M. S.; Brown, F.; Wetzel, R.; Wood, S.J.; Camilleri, P.; Roberts, G. W. Aggregation state and neurotoxic properties of Alzheimer β -amyloid peptide. *Neurodegeneration* 4:23-32; 1995.
145. Hsiao, K.; Chapman, P.; Nilsen, S.; Eckman, C.; Harigaya, Y.; Younkin, S.; Yang, F.S.; Cole, G. Correlative memory deficits, A- β elevation, and amyloid plaques in transgenic mice. *Science* 274:99-102; 1996.
146. Hsiao, K. K.; Borchelt, D. R.; Olson, K.; Johannsdottir, R.; Kitt, C.; Yunis, W.; Xu, S.; Eckman, C.; Younkin, S.; Price, D.; et al. Age-related CNS disorder and early death in transgenic FVB/N mice overexpressing Alzheimer amyloid precursor proteins. *Neuron* 15:1203-1218; 1995.
147. Hyman, B. T.; Van Hoesen, G. W.; Damasio, A. R. Memory-related neural systems in Alzheimer's disease: An anatomic study. *Neurology* 40:1721-1730; 1990.
148. Ichimiya, A.; Herholz, K.; Mielke, R.; Kessler, J.; Slansky, I.; Heiss, W. D. Difference of regional cerebral metabolic pattern between presenile and senile dementia of the Alzheimer type: A factor analytic study. *Journal of the Neurological Sciences* 123:11-17; 1994.
149. Li, M.; Sunamoto, M.; Ohnishi, K.; Ichimori, Y. β -Amyloid protein-dependent nitric oxide production from microglial cells and neurotoxicity. *Brain Research* 720:93-100; 1996.
150. Inestrosa, N. C.; Alvarez, A.; Perez, C. A.; Moreno, R. D.; Vicente, M.; Linker, C.; Soto, C.; Garrido, J. Acetylcholinesterase accelerates assembly of amyloid- β -peptides into Alzheimers fibrils: Possible role of the peripheral site of the enzyme. *Neuron* 16:881-891; 1996.
151. Ishiguro, K.; Shiratsuchi, A.; Sato, S.; Omori, A.; Arioka, M.; Kobayashi, S.; Uchida, T.; Imahori, K. Glycogen synthase kinase 3 β is identical to tau protein kinase I generating several epitopes of paired helical filaments. *FEBS Letters* 325:167-172; 1993.
152. Ishiguro, K.; Takamatsu, M.; Tomizawa, K.; Omori, A.; Takahashi, M.; Arioka, M.; Uchida, T.; Imahori, K. Tau protein kinase I converts normal tau protein into A68-like component of paired helical filaments. *Journal of Biological Chemistry* 267:10897-10901; 1992.
153. Ishii, T.; Haga, S. Immuno-electron-microscopic localization of complements in amyloid fibrils of senile plaques. *Acta Neuropathologica* 63:296-300; 1984.
154. Ishii, T.; Haga, S.; Kametari, F. Presence of immunoglobulins and complements in the amyloid plaques in the brain of patients with Alzheimer's disease. In: Pouplard-Barthelaix, A.; Emile, J.; Christen, Y. eds. *Immunology and Alzheimer's Disease*. Berlin: Springer; 1988:17-29.
155. Itagaki, S.; McGeer, P. L.; Akiyama, H.; Zhu, S.; Selkoe, D. Relationship of microglia and astrocytes to amyloid deposits of Alzheimer disease. *Journal of Neuroimmunology* 24:173-182; 1989.

156. Itoh, A.; Nitta, A.; Nadai, M.; Nishimura, K.; Hirose, M.; Hasegawa, T. Dysfunction of cholinergic and dopaminergic neuronal systems in β -amyloid protein-infused rats. *Journal of Neurochemistry* 66:1113-1117; 1996.
157. Iversen, L. L.; Rossor, M. N.; Reynolds, G. P.; Hills, R.; Roth, M.; Mountjoy, C. Q.; Foote, S. L.; Morrison, J. H.; Bloom, F. E. Loss of pigmented dopamine- β -hydroxylase positive cells from locus coeruleus in senile dementia of Alzheimer's type. *Neuroscience Letters* 39:95-100; 1983.
158. Jamada, M.; Mehraein, P. [Distribution of senile changes in the brain. The part of the limbic system in Alzheimer's disease and senile dementia]. [German]. *Archiv fur Psychiatrie und Nervenkrankheiten* 211:308-324; 1968.
159. Jellestad, F. K.; Garcia Cabrera, I. Exploration and avoidance learning after ibotenic acid and radio frequency lesions in the rat amygdala. *Behavioral & Neural Biology* 46:196-215; 1986.
160. Jellestad, F. K.; Markowska, A.; Bakke, H. K.; Walther, B. Behavioral effects after ibotenic acid, 6-OHDA and electrolytic lesions in the central amygdala nucleus of the rat. *Physiology & Behavior* 37:855-862; 1986.
161. Joachim, C. L.; Mori, H.; Selkoe, D. J. Amyloid β -protein deposition in tissues other than brain in Alzheimer's disease. *Nature* 341:226-230; 1989.
162. Joachim, C. L.; Morris, J. H.; Selkoe, D. J. Diffuse senile plaques occur commonly in the cerebellum in Alzheimer's disease. *American Journal of Pathology* 135:309-319; 1989.
163. Jonason, K. R.; Enloe, L. J. Alterations in social behavior following septal and amygdaloid lesions in the rat. *Journal of Comparative & Physiological Psychology* 75:286-301; 1971.
164. Jorgensen, O. S.; Brooksbank, B. W.; Balazs, R. Neuronal plasticity and astrocytic reaction in Down syndrome and Alzheimer disease. *Journal of the Neurological Sciences* 98:63-79; 1990.
165. Joslin, G.; Krause, J. E.; Hershey, A. D.; Adams, S. P.; Fallon, R. J.; Perlmutter, D. H. Amyloid- β peptide, substance P, and bombesin bind to the serpin-enzyme complex receptor. *Journal of Biological Chemistry* 266:21897-21902; 1991.
166. Kang, J.; Lemaire, H. G.; Unterbeck, A.; Salbaum, J. M.; Masters, C. L.; Grzeschik, K. H.; Multhaup, G.; Beyreuther, K.; Muller-Hill, B. The precursor of Alzheimer's disease amyloid A4 protein resembles a cell-surface receptor. *Nature* 325:733-736; 1987.
167. Kibbey, M. C.; Jucker, M.; Weeks, B. S.; Neve, R. L.; Van Nostrand, W. E.; Kleinman, H. K. β -Amyloid precursor protein binds to the neurite-promoting IKVAV site of laminin. *Proceedings of the National Academy of Sciences of the United States of America* 90:10150-10153; 1993.
168. Kidd, M. Alzheimer's disease. An electron microscopical study. *Brain* 87:307-320; 1964.

169. Kitaguchi, N.; Takahashi, Y.; Tokushima, Y.; Shiojiri, S.; Ito, H. Novel precursor of Alzheimer's disease amyloid protein shows protease inhibitory activity. *Nature* 331:530-532; 1988.
170. Koh, J. Y.; Yang, L. L.; Cotman, C. W. β -Amyloid protein increases the vulnerability of cultured cortical neurons to excitotoxic damage. *Brain Research* 533:315-320; 1990.
171. Kondo, J.; Honda, T.; Mori, H.; Hamada, Y.; Miura, R.; Ogawara, M.; Ihara, Y. The carboxyl third of tau is tightly bound to paired helical filaments. *Neuron* 1:827-834; 1988.
172. Koo, E. H.; Sisodia, S. S.; Archer, D. R.; Martin, L. J.; Weidemann, A.; Beyreuther, K.; Fischer, P.; Masters, C. L.; Price, D. L. Precursor of amyloid protein in Alzheimer disease undergoes fast anterograde axonal transport. *Proceedings of the National Academy of Sciences of the United States of America* 87:1561-1565; 1990.
173. Kopke, E.; Tung, Y. C.; Shaikh, S.; Alonso, A. C.; Iqbal, K.; Grundke-Iqbal, I. Microtubule-associated protein tau. Abnormal phosphorylation of a non-paired helical filament pool in Alzheimer disease. *Journal of Biological Chemistry* 268:24374-24384; 1993.
174. Korotzer, A. R.; Pike, C. J.; Cotman, C. W. β -Amyloid peptides induce degeneration of cultured rat microglia. *Brain Research* 624:121-125; 1993.
175. Kovacs, A. M.; Telegdy, G. The effects of amylin on motivated behavior in rats. *Physiology & Behavior* 60:183-186; 1996.
176. Kovacs, D. M.; Fausett, H. J.; Page, K. J.; Kim, T. W.; Moir, R. D.; Merriam, D. E.; Hollister, R. D.; Hallmark, O. G.; Mancini, R.; Felsenstein, K. M.; Hyman, B. T.; Tanzi, R. E.; Wasco, W. Alzheimer-associated presenilins 1 and 2: Neuronal expression in brain and localization to intracellular membranes in mammalian cells. *Nature Medicine* 2:224-229; 1996.
177. Kowall, N. W.; Beal, M. F. Cortical somatostatin, neuropeptide Y, and NADPH diaphorase neurons: Normal anatomy and alterations in Alzheimer's disease. *Annals of Neurology* 23:105-114; 1988.
178. Kowall, N. W.; Beal, M. F.; Busciglio, J.; Duffy, L. K.; Yankner, B. A. An in vivo model for the neurodegenerative effects of β amyloid and protection by substance P. *Proceedings of the National Academy of Sciences of the United States of America* 88:7247-7251; 1991.
179. Kowall, N. W.; McKee, A. C. The histopathology of neuronal degeneration and plasticity in Alzheimer disease. [Review]. *Advances in Neurology* 59:5-33; 1993.
180. Kowall, N. W.; McKee, A. C.; Yankner, B. A.; Beal, M. F. In vivo neurotoxicity of β -amyloid [β (1-40)] and the β (25-35) fragment. *Neurobiology of Aging* 13:537-542; 1992.
181. Kromer Vogt, L. J.; Hyman, B. T.; Van Hoesen, G. W.; Damasio, A. R. Pathological alterations in the amygdala in Alzheimer's disease. *Neuroscience* 37:377-385; 1990.
182. Ksiezak-Reding, H.; Chien, C. H.; Lee, V. M.; Yen, S. H. Mapping of the Alz 50 epitope in microtubule-associated proteins tau. *Journal of Neuroscience Research* 25:412-419; 1990.

183. Ksiezak-Reding, H.; Liu, W.-K.; Hradsky, J.; Yen, S.-H. Phosphate analysis of different tau preparations from normal and Alzheimer disease brains. *Journal of Cell Biology* 111:435a; 1990.
184. Kubos, K. L.; Pearlson, G. D.; Robinson, R. G. Intracortical kainic acid induces an asymmetrical behavioral response in the rat. *Brain Research* 239:303-309; 1982.
185. Ladner, C. J.; Czech, J.; Maurice, J.; Lorens, S. A.; Lee, J. M. Reduction of calcineurin enzymatic activity in Alzheimer's disease: Correlation with neuropathologic changes. *Journal of Neuropathology & Experimental Neurology* 55:924-931; 1996.
186. LaFerla, F. M.; Tinkle, B. T.; Bieberich, C. J.; Haudenschild, C. C.; Jay, G. The Alzheimer's A β peptide induces neurodegeneration and apoptotic cell death in transgenic mice. *Nature Genetics* 9:21-30; 1995.
187. Lai, F.; Williams, R. S. A prospective study of Alzheimer disease in Down syndrome. *Archives of Neurology* 46:849-853; 1989.
188. Lamb, B. T.; Sisodia, S. S.; Lawler, A. M.; Slunt, H. H.; Kitt, C. A.; Kearns, W. G.; Pearson, P. L.; Price, D. L.; Gearhart, J. D. Introduction and expression of the 400 kilobase amyloid precursor protein gene in transgenic mice [corrected] [published erratum appears in *Nat Genet* 1993 Nov;5(3):312]. *Nature Genetics* 5:22-30; 1993.
189. Lassmann, H.; Bancher, C.; Breitschopf, H.; Wegiel, J.; Bobinski, M.; Jellinger, K.; Wisniewski, H. M. Cell death in Alzheimer's disease evaluated by DNA fragmentation in situ. *Acta Neuropathologica* 89:35-41; 1995.
190. LeBlanc, A. C.; Xue, R.; Gambetti, P. Amyloid precursor protein metabolism in primary cell cultures of neurons, astrocytes, and microglia. *Journal of Neurochemistry* 66:2300-2310; 1996.
191. Lee, J. M.; Hejna, G.; Sigurdsson, E. M.; Singh, S.; Lorens, S. A. β -Amyloid (β /A4) 25-35 induces degeneration of median but not dorsal raphe neurons in the rat. *FASEB Journal* 6:A1916; 1992.(Abstract)
192. Levy-Lahad, E.; Wijsman, E. M.; Nemens, E.; Anderson, L.; Goddard, K. A.; Weber, J. L.; Bird, T. D.; Schellenberg, G. D. A familial Alzheimer's disease locus on chromosome 1 [see comments]. *Science* 269:970-973; 1995.
193. Li, J.; Ma, J.; Potter, H. Identification and expression analysis of a potential familial Alzheimer disease gene on chromosome 1 related to AD3. *Proceedings of the National Academy of Sciences of the United States of America* 92:12180-12184; 1995.
194. Liu, W. K.; Williams, R. T.; Hall, F. L.; Dickson, D. W.; Yen, S. H. Detection of a Cdc2-related kinase associated with Alzheimer paired helical filaments. *American Journal of Pathology* 146:228-238; 1995.
195. Lo Conte, G.; Bartolini, L.; Casamenti, F.; Marconcini-Pepeu, I.; Pepeu, G. Lesions of cholinergic forebrain nuclei: Changes in avoidance behavior and scopolamine actions. *Pharmacology, Biochemistry & Behavior* 17:933-937; 1982.

196. Lockhart, B. P.; Benicourt, C.; Junien, J. L.; Privat, A. Inhibitors of free radical formation fail to attenuate direct β -amyloid 25-35 peptide-mediated neurotoxicity in rat hippocampal cultures. *Journal of Neuroscience Research* 39:494-505; 1994.
197. Loewenstein, D. A.; Barker, W. W.; Chang, J. Y.; Apicella, A.; Yoshii, F.; Kothari, P.; Duara, R. Predominant left hemisphere metabolic dysfunction in dementia. *Archives of Neurology* 46:146-152; 1989.
198. Loffler, K. U.; Edward, D. P.; Tso, M. O. Immunoreactivity against tau, amyloid precursor protein, and β -amyloid in the human retina. *Investigative Ophthalmology & Visual Science* 36:24-31; 1995.
199. Lomedico, P. T.; Gubler, U.; Hellmann, C. P.; Dukovich, M.; Giri, J. G.; Pan, Y. C.; Collier, K.; Semionow, R.; Chua, A. O.; Mizel, S. B. Cloning and expression of murine interleukin-1 cDNA in *Escherichia coli*. *Nature* 312:458-462; 1984.
200. Loo, D. T.; Copani, A.; Pike, C. J.; Whittemore, E. R.; Walencewicz, A. J.; Cotman, C. W. Apoptosis is induced by β -amyloid in cultured central nervous system neurons. *Proceedings of the National Academy of Sciences of the United States of America* 90:7951-7955; 1993.
201. LoPresti, P.; Szuchet, S.; Papasozomenos, S. C.; Zinkowski, R. P.; Binder, L. I. Functional implications for the microtubule-associated protein tau: Localization in oligodendrocytes. *Proceedings of the National Academy of Sciences of the United States of America* 92:10369-10373; 1995.
202. Lorenzo, A.; Razzaboni, B.; Weir, G. C.; Yankner, B. A. Pancreatic islet cell toxicity of amylin associated with type-2 diabetes mellitus. *Nature* 368:756-760; 1994.
203. Lorenzo, A.; Yankner, B. A. β -Amyloid neurotoxicity requires fibril formation and is inhibited by congo red. *Proceedings of the National Academy of Sciences of the United States of America* 91:12243-12247; 1994.
204. Lowry, O. H.; Rosebrough, N. J.; Farr, A. L.; Randall, R. J. Protein measurement with folin phenol reagent. *Journal of Biological Chemistry* 193:265-267; 1951.
205. Ma, J.; Yee, A.; Brewer, H. B., Jr.; Das, S.; Potter, H. Amyloid-associated proteins α 1-antichymotrypsin and apolipoprotein E promote assembly of Alzheimer β -protein into filaments [see comments]. *Nature* 372:92-94; 1994.
206. Malherbe, P.; Richards, J. G.; Martin, J. R.; Bluethmann, H.; Maggio, J.; Huber, G. Lack of β -amyloidosis in transgenic mice expressing low levels of familial Alzheimers disease missense mutations. *Neurobiology of Aging* 17:205-214; 1996.
207. Malouf, A. T. Effect of β amyloid peptides on neurons in hippocampal slice cultures. *Neurobiology of Aging* 13:543-551; 1992.
208. Mann, D. M. Cerebral amyloidosis, ageing and Alzheimer's disease; a contribution from studies on Down's syndrome. *Neurobiology of Aging* 10:397-9; discussion 412; 1989.
209. Mann, D. M.; Esiri, M. M. The site of the earliest lesions of Alzheimer's disease [letter]. *New England Journal of Medicine* 318:789-790; 1988.

210. Mann, D. M.; Esiri, M. M. The pattern of acquisition of plaques and tangles in the brains of patients under 50 years of age with Down's syndrome. *Journal of the Neurological Sciences* 89:169-179; 1989.
211. Mann, D. M.; Tucker, C. M.; Yates, P. O. The topographic distribution of senile plaques and neurofibrillary tangles in the brains of non-demented persons of different ages. *Neuropathology & Applied Neurobiology* 13:123-139; 1987.
212. Mann, D. M.; Yates, P. O.; Marcyniuk, B.; Ravindra, C. R. The topography of plaques and tangles in Down's syndrome patients of different ages. *Neuropathology & Applied Neurobiology* 12:447-457; 1986.
213. Mantyh, P. W.; Ghilardi, J. R.; Rogers, S.; DeMaster, E.; Allen, C. J.; Stimson, E. R.; Maggio, J. E. Aluminum, iron, and zinc ions promote aggregation of physiological concentrations of β -amyloid peptide. *Journal of Neurochemistry* 61:1171-1174; 1993.
214. Masters, C. L.; Simms, G.; Weinman, N. A.; Multhaup, G.; McDonald, B. L.; Beyreuther, K. Amyloid plaque core protein in Alzheimer disease and Down syndrome. *Proceedings of the National Academy of Sciences of the United States of America* 82:4245-4249; 1985.
215. Matsuo, E. S.; Shin, R. W.; Billingsley, M. L.; Van deVoorde, A.; O'Connor, M.; Trojanowski, J. Q.; Lee, V. M. Biopsy-derived adult human brain tau is phosphorylated at many of the same sites as Alzheimer's disease paired helical filament tau. *Neuron* 13:989-1002; 1994.
216. Mattson, M. P. Antigenic changes similar to those seen in neurofibrillary tangles are elicited by glutamate and Ca^{2+} influx in cultured hippocampal neurons. *Neuron* 4:105-117; 1990.
217. Mattson, M. P.; Cheng, B.; Culwell, A. R.; Esch, F. S.; Lieberburg, I.; Rydel, R. E. Evidence for excitoprotective and intraneuronal calcium-regulating roles for secreted forms of the β -amyloid precursor protein. *Neuron* 10:243-254; 1993.
218. Mattson, M. P.; Cheng, B.; Davis, D.; Bryant, K.; Lieberburg, I.; Rydel, R. E. β -Amyloid peptides destabilize calcium homeostasis and render human cortical neurons vulnerable to excitotoxicity. *Journal of Neuroscience* 12:376-389; 1992.
219. Mattson, M. P.; Goodman, Y. Different amyloidogenic peptides share a similar mechanism of neurotoxicity involving reactive oxygen species and calcium. *Brain Research* 676:219-224; 1995.
220. Mattson, M. P.; Tomaselli, K. J.; Rydel, R. E. Calcium-destabilizing and neurodegenerative effects of aggregated β -amyloid peptide are attenuated by basic FGF. *Brain Research* 621:35-49; 1993.
221. Maurice, T.; Lockhart, B. P.; Privat, A.; Amnesia induced in mice by centrally administered β -amyloid peptides involves cholinergic dysfunction. *Brain Research* 706:181-193; 1996.

222. May, P. C.; Boggs, L. N.; Fuson, K. S. Neurotoxicity of human amylin in rat primary hippocampal cultures: Similarity to Alzheimer's disease amyloid- β neurotoxicity. *Journal of Neurochemistry* 61:2330-2333; 1993.
223. McDonald, M. P.; Dahl, E. E.; Overmier, J. B.; Mantyh, P.; Cleary, J. Effects of an exogenous β -amyloid peptide on retention for spatial learning. *Behavioral & Neural Biology* 62:60-67; 1994.
224. McDonald, M. P.; Overmier, J. B.; Bandyopadhyay, S.; Babcock, D.; Cleary, J. Reversal of β -amyloid-induced retention deficit after exposure to training and state cues. *Neurobiology of Learning & Memory* 65:35-47; 1996.
225. McGeer, P. L.; Akiyama, H.; Itagaki, S.; McGeer, E. G. Activation of the classical complement pathway in brain tissue of Alzheimer patients. *Neuroscience Letters* 107:341-346; 1989.
226. McGeer, P. L.; Akiyama, H.; Itagaki, S.; McGeer, E. G. Immune system response in Alzheimer's disease. *Canadian Journal of Neurological Sciences* 16:516-527; 1989.
227. McGeer, P. L.; Kawamata, T.; Walker, D. G.; Akiyama, H.; Tooyama, I.; McGeer, E. G. Microglia in degenerative neurological disease. [Review]. *GLIA* 7:84-92; 1993.
228. McGeer, P. L.; Rogers, J.; McGeer, E. G. Neuroimmune mechanisms in Alzheimer disease pathogenesis [see comments]. [Review]. *Alzheimer Disease & Associated Disorders* 8:149-158; 1994.
229. McLennan, H. The autoradiographic localization of L-[3 H]glutamate in rat brain tissue. *Brain Research* 115:139-144; 1976.
230. Meda, L.; Cassatella, M. A.; Szendrei, G. I.; Otvos, L., Jr.; Baron, P.; Villalba, M.; Ferrari, D.; Rossi, F. Activation of microglial cells by β -amyloid protein and interferon- γ . *Nature* 374:647-650; 1995.
231. Metzuzals, J.; Robitaille, Y.; Houghton, S.; Gauthier, S.; Leblanc, R. Paired helical filaments and the cytoplasmic-nuclear interface in Alzheimer's disease. *Journal of Neurocytology* 17:827-833; 1988.
232. Migheli, A.; Butler, M.; Brown, K.; Shelanski, M. L. Light and electron microscope localization of the microtubule-associated tau protein in rat brain. *Journal of Neuroscience* 8:1846-1851; 1988.
233. Miller, D. L.; Papayannopoulos, I. A.; Styles, J.; Bobin, S. A.; Lin, Y. Y.; Biemann, K. Peptide compositions of the cerebrovascular and senile plaque core amyloid deposits of Alzheimer's disease. *Archives of Biochemistry & Biophysics* 301:41-52; 1993.
234. Milward, E. A.; Papadopoulos, R.; Fuller, S. J.; Moir, R. D.; Small, D.; Beyreuther, K.; Masters, C. L. The amyloid protein precursor of Alzheimer's disease is a mediator of the effects of nerve growth factor on neurite outgrowth. *Neuron* 9:129-137; 1992.
235. Moossy, J.; Zubenko, G. S.; Martinez, A. J.; Rao, G. R.; Kopp, U.; Hanin, I. Lateralization of brain morphologic and cholinergic abnormalities in Alzheimer's disease. *Archives of Neurology* 46:639-642; 1989.

236. Moran, P. M.; Higgins, L. S.; Cordell, B.; Moser, P. C. Age-related learning deficits in transgenic mice expressing the 751-amino acid isoform of human β -amyloid precursor protein. *Proceedings of the National Academy of Sciences of the United States of America* 92:5341-5345; 1995.
237. Morin, P. J.; Abraham, C. R.; Amaratunga, A.; Johnson, R. J.; Huber, G.; Sandell, J. H.; Fine, R. E. Amyloid precursor protein is synthesized by retinal ganglion cells, rapidly transported to the optic nerve plasma membrane and nerve terminals, and metabolized. *Journal of Neurochemistry* 61:464-473; 1993.
238. Morishima-Kawashima, M.; Hasegawa, M.; Takio, K.; Suzuki, M.; Yoshida, H.; Ihara, Y. Proline-directed and non-proline-directed phosphorylation of PHF-tau. *Journal of Biological Chemistry* 270:823-829; 1995.
239. Motomura, N.; Seo, T. Lateral hemispheric asymmetries in senile dementia of Alzheimer's type (SDAT) assessed by I-123 IMP SPECT imaging: A preliminary report. *International Journal of Neuroscience* 63:1-3; 1992.
240. Mucke, L.; Abraham, C. R.; Ruppe, M. D.; Rockenstein, E. M.; Toggas, S. M.; Mallory, M.; Alford, M.; Masliah, E. Protection against HIV-1 gp120-induced brain damage by neuronal expression of human amyloid precursor protein. *Journal of Experimental Medicine* 181:1551-1556; 1995.
241. Mucke, L.; Masliah, E.; Johnson, W. B.; Ruppe, M. D.; Alford, M.; Rockenstein, E. M.; Forss-Petter, S.; Pietropaolo, M.; Mallory, M.; Abraham, C. R. Synaptotrophic effects of human amyloid β protein precursors in the cortex of transgenic mice. *Brain Research* 666:151-167; 1994.
242. Mullan, M.; Crawford, F.; Axelman, K.; Houlden, H.; Lilius, L.; Winblad, B.; Lannfelt, L. A pathogenic mutation for probable Alzheimer's disease in the APP gene at the N-terminus of β -amyloid. *Nature Genetics* 1:345-347; 1992.
243. Murphy, G. M., Jr.; Ellis, W. G. The amygdala in Down's syndrome and familial Alzheimer's disease: Four clinicopathological case reports. *Biological Psychiatry* 30:92-106; 1991.
244. Nabeshima, T.; Nitta, A. Memory impairment and neuronal dysfunction induced by β -amyloid protein in rats. *Tohoku Journal of Experimental Medicine* 174:241-249; 1994.
245. Namba, Y.; Tomonaga, M.; Kawasaki, H.; Otomo, E.; Ikeda, K. Apolipoprotein E immunoreactivity in cerebral amyloid deposits and neurofibrillary tangles in Alzheimer's disease and kuru plaque amyloid in Creutzfeldt-Jakob disease. *Brain Research* 541:163-166; 1991.
246. Naslund, J.; Thyberg, J.; Tjernberg, L. O.; Wernstedt, C.; Karlstrom, A. R.; Bogdanovic, N.; Gandy, S. E.; Lannfelt, L.; Terenius, L.; Nordstedt, C. Characterization of stable complexes involving apolipoprotein E and the amyloid β peptide in Alzheimer's disease brain. *Neuron* 15:219-228; 1995.

247. Naugle, R. I.; Cullum, C. M.; Bigler, E. D.; Massman, P. J. Neuropsychological and computerized axial tomography volume characteristics of empirically derived dementia subgroups. *Journal of Nervous & Mental Disease* 173:596-604; 1985.
248. Neve, R. L.; Finch, E. A.; Dawes, L. R. Expression of the Alzheimer amyloid precursor gene transcripts in the human brain. *Neuron* 1:669-677; 1988.
249. Neveu, P. J. Brain lateralization and immunomodulation. [Review]. *International Journal of Neuroscience* 70:135-143; 1993.
250. Nieto-Sampedro, M. Astrocyte mitogenic activity in aged normal and Alzheimer's human brain. *Neurobiology of Aging* 8:249-252; 1987.
251. Nishimoto, I.; Okamoto, T.; Matsuura, Y.; Takahashi, S.; Murayama, Y.; Ogata, E. Alzheimer amyloid protein precursor complexes with brain GTP-binding protein G(o) [see comments]. *Nature* 362:75-79; 1993.
252. Nordstedt, C.; Naslund, J.; Tjernberg, L. O.; Karlstrom, A. R.; Thyberg, J. The Alzheimer A β peptide develops protease resistance in association with its polymerization into fibrils. *Journal of Biological Chemistry* 269:30773-30776; 1994.
253. Norton, W. T.; Aquino, D. A.; Hozumi, I.; Chiu, F. C.; Brosnan, C. F. Quantitative aspects of reactive gliosis: a review. [Review]. *Neurochemical Research* 17:877-885; 1992.
254. O'Brien, J. T.; Egger, S.; Syed, G. M.; Sahakian, B. J.; Levy, R. A study of regional cerebral blood flow and cognitive performance in Alzheimer's disease. *Journal of Neurology, Neurosurgery & Psychiatry* 55:1182-1187; 1992.
255. O'Callaghan, J. P.; Jensen, K. F. Enhanced expression of glial fibrillary acidic protein and the cupric silver degeneration reaction can be used as sensitive and early indicators of neurotoxicity. [Review]. *Neurotoxicology* 13:113-122; 1992.
256. O'Callaghan, J. P.; Miller, D. B. Quantification of reactive gliosis as an approach to neurotoxicity assessment. [Review]. *NIDA Research Monograph* 136:188-212; 1993.
257. Olton, D. S.; Walker, J. A.; Gage, F. H. Hippocampal connections and spatial discrimination. *Brain Research* 139:295-308; 1978.
258. Palmer, A. M.; Procter, A. W.; Stratmann, G. C.; Bowen, D. M. Excitatory amino acid-releasing and cholinergic neurones in Alzheimer's disease. *Neuroscience Letters* 66:199-204; 1986.
259. Papasozomenos, S. C.; Binder, L. I. Phosphorylation determines two distinct species of Tau in the central nervous system. *Cell Motility & the Cytoskeleton* 8:210-226; 1987.
260. Paudel, H. K.; Lew, J.; Ali, Z.; Wang, J. H. Brain proline-directed protein kinase phosphorylates tau on sites that are abnormally phosphorylated in tau associated with Alzheimer's paired helical filaments. *Journal of Biological Chemistry* 268:23512-23518; 1993.
261. Paxinos, G.; Watson, C. The rat brain in stereotaxic coordinates. San Diego, CA: Academic Press; 1986.

262. Pearlson, G. D.; Robinson, R. G. Suction lesions of the frontal cerebral cortex in the rat induce asymmetrical behavioral and catecholaminergic responses. *Brain Research* 218:233-242; 1981.
263. Pearson, B. E.; Choi, T. K. Expression of the human β -amyloid precursor protein gene from a yeast artificial chromosome in transgenic mice. *Proceedings of the National Academy of Sciences of the United States of America* 90:10578-10582; 1993.
264. Pearson, R. C.; Esiri, M. M.; Hiorns, R. W.; Wilcock, G. K.; Powell, T. P. Anatomical correlates of the distribution of the pathological changes in the neocortex in Alzheimer disease. *Proceedings of the National Academy of Sciences of the United States of America* 82:4531-4534; 1985.
265. Pearson, R. C. A.; Powell, T. P. S. The neuroanatomy of Alzheimer's disease. *Reviews in Neuroscience* 2:101-122; 1989.
266. Pei, J. J.; Sersen, E.; Iqbal, K.; Grundke-Iqbal, I. Expression of protein phosphatases (PP-1, PP-2A, PP-2B and PTP-1B) and protein kinases (MAP kinase and P34cdc2) in the hippocampus of patients with Alzheimer disease and normal aged individuals. *Brain Research* 655:70-76; 1994.
267. Peinado-Manzano, M. A. The role of the amygdala and the hippocampus in working memory for spatial and non-spatial information. *Behavioural Brain Research* 38:117-134; 1990.
268. Perry, E. K.; Blessed, G.; Tomlinson, B. E.; Perry, R. H.; Crow, T. J.; Cross, A. J.; Dockray, G. J.; Dimaline, R.; Arregui, A. Neurochemical activities in human temporal lobe related to aging and Alzheimer-type changes. *Neurobiology of Aging* 2:251-256; 1981.
269. Pike, C. J.; Burdick, D.; Walencewicz, A. J.; Glabe, C. G.; Cotman, C. W. Neurodegeneration induced by β -amyloid peptides in vitro: The role of peptide assembly state. *Journal of Neuroscience* 13:1676-1687; 1993.
270. Pike, C. J.; Cummings, B. J.; Cotman, C. W. Early association of reactive astrocytes with senile plaques in Alzheimer's disease. *Experimental Neurology* 132:172-179; 1995.
271. Pike, C. J.; Cummings, B. J.; Monzavi, R.; Cotman, C. W. β -Amyloid-induced changes in cultured astrocytes parallel reactive astrocytosis associated with senile plaques in Alzheimer's disease. *Neuroscience* 63:517-531; 1994.
272. Pike, C. J.; Ramezandarab, N.; Miller, S.; Cotman, C. W. β -Amyloid increases enzyme activity and protein levels of glutamine synthetase in cultured astrocytes. *Experimental Neurology* 139:167-171; 1996.
273. Pike, C. J.; Walencewicz, A. J.; Glabe, C. G.; Cotman, C. W. In vitro aging of β -amyloid protein causes peptide aggregation and neurotoxicity. *Brain Research* 563:311-314; 1991.
274. Podlisny, M. B.; Stephenson, D. T.; Frosch, M. P.; Lieberburg, I.; Clemens, J. A. Synthetic amyloid β -protein fails to produce specific neurotoxicity in monkey cerebral cortex. *Neurobiology of Aging* 13:561-567; 1992.

275. Ponte, P.; Gonzalez-DeWhitt, P.; Schilling, J.; Miller, J.; Hsu, D.; Greenberg, B.; Davis, K.; Wallace, W.; Lieberburg, I.; Fuller, F. A new A4 amyloid mRNA contains a domain homologous to serine proteinase inhibitors. *Nature* 331:525-527; 1988.
276. Price, J. L.; Russcehn, F. T.; Amaral, D. G. The limbic region. II: The amygdaloid complex. In: Bjorklund, A.; Hokfelt, T.; Swanson, L. W. eds. *Handbook of Chemical Neuroanatomy*. Amsterdam: Elsevier Science Publishers; 1987:279-388.
277. Quon, D.; Wang, Y.; Catalano, R.; Scardina, J. M.; Murakami, K.; Cordell, B. Formation of β -amyloid protein deposits in brains of transgenic mice. *Nature* 352:239-241; 1991.
278. Rawlins, J. N.; Olton, D. S. The septo-hippocampal system and cognitive mapping. *Behavioural Brain Research* 5:331-358; 1982.
279. Rebeck, G. W.; Hyman, B. T. Neuroanatomical connections and specific regional vulnerability in Alzheimer's disease. [Review]. *Neurobiology of Aging* 14:45-7; discussion 55-6; 1993.
280. Rebeck, G. W.; Reiter, J. S.; Strickland, D. K.; Hyman, B. T. Apolipoprotein E in sporadic Alzheimer's disease: Allelic variation and receptor interactions. *Neuron* 11:575-580; 1993.
281. Robinson, R. G. Differential behavioral and biochemical effects of right and left hemispheric cerebral infarction in the rat. *Science* 205:707-710; 1979.
282. Rogers, J.; Cooper, N. R.; Webster, S.; Schultz, J.; McGeer, P. L.; Styren, S. D.; Civin, W. H.; Brachova, L.; Bradt, B.; Ward, P.; et al. Complement activation by β -amyloid in Alzheimer disease. *Proceedings of the National Academy of Sciences of the United States of America* 89:10016-10020; 1992.
283. Rogers, J.; Morrison, J. H. Quantitative morphology and regional and laminar distributions of senile plaques in Alzheimer's disease. *Journal of Neuroscience* 5:2801-2808; 1985.
284. Roher, A. E.; Ball, M. J.; Bhave, S. V.; Wakade, A. R. β -Amyloid from Alzheimer disease brains inhibits sprouting and survival of sympathetic neurons. *Biochemical & Biophysical Research Communications* 174:572-579; 1991.
285. Roher, A. E.; Lowenson, J. D.; Clarke, S.; Wolkow, C.; Wang, R.; Cotter, R. J.; Zurcher-Neely, H. A.; Heinrikson, R. L.; Ball, M. J.; et al. Structural alterations in the peptide backbone of β -amyloid core protein may account for its deposition and stability in Alzheimer's disease. *Journal of Biological Chemistry* 268:3072-3083; 1993.
286. Roozendaal, B.; Koolhaas, J. M.; Bohus, B. The central amygdala is involved in conditioning but not in retention of active and passive shock avoidance in male rats. *Behavioral & Neural Biology* 59:143-149; 1993.
287. Rossor, M. N.; Garrett, N. J.; Johnson, A. L.; Mountjoy, C. Q.; Roth, M.; Iversen, L. L. A post-mortem study of the cholinergic and GABA systems in senile dementia. *Brain* 105:313-330; 1982.

288. Rossor, M. N.; Iversen, L. L.; Reynolds, G. P.; Mountjoy, C. Q.; Roth, M. Neurochemical characteristics of early and late onset types of Alzheimer's disease. *British Medical Journal Clinical Research Ed.* 288:961-964; 1984.
289. Roth, M.; Tomlinson, B. E.; Blessed, G. The relationship between quantitative measures of dementia and of degenerative changes in the cerebral grey matter of elderly subjects. *Proceedings of the Royal Society of Medicine* 60:254-260; 1967.
290. Royston, M. C.; Mann, D.; Pickering-Brown, S.; Owen, F.; Perry, R.; Raghavan, R.; Khin-Nu, C.; Tyrer, S.; Day, K.; Crook, R.; et al. Apolipoprotein E epsilon 2 allele promotes longevity and protects patients with Down's syndrome from dementia. *Neuroreport* 5:2583-2585; 1994.
291. Rumble, B.; Retallack, R.; Hilbich, C.; Simms, G.; Multhaup, G.; Martins, R.; Montgomery, P.; Beyreuther, K.; Masters, C. L. Amyloid A4 protein and its precursor in Down's syndrome and Alzheimer's disease [see comments]. *New England Journal of Medicine* 320:1446-1452; 1989.
292. Rush, D. K.; Aschmies, S.; Merriman, M. C. Intracerebral β -amyloid(25-35) produces tissue damage: is it neurotoxic? *Neurobiology of Aging* 13:591-594; 1992.
293. Rye, D. B.; Leverenz, J.; Greenberg, S. G.; Davies, P.; Saper, C. B. The distribution of Alz-50 immunoreactivity in the normal human brain. *Neuroscience* 56:109-127; 1993.
294. Saito, T.; Ishiguro, K.; Uchida, T.; Miyamoto, E.; Kishimoto, T.; Hisanaga, S. In situ dephosphorylation of tau by protein phosphatase 2A and 2B in fetal rat primary cultured neurons. *FEBS Letters* 376:238-242; 1995.
295. Saitoh, T.; Sundsmo, M.; Roch, J. M.; Kimura, N.; Cole, G.; Schubert, D.; Oltersdorf, T.; Schenk, D. B. Secreted form of amyloid β protein precursor is involved in the growth regulation of fibroblasts. *Cell* 58:615-622; 1989.
296. Sanan, D. A.; Weisgraber, K. H.; Russell, S. J.; Mahley, R. W.; Huang, D.; Saunders, A.; Schmechel, D.; Wisniewski, T.; Frangione, B.; Roses, A. D.; et al. Apolipoprotein E associates with β amyloid peptide of Alzheimer's disease to form novel monofibrils. Isoform apoE4 associates more efficiently than apoE3. *Journal of Clinical Investigation* 94:860-869; 1994.
297. Schellenberg, G. D.; Bird, T. D.; Wijsman, E. M.; Orr, H. T.; Anderson, L.; Nemens, E.; White, J. A.; Bonnycastle, L.; Weber, J. L.; Alonso, M. E.; et al. Genetic linkage evidence for a familial Alzheimer's disease locus on chromosome 14. *Science* 258:668-671; 1992.
298. Scheuner, D.; Eckman, C.; Jensen, M.; Song, X.; Citron, M.; Suzuki, N.; Bird, T. D.; Hardy, J.; Hutton, M.; Kukull, W.; Larson, E.; Levylahad, E.; Viitanen, M.; Peskind, E.; Poorkaj, P.; Schellenberg, G.; Tanzi, R.; Wasco, W.; Lannfelt, L.; Selkoe, D.; Younkin, S. Secreted amyloid β -protein similar to that in the senile plaques of Alzheimers disease is increased in vivo by the presenilin 1 and 2 and APP mutations linked to familial Alzheimers disease. *Nature Medicine* 2:864-870; 1996.
299. Schmechel, D. E.; Saunders, A. M.; Strittmatter, W. J.; Crain, B. J.; Hulette, C. M.; Joo, SH; Pericak-Vance, M. A.; Goldgaber, D.; Roses, A. D. Increased amyloid β -peptide deposition in cerebral cortex as a consequence of apolipoprotein E genotype in late-onset

Alzheimer disease. *Proceedings of the National Academy of Sciences of the United States of America* 90:9649-9653; 1993.

300. Schobitz, B.; De Kloet, E. R.; Holsboer, F. Gene expression and function of interleukin 1, interleukin 6 and tumor necrosis factor in the brain. [Review]. *Progress in Neurobiology* 44:397-432; 1994.

301. Schubert, D. The possible role of adhesion in synaptic modification. [Review]. *Trends in Neurosciences* 14:127-130; 1991.

302. Schubert, D.; Behl, C. The expression of amyloid β protein precursor protects nerve cells from β -amyloid and glutamate toxicity and alters their interaction with the extracellular matrix. *Brain Research* 629:275-282; 1993.

303. Schubert, D.; Jin, L. W.; Saitoh, T.; Cole, G. The regulation of amyloid β protein precursor secretion and its modulatory role in cell adhesion [published erratum appears in *Neuron* 1990 May;4(5):813]. *Neuron* 3:689-694; 1989.

304. Schultz, J.; Schaller, J.; McKinley, M.; Bradt, B.; Cooper, N.; May, P.; Rogers, J. Enhanced cytotoxicity of amyloid β -peptide by a complement dependent mechanism. *Neuroscience Letters* 175:99-102; 1994.

305. Schwartzbaum, J. S.; Gay, P. E. Interacting behavioral effects of septal and amygdaloid lesions in the rat. *Journal of Comparative & Physiological Psychology* 61:59-65; 1966.

306. Seltzer, B.; Sherwin, I. A comparison of clinical features in early- and late-onset primary degenerative dementia. One entity or two? *Archives of Neurology* 40:143-146; 1983.

307. Seubert, P.; Vigo-Pelfrey, C.; Esch, F.; Lee, M.; Dovey, H.; Davis, D.; Sinha, S.; Schlossmacher, M.; Whaley, J.; Swindlehurst, C.; et al. Isolation and quantification of soluble Alzheimer's β -peptide from biological fluids [see comments]. *Nature* 359:325-327; 1992.

308. Shearman, M. S.; Ragan, C. I.; Iversen, L. L. Inhibition of PC12 cell redox activity is a specific, early indicator of the mechanism of β -amyloid-mediated cell death. *Proceedings of the National Academy of Sciences of the United States of America* 91:1470-1474; 1994.

309. Sheng, J. G.; Mrak, R. E.; Griffin, W. S. Microglial interleukin-1 α expression in brain regions in Alzheimer's disease: Correlation with neuritic plaque distribution. *Neuropathology & Applied Neurobiology* 21:290-301; 1995.

310. Sherrington, R.; Rogaev, E. I.; Liang, Y.; Rogaeva, E. A.; Levesque, G.; Ikeda, M.; Chi, H.; Lin, C.; Li, G.; Holman, K.; et al. Cloning of a gene bearing missense mutations in early-onset familial Alzheimer's disease [see comments]. *Nature* 375:754-760; 1995.

311. Shimohama, S.; Fujimoto, S.; Taniguchi, T.; Kameyama, M.; Kimura, J. Reduction of low-molecular-weight acid phosphatase activity in Alzheimer brains. *Annals of Neurology* 33:616-621; 1993.

312. Shin, R. W.; Bramblett, G. T.; Lee, V. M.; Trojanowski, J. Q. Alzheimer disease A68 proteins injected into rat brain induce codeposits of β -amyloid, ubiquitin, and alpha 1-antichymotrypsin. *Proceedings of the National Academy of Sciences of the United States of America* 90:6825-6828; 1993.
313. Shoji, M.; Golde, T. E.; Ghiso, J.; Cheung, T. T.; Estus, S.; Shaffer, L. M.; Cai, X. D.; McKay, D. M.; Tintner, R.; Frangione, B.; et al. Production of the Alzheimer amyloid β protein by normal proteolytic processing. *Science* 258:126-129; 1992.
314. Sigurdsson, E. M.; Hejna, M. J.; Lee, J. M.; Lorens, S. A. β -Amyloid 25-35 and/or quinolinic acid injections into the basal forebrain of young male Fischer-344 rats: Behavioral, neurochemical and histological effects. *Behavioural Brain Research* 72:141-156; 1995.
315. Sigurdsson, E. M.; Lee, J. M.; Dong, X.-W.; Hejna, M. J.; Lorens, S. A. Laterality in the histological effects of injections of amyloid- β 25-35 into the amygdala of young Fischer rats. *Journal of Neuropathology & Experimental Neurology*, in press.
316. Sigurdsson, E. M.; Lee, J. M.; Dong, X.-W.; Hejna, M. J.; Lorens, S. A. Time course of the histopathological effects of injections of amyloid- β 25-35 into the amygdala of young male Fischer rats. Submitted.
317. Sigurdsson, E. M.; Lorens, S. A.; Hejna, M. J.; Dong, X.-W.; Lee, J. M. Local and distant histopathological effects of unilateral amyloid- β 25-35 injections into the amygdala of young F344 rats. *Neurobiology of Aging* 17:893-901; 1996.
318. Sisodia, S. S.; Koo, E. H.; Beyreuther, K.; Unterbeck, A.; Price, D. L. Evidence that β -amyloid protein in Alzheimer's disease is not derived by normal processing. *Science* 248:492-495; 1990.
319. Smith, C. D.; Carney, J. M.; Starke-Reed, P. E.; Oliver, C. N.; Stadtman, E. R.; Floyd; RA; Markesbery, W. R. Excess brain protein oxidation and enzyme dysfunction in normal aging and in Alzheimer disease. *Proceedings of the National Academy of Sciences of the United States of America* 88:10540-10543; 1991.
320. Smyth, M. D.; Kesslak, J. P.; Cummings, B. J.; Cotman, C. W. Analysis of brain injury following intrahippocampal administration of β -amyloid in streptozotocin-treated rats. *Neurobiology of Aging* 15:153-159; 1994.
321. Snow, A. D.; Sekiguchi, R.; Nochlin, D.; Fraser, P.; Kimata, K.; Mizutani, A.; Schreier, W. A.; Morgan, D. G. An important role of heparan sulfate proteoglycan (Perlecan) in a model system for the deposition and persistence of fibrillar A β -amyloid in rat brain. *Neuron* 12:219-234; 1994.
322. St George-Hyslop, P.; Haines, J.; Rogaeve, E.; Mortilla, M.; Vaala, G.; Pericak-Vance, M.; Foncin, J. F.; Montesi, M.; Bruni, A.; Sorbi, S.; et al. Genetic evidence for a novel familial Alzheimer's disease locus on chromosome 14. *Nature Genetics* 2:330-334; 1992.
323. Strijbos, P. J.; Rothwell, N. J. Interleukin-1 β attenuates excitatory amino acid-induced neurodegeneration in vitro: Involvement of nerve growth factor. *Journal of Neuroscience* 15:3468-3474; 1995.

324. Strittmatter, W. J.; Saunders, A. M.; Goedert, M.; Weisgraber, K. H.; Dong, L. M.; Jakes, R.; Huang, D. Y.; Pericak-Vance, M.; Schmechel, D.; Roses, A. D. Isoform-specific interactions of apolipoprotein E with microtubule-associated protein tau: Implications for Alzheimer disease. *Proceedings of the National Academy of Sciences of the United States of America* 91:11183-11186; 1994.
325. Strittmatter, W. J.; Saunders, A. M.; Schmechel, D.; Pericak-Vance, M.; Enghild, J.; Salvesen, G. S.; Roses, A. D. Apolipoprotein E: High-avidity binding to β -amyloid and increased frequency of type 4 allele in late-onset familial Alzheimer disease. *Proceedings of the National Academy of Sciences of the United States of America* 90:1977-1981; 1993.
326. Strittmatter, W. J.; Weisgraber, K. H.; Huang, D. Y.; Dong, L. M.; Salvesen, G. S.; Pericak-Vance, M.; Schmechel, D.; Saunders, A. M.; Goldgaber, D.; Roses, A. D. Binding of human apolipoprotein E to synthetic amyloid β peptide: Isoform-specific effects and implications for late-onset Alzheimer disease. *Proceedings of the National Academy of Sciences of the United States of America* 90:8098-8102; 1993.
327. Struble, R. G.; Powers, R. E.; Casanova, M. F.; Kitt, C. A.; Brown, E. C.; Price, D. L. Neuropeptidergic systems in plaques of Alzheimer's disease. [Review]. *Journal of Neuropathology & Experimental Neurology* 46:567-584; 1987.
328. Su, J. H.; Anderson, A. J.; Cummings, B. J.; Cotman, C. W. Immunohistochemical evidence for apoptosis in Alzheimer's disease. *Neuroreport* 5:2529-2533; 1994.
329. Sullivan, R. M.; Szechtman, H. Left/right nigrostriatal asymmetry in susceptibility to neurotoxic dopamine depletion with 6-hydroxydopamine in rats. *Neuroscience Letters* 170:83-86; 1994.
330. Sutherland, R. J.; McDonald, R. J. Hippocampus, amygdala, and memory deficits in rats. *Behavioural Brain Research* 37:57-79; 1990.
331. Suzuki, N.; Cheung, T. T.; Cai, X. D.; Odaka, A.; Otvos, L., Jr.; Eckman, C.; Golde, T. E.; Younkin, S. G. An increased percentage of long amyloid β protein secreted by familial amyloid β protein precursor (β APP717) mutants. *Science* 264:1336-1340; 1994.
332. Takashima, A.; Noguchi, K.; Sato, K.; Hoshino, T.; Imahori, K. Tau protein kinase I is essential for amyloid β -protein-induced neurotoxicity. *Proceedings of the National Academy of Sciences of the United States of America* 90:7789-7793; 1993.
333. Tanzi, R. E.; McClatchey, A. I.; Lamperti, E. D.; Villa-Komaroff, L.; Gusella, J. F.; Neve, R. L. Protease inhibitor domain encoded by an amyloid protein precursor mRNA associated with Alzheimer's disease. *Nature* 331:528-530; 1988.
334. Tate, B.; Aboody-Guterman, K. S.; Morris, A. M.; Walcott, E. C.; Majocha, R. E.; Marotta, C. A. Disruption of circadian regulation by brain grafts that overexpress Alzheimer β /A4 amyloid. *Proceedings of the National Academy of Sciences of the United States of America* 89:7090-7094; 1992.
335. Terry, R. D. The fine structure of neurofibrillary tangles in Alzheimer's disease. *Journal of Neuropathology & Experimental Neurology* 22:629-642; 1963.

336. Turner, R. S.; Suzuki, N.; Chyung, A. S. C.; Younkin, S. G.; Lee, V. M. Y. Amyloids $\beta(40)$ and $\beta(42)$ are generated intracellularly in cultured human neurons and their secretion increases with maturation. *Journal of Biological Chemistry* 271:8966-8970; 1996.
337. Ueda, K.; Masliah, E.; Saitoh, T.; Bakalis, S. L.; Scoble, H.; Kosik, K. S. Alz-50 recognizes a phosphorylated epitope of tau protein. *Journal of Neuroscience* 10:3295-3304; 1990.
338. Urbanyi, Z.; Lakics, V.; Erdo, S. L. Serum amyloid P component-induced cell death in primary cultures of rat cerebral cortex. *European Journal of Pharmacology* 270:375-378; 1994.
339. Van Nostrand, W. E.; Wagner, S. L.; Shankle, W. R.; Farrow, J. S.; Dick, M.; Rozemuller, J.M.; Kuiper, M. A.; Wolters, E. C.; Zimmerman, J.; Cotman, C. W.; et al. Decreased levels of soluble amyloid β -protein precursor in cerebrospinal fluid of live Alzheimer disease patients. *Proceedings of the National Academy of Sciences of the United States of America* 89:2551-2555; 1992.
340. Vereecken, T. H.; Vogels, O. J.; Nieuwenhuys, R. Neuron loss and shrinkage in the amygdala in Alzheimer's disease. *Neurobiology of Aging* 15:45-54; 1994.
341. Vincent, I. J.; Davies, P. A protein kinase associated with paired helical filaments in Alzheimer disease. *Proceedings of the National Academy of Sciences of the United States of America* 89:2878-2882; 1992.
342. Vlajkovic, S.; Nikolic, V.; Nikolic, A.; Milanovic, S.; Jankovic, B. D. Asymmetrical modulation of immune reactivity in left- and right-biased rats after ipsilateral ablation of the prefrontal, parietal and occipital brain neocortex. *International Journal of Neuroscience* 78:123-134; 1994.
343. Wang, J. Z.; Gong, C. X.; Zaidi, T.; Grundke-Iqbal, I.; Iqbal, K. Dephosphorylation of Alzheimer paired helical filaments by protein phosphatase-2A and -2B. *Journal of Biological Chemistry* 270:4854-4860; 1995.
344. Wasco, W.; Pettingell, W. P.; Jondro, P. D.; Schmidt, S. D.; Gurubhagavatula, S.; Rodes, L.; DiBlasi, T.; Romano, D. M.; Guenette, S. Y.; Kovacs, D. M.; et al. Familial Alzheimer's chromosome 14 mutations [letter]. *Nature Medicine* 1:848-1995.
345. Watanabe, A.; Hasegawa, M.; Suzuki, M.; Takio, K.; Morishima-Kawashima, M.; Arai, T.; Kosik, K. S.; Ihara, Y. In vivo phosphorylation sites in fetal and adult rat tau. *Journal of Biological Chemistry* 268:25712-25717; 1993.
346. Watanabe, N.; Takio, K.; Hasegawa, M.; Arai, T.; Titani, K.; Ihara, Y. Tau 2: a probe for a Ser conformation in the amino terminus of tau. *Journal of Neurochemistry* 58:960-966; 1992.
347. Watt, J. A.; Pike, C. J.; Walencewicz-Wasserman, A. J.; Cotman, C. W. Ultrastructural analysis of β -amyloid-induced apoptosis in cultured hippocampal neurons. *Brain Research* 661:147-156; 1994.
348. Webster, S.; O'Barr, S.; Rogers, J. Enhanced aggregation and β structure of amyloid β peptide after coincubation with C1q. *Journal of Neuroscience Research* 39:448-456; 1994.

349. Weidemann, A.; Konig, G.; Bunke, D.; Fischer, P.; Salbaum, J. M.; Masters, C. L.; Beyreuther, K. Identification, biogenesis, and localization of precursors of Alzheimer's disease A4 amyloid protein. *Cell* 57:115-126; 1989.
350. Werka, T.; Skar, J.; Ursin, H. Exploration and avoidance in rats with lesions in amygdala and piriform cortex. *Journal of Comparative & Physiological Psychology* 92:672-681; 1978.
351. Whitehouse, P. J.; Price, D. L.; Struble, R. G.; Clark, A. W.; Coyle, J. T.; Delon, M. R. Alzheimer's disease and senile dementia: Loss of neurons in the basal forebrain. *Science* 215:1237-1239; 1982.
352. Whitson, J. S.; Appel, S. H. Neurotoxicity of A β amyloid protein in vitro is not altered by calcium channel blockade. *Neurobiology of Aging* 16:5-10; 1995.
353. Whitson, J. S.; Selkoe, D. J.; Cotman, C. W. Amyloid β protein enhances the survival of hippocampal neurons in vitro. *Science* 243:1488-1490; 1989.
354. Winkler, J.; Connor, D. J.; Frautschy, S. A.; Behl, C.; Waite, J. J.; Cole, G. M.; Thal, L.J. Lack of long-term effects after β -amyloid protein injections in rat brain. *Neurobiology of Aging* 15:601-607; 1994.
355. Wischik, C. M.; Novak, M.; Edwards, P. C.; Klug, A.; Tichelaar, W.; Crowther, R. A. Structural characterization of the core of the paired helical filament of Alzheimer disease. *Proceedings of the National Academy of Sciences of the United States of America* 85:4884-4888; 1988.
356. Wischik, C. M.; Novak, M.; Thogersen, H. C.; Edwards, P. C.; Runswick, M. J.; Jakes, R.; Milstein, C.; Roth, M.; Klug, A. Isolation of a fragment of tau derived from the core of the paired helical filament of Alzheimer disease. *Proceedings of the National Academy of Sciences of the United States of America* 85:4506-4510; 1988.
357. Wisniewski, K.; Jervis, G. A.; Moretz, R. C.; Wisniewski, H. M. Alzheimer neurofibrillary tangles in diseases other than senile and presenile dementia. *Annals of Neurology* 5:288-294; 1979.
358. Wisniewski, K. E.; Wisniewski, H. M.; Wen, G. Y. Occurrence of neuropathological changes and dementia of Alzheimer's disease in Down's syndrome. *Annals of Neurology* 17:278-282; 1985.
359. Wisniewski, T.; Castano, E. M.; Golabek, A.; Vogel, T.; Frangione, B. Acceleration of Alzheimer's fibril formation by apolipoprotein E in vitro. *American Journal of Pathology* 145:1030-1035; 1994.
360. Wisniewski, T.; Frangione, B. Apolipoprotein E: a pathological chaperone protein in patients with cerebral and systemic amyloid. *Neuroscience Letters* 135:235-238; 1992.
361. Wittling, W. Brain asymmetry in the control of autonomic-physiologic activity. In: Davidson, R. J.; Hugdahl, K. eds. *Brain asymmetry*. Cambridge: MIT Press; 1995:305-357.

362. Wolozin, B.; Iwasaki, K.; Vito, P.; Ganjei, J. K.; Lacana, E.; Sunderland, T.; Zhao, B. Y.; Kusiak, J. W.; Wasco, V.; Dadamio, L. Participation of presenilin 2 in apoptosis: Enhanced basal activity conferred by an Alzheimer mutation. *Science* 274:1710-1713; 1996.
363. Woolf, N. J.; Butcher, L. L. Cholinergic projections to the basolateral amygdala: A combined Evans Blue and acetylcholinesterase analysis. *Brain Research Bulletin* 8:751-763; 1982.
364. Yamaguchi, F.; Richards, S. J.; Beyreuther, K.; Salbaum, M.; Carlson, G. A.; Dunnett, S. B. Transgenic mice for the amyloid precursor protein 695 isoform have impaired spatial memory. *Neuroreport* 2:781-784; 1991.
365. Yamazaki, T.; Selkoe, D. J.; Koo, E. H. Trafficking of cell surface β -amyloid precursor protein: Retrograde and transcytotic transport in cultured neurons. *Journal of Cell Biology* 129:431-442; 1995.
366. Yamazaki, T.; Yamaguchi, H.; Nakazato, Y.; Ishiguro, K.; Kawarabayashi, T.; Hirai, S. Ultrastructural characterization of cerebellar diffuse plaques in Alzheimer's disease. *Journal of Neuropathology & Experimental Neurology* 51:281-286; 1992.
367. Yan, S. D.; Chen, X.; Fu, J.; Chen, M.; Zhu, H. J.; Roher, A.; Slattery, T.; Zhao, L.; Nagashima, M.; Morser, J.; Migheli, A.; Nawroth, P.; Stern, D.; Schmidt, A. M. RAGE and amyloid- β peptide neurotoxicity in Alzheimers disease. *Nature* 382:685-691; 1996.
368. Yankner, B. A.; Caceres, A.; Duffy, L. K. Nerve growth factor potentiates the neurotoxicity of β amyloid. *Proceedings of the National Academy of Sciences of the United States of America* 87:9020-9023; 1990.
369. Yankner, B. A.; Dawes, L. R.; Fisher, S.; Villa-Komaroff, L.; Oster-Granite, M. L. Neurotoxicity of a fragment of the amyloid precursor associated with Alzheimer's disease. *Science* 245:417-420; 1989.
370. Yankner, B. A.; Duffy, L. K.; Kirschner, D. A. Neurotrophic and neurotoxic effects of amyloid β protein: Reversal by tachykinin neuropeptides. *Science* 250:279-282; 1990.
371. Zheng, H.; Jiang, M.; Trumbauer, M. E.; Sirinathsinghji, D. J.; Hopkins, R.; Smith; DW; Heavens, R. P.; Dawson, G. R.; Boyce, S.; Conner, M. W.; et al. β -Amyloid precursor protein-deficient mice show reactive gliosis and decreased locomotor activity. *Cell* 81:525-531; 1995.

VITA

The author, Einar Mar Sigurdsson, was born on January 14, 1965 in Kopavogur, Iceland to Sigurdur Jonsson and Palina Johannesdottir. He received his college education in Natural Sciences at the College of Reykjavik, Iceland, graduating in 1984. He studied French at the University of Aix-Marseilles from 1984-1985. In the autumn of 1985, Einar entered the University of Iceland, where he studied Pharmacy. He graduated with a Cand. Pharm. degree in Pharmacy in May, 1990. During the summer of 1990, Einar worked as a pharmacist in Akraness Pharmacy, Akranes, Iceland. From September 1990 to August 1991, Einar worked as a pharmacist and laboratory instructor in Medicinal Chemistry in the Department of Pharmacy at the University of Iceland.

In August 1991, Einar entered the Department of Pharmacology and Experimental Therapeutics of the Graduate School at Loyola University Chicago. In 1992, he joined the laboratory of Dr. Stanley A. Lorens to pursue research in the development of an animal model for Alzheimer's disease.

DISSERTATION APPROVAL SHEET

The dissertation submitted by Einar M. Sigurdsson has been read and approved by the following committee:

Stanley A. Lorens, Ph.D., Director
Professor, Department of Pharmacology
Loyola University Chicago

John M. Lee, M.D., Ph.D.
Assistant Professor, Departments of Pathology and Pharmacology
Loyola University Chicago

Thackery S. Gray, Ph.D.
Associate Professor, Department of Cell Biology, Neurobiology and Anatomy
Loyola University Chicago

Nancy A. Muma, Ph.D.
Associate Professor, Department of Pharmacology
Loyola University Chicago

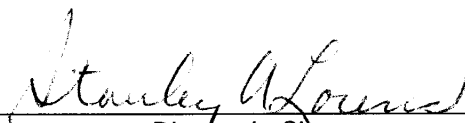
T. Celeste Napier, Ph.D.
Professor, Department of Pharmacology
Loyola University Chicago

The final copies have been examined by the director of the dissertation and the signature which appears below verifies the fact that any necessary changes have been incorporated and that the dissertation is now given final approval by the committee with reference to content and form.

The dissertation is, therefore, accepted in partial fulfillment of the requirements for the degree of Doctor of Philosophy.

4/7-97

Date


Director's Signature